STATISTICAL AND BEHAVIORAL MODELING OF DRIVER BEHAVIOR ON SIGNALIZED INTERSECTION APPROACHES

Ahmed Mohamed Mostafa Amer

Dissertation submitted to the faculty of the
Virginia Polytechnic Institute and State University
in partial fulfillment of the
requirements for the degree of

Doctor of Philosophy
in
Civil Engineering

Hesham A. Rakha, Chair
Ihab E. El-Shawarby, Co-Chair
Vicki R. Lewis
Antoine G. Hobeika
Montasir M. Abbas

December 8th, 2010
Blacksburg, VA

Keywords: Driver Behavior, Onset of Yellow, Perception-Reaction Time, Deceleration Behavior, Dilemma Zone, Red Light Running

STATISTICAL AND BEHAVIORAL MODELING OF DRIVER BEHAVIOR ON SIGNALIZED INTERSECTION APPROACHES

Ahmed Mohamed Mostafa Amer

ABSTRACT

The onset of a yellow indication is typically associated with the risk of vehicle crashes resulting from dilemma-zone and red-light-running problems. Such risk of vehicle crashes is greater for high-speed signalized intersection approaches. The research presented in this dissertation develops statistical as well as behavioral frameworks for modeling driver behavior while approaching high-speed signalized intersection approaches at the onset of a yellow indication. The analysis in this dissertation utilizes two sources of data. The main source is a new dataset that was collected as part of this research effort during the summer of 2008. This experiment includes two instructed speeds; 72.4 km/h (45 mph) with 1727 approaching trials (687 running and 1040 stopping), and 88.5 km/h (55 mph) with 1727 approaching trials (625 running and 1102 stopping). The complementary source is an existing dataset that was collected earlier in the spring of 2005 on the Virginia Smart Road facility. This dataset includes a total of 1186 yellow approaching trials (441 running and 745 stopping).

The adopted analysis approach comprises four major parts that fulfill the objectives of this dissertation. The first part is concerned with the characterization of different driver behavioral attributes, including driver yellow/red light running behavior, driver stop-run decisions, driver perception-reaction times (PRT), and driver deceleration levels. The characterization of these attributes involves analysis of variance (ANOVA) and frequency distribution analyses, as well as the calibration of statistical models. The second part of the dissertation introduces a novel approach for computing the clearance interval duration that explicitly accounts for the reliability of the design (probability that drivers do not encounter a dilemma zone). Lookup tables are developed to assist practitioners in the design of yellow timings that reflects the stochastic nature of driver PRT and deceleration levels. An extension of the proposed approach is presented that can be integrated with the IntelliDrive^{SM} initiative.

Furthermore, the third part of the dissertation develops an agent-based Bayesian statistics approach to capture the stochastic nature of the driver stop-run decision. The Bayesian model parameters are calibrated using the Markov Chain Monte Carlo (MCMC) slice procedure implemented within the MATLAB® software. In addition, two procedures for the Bayesian model application are illustrated; namely Cascaded regression and Cholesky decomposition. Both procedures are demonstrated to produce replications that are consistent with the Bayesian model realizations, and capture the parameter correlations without the need to store the set of parameter realizations. The proposed Bayesian approach is ideal for modeling multi-agent systems in which each agent has its own unique set of parameters. Finally, the fourth part of the dissertation introduces and validates a state-of-the-art behavioral modeling framework that can be used as a tool to simulate driver behavior after the onset of a yellow indication until he/she reaches the intersection stop line. The behavioral model is able to track dilemma zone drivers and update the information available to them every time step until they reach a final decision. It is anticipated that this behavioral model will be implemented in microscopic traffic simulation software to enhance the modeling of driver behavior as they approach signalized intersections.

ACKNOWLEDGEMENTS

All praise is due to Allah, our lord. I thank him for giving me the guidance, patience, and determination to finish this work. I hope and pray that this work will find its way to being a little step towards helping all humanity live better lives.

With all words full of gratitude and appreciation, I would like to thank my advisor, Dr. Hesham Rakha, who generously supervised this dissertation, for his valuable guidance and continuous support, academically and financially. His friendly personality, calm character, and valuable input were my most important resource in the past four years. Dr. Rakha provided extensive guidance toward all the chapters of this dissertation. He also aided in the analysis carried out in Chapters 5 and 8, and in the concepts discussed in Chapters 7, 8 and 9. In addition, many thanks and deep appreciations are due to my co-advisor, Dr. Ihab El-Shawarby, for his sincere support, attention, discussion and warm encouragement. Dr. El-Shawarby supervised the preparation, organization and implementation of the data collection experiment illustrated in Chapter 4. He also aided in the analysis carried out in Chapters 5 and 6. I would like also to thank Dr. Vicki Lewis, Dr. Antoine Hobeika, and Dr. Montasir Abbas; who kindly agreed to serve as members on my dissertation committee.

The experimental effort in this work was sponsored by grants from the Virginia Transportation Research Council (VTRC), SAFETEA-LU funding, and the Mid-Atlantic Universities Transportation Center (MAUTC). In addition, deep recognition is given to all my colleagues at the Center for Sustainable Mobility for their continuous encouragement and cooperation. I specially acknowledge the support of Yu Gao, Sangjun Park, Aly Tawfik (my academic career companion since 1997), Sashikanth Gurram, Stephanie Shupe, Maha El-Metwally, Molataf Al-Aromah, and the Center for Technology Development at VTTI for running the tests. I would like also to thank Dr. Abdel-Salam G. Abdel-Salam for providing valuable comments in the statistical analysis in Chapters 5 and 6.

All my appreciations are due to all my family members back home; my parents, my sister, my parents-in-law, and my sisters-in-law; whom I am missing all the time. I specially dedicate this work to my mother and my father, and hope it would make them feel proud of their son. Last but not least, my warm feelings and affection go to my beloved wife, Maha, the mom-to-be, for her continuous care and sacrifice. She always endures my tempers and accommodates me in the hard times.

Ahmed Amer

TABLE OF CONTENTS

LIST OF FIGURES

LIST OF TABLES

CHAPTER 1 INTRODUCTION

Traffic signals were introduced to the highway system infrastructure in order to regulate the movement of vehicles traveling in conflicting directions at roadway intersections. In order to provide a smooth transition between the various movements during different signal phases, a yellow interval is provided at the conclusion of each green indication. According to the Manual on Uniform Traffic Control Devices (MUTCD) [1], "*the yellow signal indication warns the vehicles that their green movement is being terminated and a red signal indication will be exhibited immediately*".

Upon the onset of a yellow indication, a driver has a choice set of two alternatives; the first is to come to a safe and complete stop before the stop line, whereas the second is to continue moving with the approaching speed or accelerate to or even beyond the speed limit in order to clear the intersection before the onset of the red indication. Several problems are associated with the yellow interval arising from the incompatibility between the obligations a driver faces, either to stop safely or to proceed before the red indication. These obligations are influenced by the technical feasibility of the vehicle kinematics and behavioral attributes of the driver.

The onset of a yellow indication is typically associated with the risk of vehicle crashes resulting from dilemma-zone and red-light-running problems. Such risk of vehicle crashes is greater for high-speed signalized intersection approaches, whose speed limit is greater than 30 mph. In general, the driver is considered to be trapped in a dilemma zone, if at the onset of yellow, the driver's perceived distance to the intersection is neither greater than the distance required for safe stopping, nor less than to the distance required to run, and, in some jurisdictions clear the intersection before the yellow indication ends. It was reported, based on the General Estimates System (GES) of the NHTSA that in 1999 and 2000, there were 523,000 and 545,000 crossing crashes, respectively, at signalized intersections nationwide, and about 45% of which involved different injury levels [2].

Alternatively, another definition for the dilemma zone is the zone from the point beyond which 90 percent of the drivers would stop to the point at which only 10 percent of the drivers would stop [3]. In general, the dilemma zone is defined either in time or space. If the driver decides to stop when he/she should have proceeded, rear-end crashes could occur. While if the driver proceeds when he/she should have stopped, he/she would run the red light and a right-

angle crash with side-street traffic could occur. In 2001, approximately 218,000 red-light-running crashes occurred at signalized intersections in the United States. These crashes resulted in nearly 181,000 injuries and 880 fatalities and an economic loss of 14 billion dollars [4].

1.1 PROBLEM STATEMENT

Driver behavior while approaching high-speed signalized intersections at the onset of a yellow indication varies as a function of many parameters. Some of these parameters are related to the driver's attributes; for example, age, gender, perception-reaction time (PRT), and the safe acceptable acceleration/deceleration rates the driver is willing to exert to either run or stop. Other parameters are related to the intersection; e.g., approaching speed, distance and time to the intersection at the onset of the yellow indication, and the maximum acceleration/deceleration rates the vehicle kinematics permit. Nevertheless, the current traffic signal timing guidelines assume that the driver dilemma zone is fixed (ranging between 5.5 to 2.5 s from the intersection), considering a 1.0 s PRT (85^{th} percentile PRT) and a deceleration rate of 3.0 m/s^2 (10.0 ft/s^2) [5, 6, 7]. However, it is not clear how driver PRT and accepted deceleration rates vary as a function of the driver characteristics (age, gender, etc.), intersection characteristics (approaching speed, speed limit, time-to-intersection, etc.), and roadway surface conditions. Consequently, there is a need to enhance the yellow timing design guidelines to reflect various driver behavior attributes and intersection configurations.

Moreover, several research efforts have attempted to address the dilemma zone problem using various Intelligent Transportation System (ITS) strategies. These strategies include, but are not limited to, green-extension and green-termination systems [8, 9], Detection-Control Systems (D-CS) [10, 11, 12], LHOVRA (where each letter—L, H, O, V, R, and A—represents a function of operation) and Self Optimizing Signal (SOS) system [13, 14, 15]. Even though most of the dilemma zone mitigation systems account for the average intersection-related variables, they still assume constant values for the driver-specific variables. Such an assumption does not consider the variations among different drivers approaching the yellow indication.

Furthermore, one of the most attractive applications in the ITS Strategic Research Plan of the U.S. Department of Transportation (U.S. DOT) ITS research plan is the IntelliDrive^{SM} initiative, formerly known as the Vehicle Infrastructure Integration (VII) initiative [16]. Overall, the IntelliDrive^{SM} Systems Initiative explores the potential for using ITS to bring connectivity to

transportation through advanced wireless technologies that enable safe, interoperable networked wireless communications among vehicles, the infrastructure, and users' personal communications devices. The deployment of the IntelliDrive[SM] initiative requires developing and introducing various applications including safety applications that have the potential to reduce crashes through advisories and warnings, such as dilemma zone and red-light running warnings.

1.2 RESEARCH OBJECTIVES

Based on the above discussion and in light of the current deficiencies in modeling driver behavior, the research effort presented in this dissertation attempts to enhance the modeling of driver behavior at the onset of a yellow indication at high-speed traffic signalized approaches. In order to fulfill this goal, intersection field data were collected based on a designed experiment and used to address the specific objectives listed hereinafter.

1. Design and conduct an intersection controlled field experiment on the Virginia Smart Road facility in order to collect driver behavior data that will serve as the main data source for the analyses carried out in this dissertation.
2. Characterize the impacts of the different surrounding parameters on the driver stop-run decision at the onset of a yellow indication as well as the driver yellow/red light running behavior for those drivers who decide to run the yellow light.
3. Characterize the stochastic nature of driver stopping behavior attributes, including PRT and deceleration level, at the onset of a yellow indication as a function of various driver characteristics (age and gender), surrounding traffic stream characteristics (alone, following, or leading), and time to intersection (TTI) at the onset of the yellow.
4. Develop a new and novel framework for computing yellow indication durations that accounts for the stochastic nature of driver behavior and provides the designer with a level of design reliability, and introduce an extension for the framework that can serve within the IntelliDrive[SM] initiative to provide customizable driver-specific change interval warnings.
5. Develop an agent-based Bayesian statistical stop-run decision model that captures the stochastic variations of different drivers as a function of the surrounding variables, and introduce a model application procedure that captures parameter correlations without the need to store all parameters realizations.

6. Develop a novel behavioral modeling framework for modeling driver deliberation at the onset of yellow indication at high-speed signalized intersections that tracks vehicle motion through the intersection approach and can be implemented within microscopic simulation software and can be used to test the dilemma zone mitigation strategies.

1.3 RESEARCH SCOPE

As discussed earlier, the scope of the analysis presented in this dissertation covers high-speed signalized intersection approaches. This stems from the fact that driver behavior associated with low-speed intersections may be different from that at high-speed intersections. For instance, drivers at low-speed intersections would adopt lower deceleration levels in order to stop compared to those applied at high-speed intersections. Furthermore, due to budget limitations, the data collection effort carried out for the analysis is limited to capturing driver behavior for light-duty vehicles only, without consideration of heavy-duty vehicles in the traffic composition. In addition, the field testing was executed during daylight clear and dry weather conditions. The experiment also extends to consider the car-following effect on the driver behavior, whether following, leading or driving alone, while approaching the intersection at the onset of yellow. Nevertheless, the experiment did not account for the lane changing effect, as the testing was carried out on a single lane approach.

1.4 RESEARCH CONTRIBUTIONS

The research presented in this dissertation has many unique contributions to the body of knowledge related to traffic signal systems and driver characteristics. The dissertation first begins by thoroughly investigating the previous research efforts related to driver behavior at signalized intersections, and offers an in-depth synthesis of the relevant literature (Chapter 2).

The research constructs a unique dataset of signalized intersection controlled field data, with more than 3,000 yellow time approaching trials, each includes a complete tracking of data every deci-second of the subject vehicle within approximately 150 m (500 ft) before and after the intersection (Chapter 4).

Furthermore, the dissertation develops a complete characterization of driver behavior at the onset of a yellow indication, including the driver stop-run decision, yellow/red light running behavior, and stopping behavior attributes (PRT and deceleration behavior). The characterization

comprises empirical analysis and statistical modeling of the variables versus the different surrounding attributes (Chapter 5 and Chapter 6).

The research then develops a novel procedure for the computation of the traffic signal clearance interval that accounts for the reliability in the design. This procedure also captures individual driver attributes (age and gender) on the required clearance time and thus is suitable for the integration within the IntelliDrive^{SM} initiative (Chapter 7).

Moreover, a state-of-the-art agent-based Bayesian statistical modeling framework for the driver stop-run decision is developed in order to capture individual personal differences. The application of this Bayesian modeling framework requires extensive computing capabilities to store the model parameter realizations. However, the dissertation introduces a novel procedure to apply the model utilizing two mathematical techniques to enable the model to store only 14 parameters making the framework easily implementable within traffic simulation software (Chapter 8).

Finally, the dissertation outlines the general framework for an agent-based behavioral modeling structure that is capable of simulating the complete driver behavior while approaching an intersection approach from the instant of the onset of yellow to the instant the driver reaches the intersection stop line. The behavior framework can track the dilemma zone drivers and update the information available to them every time step until they reach a final decision (Chapter 9).

1.5 DISSERTATION LAYOUT

After this introduction chapter, an extensive review of the literature relevant to different topics covered in the dissertation is presented in Chapter 2. Thereafter, Chapter 3 sheds light on the different tasks that are proposed in order to fulfill the objectives of the dissertation, in addition to the techniques and methods used in the adopted analysis approach are discussed. Chapter 4 provides the details of the experimental design and the available datasets for the analysis. Thereafter, Chapter 5 and Chapter 6 present the characterization of the different driver behavior attributes, namely stop-run decision, yellow/red light running behavior (Chapter 5), PRT and deceleration level (Chapter 6). Furthermore, the details of the proposed yellow timing procedure and the clearance interval lookup tables are presented in Chapter 7. The agent-

based Bayesian stop-run decision model then is calibrated in Chapter 8, along with the adopted model application techniques. Afterwards, Chapter 9 presents the general framework of the proposed behavioral model and its different components. Finally, Chapter 10 provides the overall conclusions drawn from the dissertation as well as recommendations for further research.

CHAPTER 2 LITERATURE REVIEW

2.1 INTRODUCTION

As mentioned in Chapter 1, the dissertation attempts to characterize the different aspects and issues related to the driver behavior while approaching high-speed signalized intersections at the onset of yellow indication. There is a diversity of research efforts that have addressed different aspects and issues, and that have attempted to present various ITS strategies to address the problems associated with the onset of yellow. Examples of these problems are the dilemma zone trap as well as the red-light running violation. Accordingly, this chapter sheds light on relevant literature concerned with driver behavior at the onset of a yellow indication at high-speed signalized intersections, and its corresponding aspects and issues. First, the chapter starts with the driver-related parameters, namely PRT and deceleration behavior, and how they are affected by the surrounding variables. Then, it moves to the stop-run behavior and the issue of option and dilemma zone with the problems associated with it and its different mitigation strategies. Finally, the chapter discusses red-light running behavior, its underlying factors, and the various enforcement techniques.

2.2 DRIVER-RELATED PARAMETERS

2.2.1 Perception-Reaction Time

As discussed earlier, PRT is an important component of the driver behavior while approaching signalized intersections. In the context of this research, PRT is defined as the time elapsed between the onset of the yellow indication and the instant the driver started to press the brake pedal.

In general, PRT is of significant importance in highway design. For example, it is used to estimate the stopping sight distance in the computation of horizontal and vertical profiles in highway design [17] and as well used in the calculation of the yellow interval duration in traffic signal design [18]. As argued earlier, at the onset of a yellow- indication transition on high-speed signalized intersections, each driver has to decide either to stop safely or to proceed through the intersection before the end of the yellow interval. Accordingly, the proper design of traffic signals requires the computation of a yellow interval that entails an estimate of the driver PRT. The state-of-practice in different dilemma zone alleviation strategies typically recommends a 1.0

s PRT, which is assumed to equal or exceed the 85th percentile brake PRT [19]. However, a number of studies have demonstrated that brake PRTs are much longer than 1.0 s and that the 85th percentile PRT is more in the range of 1.5 to 1.9 s [20]. These studies have also demonstrated that the PRTs on high-speed intersection approaches (greater than 64 km/h) are lower, with 85th percentile PRTs in the range of 1.1 to 1.3 s. Nevertheless, the driver behavior during the yellow interval is a problem that has been examined in the literature since 1960 by Gazis et al. [21]. In their paper they examined the driver behavior in response to the onset of a yellow indication. That study measured the drivers braking reaction time on the basis of 87 observations and was found to have a mean of 1.14 s.

A review of the fundamental concepts associated with reaction times provides a better understanding of the factors related to PRT and driver behavior at the onset of yellow and within a dilemma zone. When a driver responds to a sensory input, such as the onset of a yellow light at a traffic signal, the total PRT can be split into a mental processing time (the time required for the driver to perceive the sensory input and to decide on a response) and a movement time (the time used to perform the programmed movement, such as lifting the foot from the accelerator and touching the brake). It is worth mentioning here that these PRT times can be greatly affected by driver's level of distraction, either cognitive or visual. However, the effect of distraction is outside the scope of this study. Because the mental processing time is an internal quantity that cannot be measured directly and objectively without a physical response, it is usually measured jointly with the movement time [22]. In the case of a driver arriving at a signalized intersection when the indication changes from green to yellow, the time interval from the onset of the yellow light to the instant when the brake pedal is pressed is called the *perception-reaction time* [18, 23], *perception response time* [24], *brake reaction time* [22, 25], *perception-braking response time* [26], *yellow response time* [27], or *brake-response time* [28]. The present research will refer to it as the PRT. Another interesting study by Doerzaph [29] put together the different reaction time components that were reported across the literature, as listed in Table 1. Doerzaph also presented the overlap of those various components in temporal and spatial domains, as presented in Figure 1.

Table 1: Description of Reaction Time Components across Literature [29]

Component		Description
Time to accelerator release	TAR	Time from initial stimulus appearance to beginning of accelerator release.
Time to steering	TS	Time from initial stimulus appearance to initiation of steering input.
Time to severe steering	TSS	Time from initial stimulus appearance and initiation of a severe steering input. While no set definition is available, lateral acceleration values over 0.2g caused by steering can be considered moderate.
Time to brake	TB	
Time to full brake	TFB	Time from the stimulus until the brake pedal was fully depressed.
Transition time from accelerator to brake	TSAB	Time from the beginning of accelerator release to the point where the foot was positioned over the brake.
Transition time from accelerator to full brake	TSAFB	Time from the beginning of accelerator release until the foot fully depresses the brake.
Transition time from brake to full brake	TSBFB	Time from initiation of braking to full braking.
Time to initial driver action	TIDA	Time between stimulus and first subject action performed.
Time from glance to driver action	TGDA	Time between the driver's first glance at the stimulus and the first action performed.
Time to full stop	TFS	Time to come to a full stop measured from initial stimulus appearance.

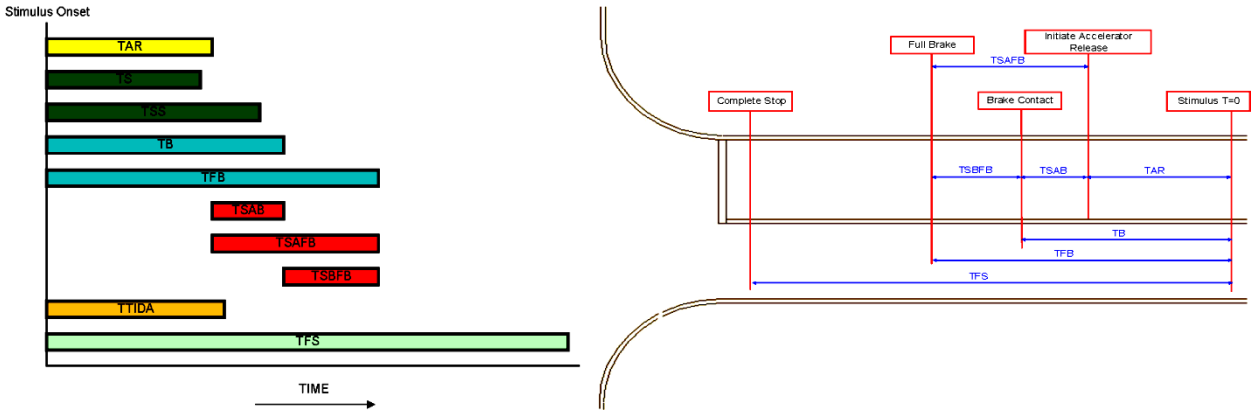

(a) Temporal Presentation (b) Spatial Presentation

Figure 1: Temporal and Spatial Presentation of Reaction Time Components [29]

Furthermore, Taoka [20] stresses that PRTs measured under anticipatory conditions, when drivers are aware that their PRTs are recorded, are shorter than the expected values under normal driving conditions. In a comprehensive survey which summarized PRT results from most

studies published until 2000, Green [22] classified PRT studies into three basic types: simulator studies, controlled road studies, and naturalistic observations. Controlled road studies and naturalistic observation are both field approaches but differ in the sense that, in the latter, the driver is unaware of the data collection effort. Each type of study has limitations to the degree in which results can be generalized to normal driving conditions. PRT measurements from driving simulators are typically shorter than those measured in vehicles because simulators typically have simplified visuals, smaller fields of view, no depth, no non-visual cues, and small cognitive loads. Although some may argue that the cognitive load is higher in simulators. Controlled-road studies may also produce shorter PRT measurements because drivers may be more alert than in normal driving conditions. Both simulator and controlled-road studies create practice effects because of the many trials used to gather data for each driver. Alternatively, naturalistic studies have the highest validity, but are also limited because it is not possible to test effects of independent variables, place drivers in emergency or even urgent situations, measure perception and movement times separately, or control driver demographics to avoid sample bias [22].

Wortman and Matthias [30] used a time-lapse camera to study driver behavior at six intersections in the Phoenix and Tucson, AZ metropolitan areas. They observed a mean PRT of 1.3 s with 85^{th} percentile times ranging from 1.5 to 2.1 s. PRTs at traffic signals also include some lag time because the onset of the yellow does not always require immediate braking reaction unless the driver is close to the intersection. In a study by Chang et al. [27], seven intersections were observed and driver PRTs (defined as "the time elapsed from the onset of the yellow until the brake light is observed") were recorded, this lag should be small or nonexistent on high-speed signalized approaches because the high speed requires immediate reactions to avoid excessive deceleration or even collisions with other vehicles. The study focused on the effect of the distance from the intersection at the onset of a yellow indication because, according to its authors, drivers tend to react faster as vehicles move closer to the intersection; when vehicles are farther away, the PRT might be longer because the urgency to make a decision is not as great. Accordingly, the study produced curves demonstrating significant variability in driver PRT as a function of the vehicle speed (different lines represent speeds in km/h) and distance to intersection (DTI) at the instant the traffic signal turned yellow, as illustrated in Figure 2. In addition, the present dissertation demonstrates that if the x-axis were replaced with the time-to-intersection instead of distance-from-intersection, the lines approach one another (Figure 2).

Consequently, it appears that TTI would be a better explanatory variable because it combines two explanatory variables, as will be demonstrated later in the consequent chapters. The results of Chang et al. study suggest that speed effectively influences the median PRT, which converges to 0.9 s at speeds equal to or greater than 72 km/h (45 mi/h). Other research efforts have also considered the use of TTI as an explanatory variable [31, 32]. Another study [33] that used a driving simulator to analyze the behavior of 77 drivers approaching signalized intersections at 70 km/h concluded that the TTI significantly affected the PRT whereas age did not. The PRT grand mean was 0.96 s, ranging from 0.86 s for drivers closest to the intersection stop line to 1.03 s for drivers farthest from it [33].

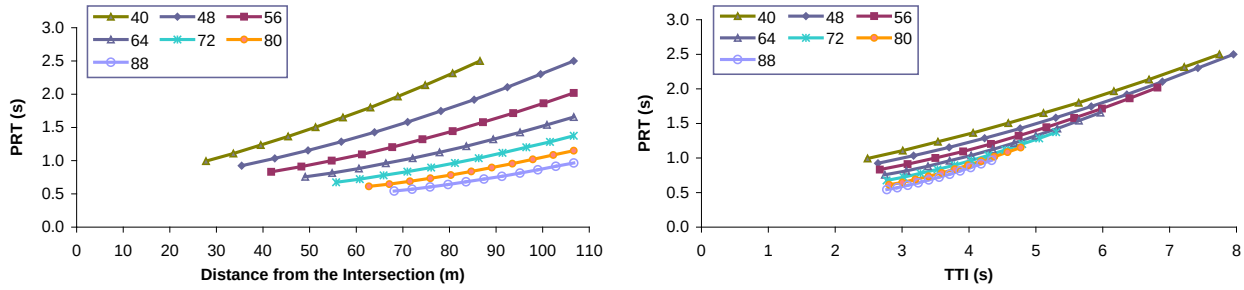

Figure 2: Driver PRT based on Distance and Time to Intersection and Approach Speed (Based on [27])

In order to overcome the effect of the distance from the intersection on the PRT at the yellow indication onset, Diew and Kai [26] used a transitional (dilemma) zone, defined as the zone in which drivers are required to make a decision quickly or be forced to cross. Drivers before the transitional zone must stop at the intersection (because they cannot legally cross); drivers after the transitional zone must cross the intersection. The transitional zone was defined in terms of the TTI, measured as the actual travel time for those vehicles that crossed the intersection and as the projected travel time for those that stopped. For the three intersections analyzed in Singapore in this study [26], the dilemma zone was defined as lying between 4.2 and 2.3 s from the intersection stop bar. PRT was defined as the time elapsed from the yellow indication onset until the brake lights became visible. PRT values found for the transitional zone were 0.84 s (median), 0.86 s (mean), 0.64 s (15^{th} percentile), and 1.08 s (85^{th} percentile), following a log-normal distribution; this finding is consistent with other studies [20]. In another paper [24], the authors reported shorter reaction times at intersections with red light surveillance cameras: 0.80 s for the median and mean and 1.00 s for the 85^{th} percentile.

Another recent study by Gates et al. [28] recorded vehicles behavior at six signalized intersections in the Madison, WI area comprising 463 first-to-go and 538 last-to-go records. The analysis of the brake-response time first-to-stop vehicles showed that the 15^{th}, 50^{th}, and 85^{th} percentile brake-response times were 0.7, 1.0, and 1.6 s, respectively.

2.2.2 Deceleration Behavior

Deceleration characteristics of drivers, at the onset of a yellow- indication transition on high-speed approaches to a signalized intersection, affect appropriate yellow-phase timing because the length of the yellow indication should be sufficient for drivers to either stop safely or to proceed through the intersection before the end of the yellow interval. Driver deceleration rates play a critical role in most traffic simulation software and vehicle fuel consumption and emission models. Also intersection and deceleration lane design are governed by vehicle rates of acceleration and deceleration.

Early in 1960, Gazis et al. [21] examined the driver behavior in response to yellow signal phasing. In their study, they suggested a method to calculate the time required to stop a vehicle at a speed of 72 km/h (45 mi/h) assuming a deceleration rate of 4.9 m/s^2 (16 ft/s^2). On the other hand, Williams [32] suggested in his study at an intersection in Connecticut that 2.95 m/s^2 (9.7 ft/s^2) was the average maximum deceleration rate of stopping for vehicle speeds of 16.1 to 40.2 km/h (10 to 25 mi/h), while Parsonson and Santiago [34] reported that 3 m/s^2 (10 ft/s^2) was a more reasonable value for the deceleration rate based on a study of 54 intersection approaches in four counties in the southeastern United States.

Wortman and Matthias [30] conducted a study at a total of six intersections in metropolitan areas in Phoenix and Tucson, AZ. They found that the mean deceleration rate ranged from 2.1 m/s^2 (7.0 ft/s^2) to 4.2 m/s^2 (13.9 ft/s^2) with a mean value of 3.5 m/s^2 (11.6 ft/s^2) for all observations at posted speed limits that ranged from 48.3 to 80.5 km/h (30–50 mph). Another project by Wortman et al. [35] was undertaken and further field studies were conducted at four intersections. Again, the results revealed considerable variation in the traffic characteristics with mean intersection approach speeds ranging from 57.6 to 76.4 km/h (35.8 to 47.5 mph). The mean deceleration rates for the intersections in the later study ranged from 2.5 m/s^2 (8.3 ft/s^2) to 4 m/s^2 (13.2 ft/s^2).

According to the study by Chang et al. [27], in which the driver behavior to traffic signal change intervals at seven intersections were observed, the mean driver deceleration rate for passengers cars approaching at speeds higher than 32 km/h (20 mi/h) was 2.9 m/s^2 (9.5 ft/s^2) and the median was 2.8 m/s^2 (9.2 ft/s^2). The study concluded that driver-selected deceleration rates were affected by the approach speed, the distance to the intersection at the yellow onset, the time available to reach the stop line after the yellow onset, and the distance traveled during the yellow response time. Similar to those curves produced for PRT in Figure 2, curves for deceleration level were produced, and x-axis was replaced with the time-to-intersection instead of distance-from-intersection, as shown in Figure 3. Similar behavior is observed for vehicle decelerations,, however, in the case of vehicle deceleration levels the effect of speed still appears to be significant.

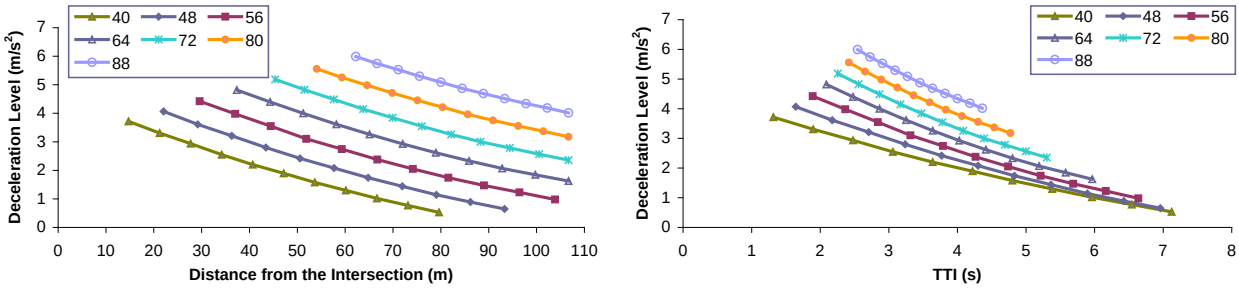

Figure 3: Driver Deceleration Level based on Distance and Time to Intersection and Approach Speed (Based on [27])

Furthermore, Bennett and Dunn [36] conducted a study to monitor vehicle deceleration behavior at the exit ramp on a freeway in New Zealand. While their approach did not identify the deceleration rates of individual drivers, the plotted data of vehicle speed versus time showed a wide range of observed speeds for the decelerated vehicles, which implies a wide range of deceleration rates.

Haas et al. [37] reported in their study the deceleration and acceleration rates observed at rural stop-sign controlled intersections in southern Michigan. The study analysis seemed to indicate that drivers show wide variability in rates of deceleration and acceleration and that the initial speed accounted for about 18% of the variation in deceleration rates while each of the other factors (driver demographics and time-of-day) accounted for only about 5% of the variation. Wang et al. [38] studied the deceleration behaviors for passenger cars at stop-sign controlled intersections on urban streets based on in-vehicle global positioning system (GPS)

data. They found that the recommended maximum deceleration rate of 3.4 m/s^2 (11.2 ft/s^2) was applicable to most drivers with 92.5% of the measured deceleration trips having maximum deceleration rates less than 3.4 m/s^2 (11.2 ft/s^2) and 87.6% of the deceleration trips having maximum deceleration rates less than 3 m/s^2 (10 ft/s^2).

The performance of 77 participants (older and younger drivers) while approaching signalized intersections at an approach speed of 70 km/h (42 mi/h) when traffic signals changed from green to yellow was measured by Caird et al. [33] using a moderate-fidelity driving simulator. The study found that older driver deceleration rates (3.7 m/s^2) were significantly lower than younger age group deceleration rates (4.2 m/s^2). Another study by Hicks et al. [39] at nine intersections in Maryland, found that driver stopping/passing behavior and vehicle speed performance in response to a yellow-light interval were affected by the driver's gender and age and found that vehicles with higher enter or initial speed, if stopped, were more likely to experience a sharp stop, using deceleration rates greater than 3.4 m/s^2 (11.2 ft/s^2).

A recent study [28] analyzed vehicle behavior upstream six signalized intersections in the Madison, WI area at the start of a yellow interval. First-to-stop vehicles approaching at speeds > 64.4 km/h (40 mi/h) applied greater deceleration levels than those approaching at speeds ≤ 64.4 km/h (40 mi/h). The analysis of the deceleration levels for first-to-stop vehicles showed that the 15^{th}, 50^{th}, and 85^{th} percentile deceleration levels were 2.19, 3.02, and 3.93 m/s^2 (7.2, 9.9, and 12.9 ft/s^2), respectively. A deceleration level of 3.05 m/s^2 (10 ft/s^2) was the 69^{th} percentile and the 26^{th} percentile for vehicle approach speeds of > 64.4 km/h (40 mi/h) and ≤ 64.4 km/h (40 mi/h), respectively. In another study by El-Shawarby et al. [40], a field data collection effort funded by the Federal Highway Administration (FHWA) collected data on 60 subjects approaching a signalized intersection at the Virginia Department of Transportation's (VDOT) Smart Road facility. The results indicated that mean deceleration levels vary from 2.2 m/s^2 (7.2 ft/s^2) for the longest time to stop-line (5.6 s) to 5.9 m/s^2 (19.4 ft/s^2) for the shortest time to stop-line (1.6 s), demonstrating that drivers use more time to decelerate if they are sufficiently away from the intersection. Statistical analyses demonstrated that male drivers appear to show slightly higher levels of deceleration when compared to female drivers and increases as the trigger time to stop-line decreases. Younger drivers (under 40-years-old) and older drivers (60 years of age or older) exhibit greater deceleration levels when compared to drivers in the 40 to 59 age group [40].

2.3 DRIVER BEHAVIOR AT THE ONSET OF YELLOW

2.3.1 Dilemma Zone and Option Zone

The yellow signal interval is designed to warn approaching drivers of an impending loss of right-of-way for the traffic crossing a signalized intersection in the previous green signal phase. When a yellow indication is triggered, the driver decides whether to stop safely or to proceed through the intersection before the end of the yellow interval. Incorrect driver decisions may result in either a rear-end collision, if the driver fails to come to a safe stop, or a straight crossing-path crash, if the driver does not have enough time to safely cross the intersection before the conflicting flow is released.

The dilemma zone problem has been examined in the literature since its initial formulation by Gazis et al. [21], that observed the existence of dilemma zones at approaches to signalized intersections and developed the first dilemma zone model, as a binary decision problem to either stop or proceed when a yellow indication is triggered. According to Gazis et al. [21], the dilemma zone is defined as "*a situation in which a driver may neither be able to stop safely after the onset of yellow indication nor be able to clear an intersection before the end of the yellow duration*". Accordingly, the yellow interval dilemma is considered as an example of the incompatibility of man-made laws and physically attainable human behavior [21].

Nevertheless, an analysis of the literature demonstrates a lack of consensus in defining the dilemma zone. For example, Sheffi and Mahmassani [41] define the dilemma zone as "*that zone within which the driver can neither come to a safe stop nor proceed through the intersection before the end of the yellow phase*". This definition represents the design definition of a dilemma zone. Senders [42] demonstrated for a specific signalized intersection that a design dilemma zone existed in which a driver traveling at the speed limit had no feasible option and would have to break the law. Alternatively, Zegeer [3] defines the dilemma zone from a driver's perspective as "*the zone in which between 10 to 90 percent of the drivers stop*". Sheffi and Mahmassani [41] summarize the approach to modeling this problem as developing dilemma zone curves of "percent drivers stopping" versus "distance from stop bar" at the instant when the signal indication changes from green to yellow and that the driver behavior at high speed signalized intersections when faced with a yellow indication can be viewed as a binary choice process, where the relevant decisions are either to stop or proceed through the intersection [41]. Research has shown that dilemma zone protection can help reduce crashes at high speed

signalized intersections. For example, Parsonson [43] developed detector-controller solutions for the dilemma zone problem at high speed signalized approaches by establishing option zone boundaries within the range of 10 to 90 percent probability of stopping for various speeds.

Furthermore, it is important to describe the different situations that the driver encounters while approaching the intersection at the onset of a yellow indication; namely the dilemma and option zones. An earlier study by El-Shawarby et al. [44] summarized the difference between dilemma and option zones, stating that the driver's approach speed and distance from a signalized intersection at the onset of a yellow indication affect his/her stop/go decision. Drivers can either come to a safe stop if they are far enough from the intersection or clear the intersection if they are close enough to the intersection. The inability to perform either option successfully is attributed to a shortcoming in the design of the signal timings and is termed the design dilemma zone [41]. This dilemma zone is created when the minimum stopping distance (d_s) is greater than the maximum running (clearing) distance (d_r) which is the distance within which the vehicle can clear the intersection before the end of the yellow interval. The stopping distance, which is a function of the vehicle's speed; the driver's PRT; and an acceptable deceleration rate, is defined as the distance required for a vehicle to come to a complete stop upstream of the intersection stop line by considering the braking, aerodynamic, rolling, and grade resistance forces as in Equation (1).

$$d_s = v\,t + \frac{\gamma_b W}{2g\,k_a}\ln\left[1+\frac{k_a v^2}{\eta_b \mu W + f_{rl} W \pm WG}\right] \quad (1)$$

where d_s is the distance required for a vehicle to stop at the stop line (m),
v is the speed of the approaching vehicle (m/s),
t is the driver PRT (s),
γ_b is the mass factor accounting for moments of inertia during braking (recommended 1.04),
W is the vehicle weight (N),
g is the gravitational acceleration (9.81 m/s^2),
k_a is the aerodynamic coefficient ($k_a=\rho/2C_DA_f$),
ρ is the air density kg/m^3,
C_D is the drag coefficient,
A_f is the vehicle's frontal area (m^2),
η_b is the braking efficiency,
μ is the coefficient of roadway adhesion,
f_{rl} is the rolling coefficient ($f_{rl} \approx 0.01(1+v/44.73)$),

G is the roadway grade (decimal).

Typically the aerodynamic and the rolling resistance forces are ignored and the stopping distance is computed as

$$d_s = v\,t + \frac{v^2}{2g\left(\eta_b \mu \pm WG\right)} = v\,t + \frac{v^2}{2d \pm 2gG} \tag{2}$$

where d is the deceleration rate (m/s^2).

Equation (2) is typically used in the literature to compute a vehicle's stopping distance and this equation is identical to the ITE formula that is used in yellow interval calculation [45, 46], as shown in Equation (3).

$$y = t + \frac{v}{2\left(d \pm gG\right)} \tag{3}$$

where y is the duration of the yellow interval (s).

On the other hand, a vehicle that is closer than d_s from the stop line when the yellow is displayed will not have sufficient distance to decelerate to a stop before reaching the stop line. In this case, the driver has to clear the intersection at the speed limit before the yellow interval ends. Considering the approach speed, the running distance required for a vehicle to enter the intersection prior to the end of the yellow interval is computed in Equation (4).

$$d_r = v \cdot y \tag{4}$$

where d_r is distance required for a vehicle traveling at v to reach the stop line (m).

A vehicle should be able to safely come to a stop or proceed through the intersection before the end of the yellow interval. An option zone is defined as the zone within which the driver can safely come to a stop during the signal yellow interval and also can clear the intersection during the same interval. Figure 4 illustrates the definition of option and dilemma zones that a driver faces when approaching a high-speed signalized intersection. When a vehicle approaches an intersection during a yellow warning interval, if $d_s < d_r$ and if the vehicle is farther than d_s or closer than d_r such that $d_s < d < d_r$, then an option zone exists where a driver can choose between stopping and clearing the intersection. If $d_s > d_r$ and the vehicle is placed between them such that $d_r < d < d_s$, then a design dilemma zone exists where a vehicle can neither stop nor clear the intersection.

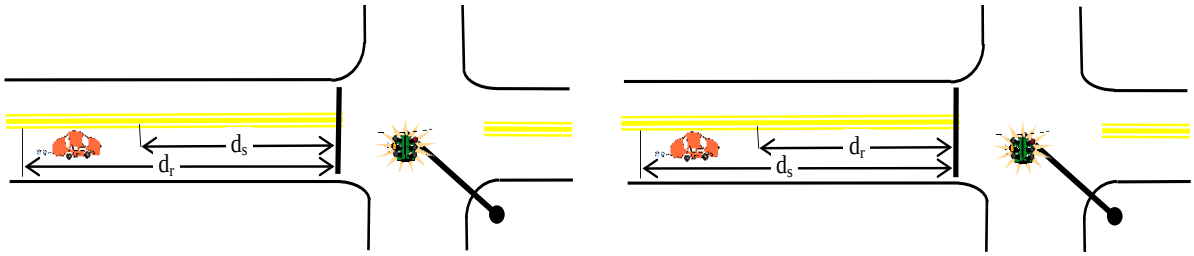

(a) Option Zone $d_s < d_r$ (b) Dilemma Zone $d_s > d_r$

Figure 4: Option and Dilemma Zones at Signalized Intersection [44]

An interesting illustration for dilemma and option zones was presented in another paper [47], that summarizes the situations the driver encounters at the onset of a yellow indication as represented by the approach speed and the distance from the stop line for different yellow times, as shown in Figure 5. The figure is divided into 4 zones; running, stopping, option, and dilemma zones. It can be seen that increasing the yellow time could free many drivers from being trapped in the dilemma zone. In comparison to this illustration, the current research composed a similar relationship by varying the deceleration level from 0.31*g* (3 m/s^2) to 0.51*g* (5 m/s^2), as illustrated in Figure 6. The figure demonstrates that a driver encounters a dilemma zone if they travel faster than the design speed. The driver may avoid the dilemma zone by decelerating at a more aggressive level.

2.3.2 Dilemma Zone Mitigation Strategies

Furthermore, reviewing the different strategies that are adopted for eliminating drivers from being trapped in dilemma zone is worthy, in order to shed some light on the gaps in the current state-of-practice. A comprehensive review by Li [48], summarizes these various mitigation strategies as listed hereinafter.

Multi-detector Green Extension System (GES): that extends the green, by placing several advance detectors, to allow fast vehicles to clear the dilemma zone and ends the green before slow vehicles enter the dilemma zone.

Microprocessor Optimized Vehicle Actuation System (MOVA) [49]: that has three kinds of detectors; IN, EXIT, and OUT detectors, to count the vehicles between the stop bar and the EXIT detector, and between the IN and the EXIT detectors in each lane, to end the green based on comparing the “benefits” of preventing vehicles from being caught in the dilemma zone and the possible delay caused by ending the green.

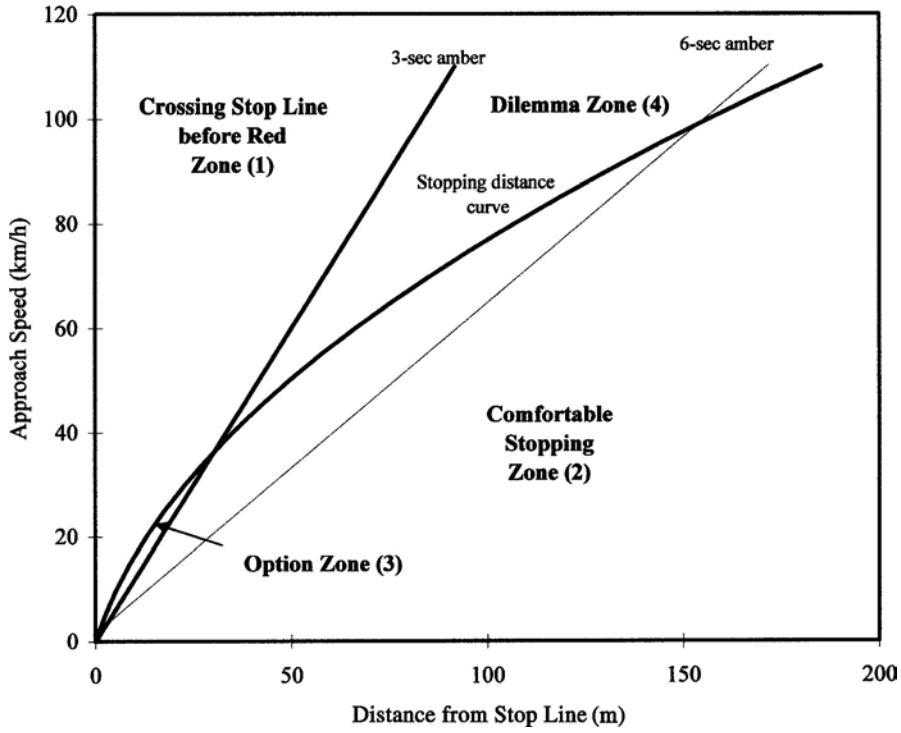

Figure 5: Driver's Situations at the Onset of Yellow for Different Yellow Times [47]

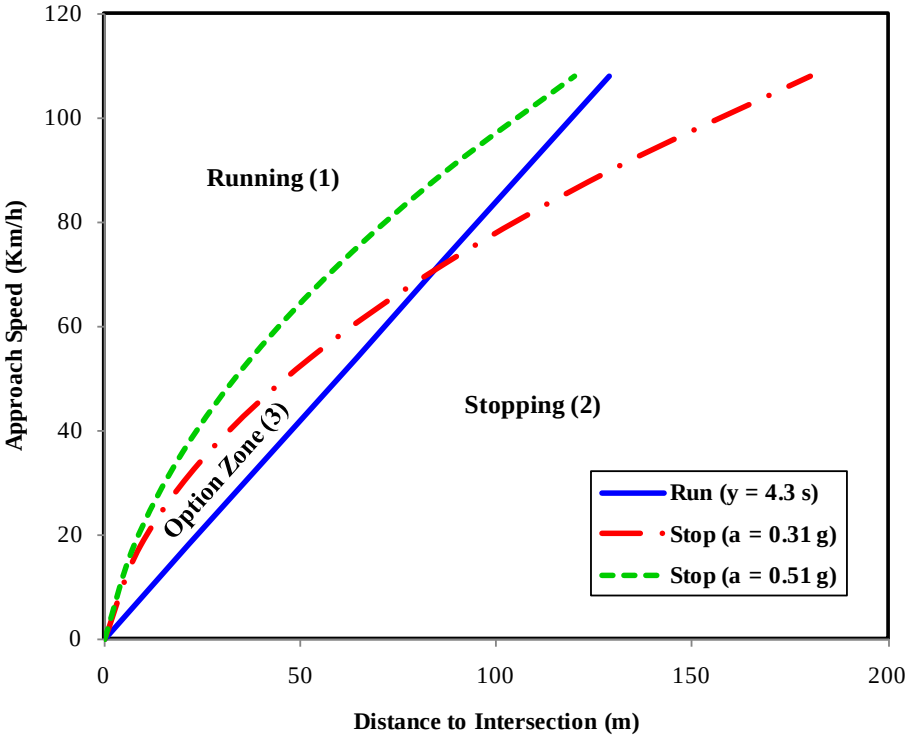

Figure 6: Driver's Situations at the Onset of Yellow for Different Deceleration Levels

LHOVRA [13, 15]: that is the acronym of six function modules: truck priority (L), primary road priority (H), accident reduction (O), variable amber (V), control of red-light running (R) and changes of mind at all-red (A), from which module O minimizes the number of vehicles caught in the dilemma zone by extending the green, whereas module L holds the green if a truck is detected until it leaves the dilemma zone.

TTI Truck Priority System [50]: that is similar to LHOVRA and developed by TTI, which can even override the controller phasing and hold the phase longer than maximum green until the trucks leave the dilemma zone.

Self-Optimizing Signal System (SOS) [14]: that is also called "green termination system", and is similar to LHOVRA except module O, where the decision whether to end the green is made by comparing the possible dilemma zone-associated benefits and the possible control delay.

Advance Detection with Advance Warning Flasher (AWF) [51]: that flashes the advance warning flashers for three seconds, when the green duration reaches the maximum green and an approaching vehicle is detected, and it can provide dilemma zone protection for those vehicles at speeds up to 81 mi/h at 65-mi/h intersections.

Advance Warning Systems for End of Green Phase System (AWEGS) [52, 53]: that is designed to supplement the green extension systems, by using additional "two-detectors speed trap" and having a fail-safe design, which divides all possible scenarios into three levels; both speed trap detectors fail, one of the detectors fails, or both detectors work.

Detection-Control System (D-CS) [10, 11, 12]: that uses a two-detector speed trap at 300 m upstream of the intersection to detect and measure the speed of individual vehicles, and assuming a constant dilemma zone, defined by TTIs ranging between 5.5 and 2.5 s. Then, it implements a 2-step gap-out strategy to reduce the probability of max-out and thus reduce the probability of trapping vehicles in the dilemma zone.

Platoon Identification Accommodation System (PIA) [54]: that provides "green preemption" for approaching traffic platoons, with advance detectors and installed PIA program that monitors approaching vehicles all the time and, if certain conditions are satisfied, sends a low-priority preemption request to the controller to end the red or extend the green.

Furthermore, Li and Abbas in 2010 [55] proposed a dilemma hazard model that assigns a hazard weight for each vehicle in the dilemma zone according to its position and speed at the onset of yellow, which can be used as a safety measure for dilemma zone protection systems.

A survey questionnaire of practitioners within state DOTs was conducted in 2007 by Jones and Sisiopiku [56], in order to identify efforts to address operational and safety issues associated with two mitigation strategies; green extension and advance warning. Out of 60 surveys were mailed out, 27 respondent agencies were obtained. The survey indicated that advanced warning was perceived effective by DOTs not using any mitigation strategies, whereas green extension was found more effective by those using such strategies. In addition, potential obstacles to deploy such strategies are liability, equipment-related issues, training of maintenance personnel, and cost.

2.3.3 Driver Stop-Run Decision

Driver behavior on high-speed signalized intersection approaches in response to yellow phasing has been studied for many years. For example, Shinar and Compton [57] observed the aggressive driving behavior of more than 2000 drivers over a total of 72 hours in the immediate proximity of an intersection or an interchange at six different sites with posted speed limits ranging from 70 to 80 km/h (43 to 50 mi/h). The study concluded that aggressive driving is associated with both situational variables and individual characteristics, men were more aggressive than women, young drivers (less than 45-years-old) were more aggressive than older drivers, and the presence of passengers was associated with lower rates of aggressive driving. Furthermore, the performance of 77 participants (older and younger drivers) while approaching signalized intersections at 70 km/h (43 mi/h) when traffic signals changed from green to yellow was measured by Caird et al. [33] in Calgary, Canada using a moderate-fidelity driving simulator. They found that older drivers (55 years of age and older) were significantly less likely to stop than those in the younger age groups at the longest time to stop-line and those older drivers who chose to go through the yellow light were more likely to be in the intersection when the light changed to red.

Another study by Hicks et al. [39] at nine intersections in Maryland found that driver stopping/passing behavior and vehicle speed performance in response to a yellow-light interval were affected by multiple factors. Driver’s gender, age, and the use of cellular phones were

found to be significant human factors affecting driver behavior and vehicle speed at intersections during yellow intervals. The study also concluded that the initial position of a vehicle when a yellow-light phase is displayed significantly affects drivers' stopping/passing behavior. The decision of stopping or proceeding through the yellow light is related to the distance to the intersection, the travel time to the stop bar, and the approach speed. Another recent study by Gates et al. [28] evaluated the behavior of vehicles trapped in the dilemma zone; defined by the authors to be between 2.0 and 5.5 s. The study can be classified as a naturalistic observation study that recorded vehicles behavior at six signalized intersections in the Madison, Wisconsin area comprising 463 first-to-go and 538 last-to-go records. The analysis showed that the TTI was found to be, by far, the strongest variable affecting the stop/go decision among all other factors. Drivers were found to be more likely to stop rather than to go with greater TTI.

On the other hand, drivers are typically indecisive within the option zone and thus respond differently during the signal change interval. A driver approaching a signalized intersection while the traffic signal changes from green to yellow has two alternatives, either to stop at the intersection or to continue to clear the intersection before the signal turns red. A driver in such a situation is experiencing a state of uncertainty and anxiety because he/she has to evaluate many parameters before taking his/her final decision. An equation to measure the degree of uncertainty to help characterize the difficulty of choosing between different alternatives in a choice situation was proposed by Yager [58] as in Equation (5).

$$A = 1 - \int_{0}^{\alpha_{\max}} \frac{1}{|A_{\alpha}|} d\alpha \tag{5}$$

where A is the degree of uncertainty (anxiety measure),
A_{α} is the number of alternatives whose probabilities are greater than α.

This measure attempts to capture the uncertainty that one experiences in selecting an alternative. Consider a decision in which we must choose from a collection of alternatives. The degree of uncertainty is lowest when the choice is clear, this situation occurs when only one alternative is supported and all other alternatives are not supported, i.e. one element has a probability of one and all other elements have a probability of zero. Uncertainty increases as more elements get support and are not equal to zero, here we are faced with the problem of choosing among some equally good solutions. A greater degree of uncertainty occurs in situations when we have no support for any of the alternatives and all the elements have a

probability near to zero. In this case, we must choose among all equally bad alternatives. In the case of only a two-choice situation, such as our case "stopping" or "running," equation, Equation (5), for the measurement of uncertainty, as introduced by Kikuchi et al. [59] and Yager and Kikuchi [60], is reduced to

$$A = 1 - \max(P_s, P_r) + \frac{1}{2}\min(P_s, P_r) \quad (6)$$

where P_s is the probability of stopping,
P_r is the probability of running.

The uncertainty measure is equal to 0 when one of the two probabilities is equal to one and the other is zero, and is equal to 0.75 when the value of the two probabilities are both equal to 0.5. This means that uncertainty is lowest when the probability of only one action is fully supported while the other is not, and is highest when the probability of the two conflicting actions are equal, indicating that either action is equally possible and only one has to be chosen.

2.3.4 Red-Light Running

Many studies were conducted in order to capture the parameters affecting the driver red light running behavior, as well as to introduce and evaluate different mitigation strategies for the red light running problems, such as red light enforcement cameras.

In another recent study, two methods for reducing red light running were evaluated at two intersections in Philadelphia, PA [61]. The first method involved extending the yellow duration by one second; demonstrating a reduction in the red light violation rates between 21 to 63% at all sites. The second method involved the installation of red light running cameras; reducing the violation rates by 87 to 100%. The paper confirmed that adequate yellow duration timing is important for reducing red light running. However, red light running remains a problem that can be reduced further through the use of camera enforcement.

In 1999, Retting et al. [62] employed a before/after design in order to evaluate the influence of red light camera (RLC) enforcement on red light violation in Oxnard, CA. The design comprised 14 intersections, of which nine were camera sites, three were non-camera sites, and two were control sites. On the camera sites, RLC is triggered when any vehicle passes over a stop bar sensor faster than a preset minimum speed of 15 mph and after 0.4 s after red. On the non-camera and control sites, an observer was assigned to apply the same criteria to the red light running. They found that the red light violations in both camera and non-camera sites were

reduced by approximately 42% with no significant difference. In another study in 1999, Retting et al. [63] examined the prevalence of red light running crashes across the United States on cities with high rates of fatal crashes, were two databases were employed in this paper; the Fatality Analysis Reporting System (FARS) data and the General Estimates System (GES) data. The analysis indicated that red light runners were more likely to be young males and to be fatally injured in red light crashes than non-runners. In addition, fatally injured red light runners were much more likely to have high blood alcohol concentrations and to have been driving with suspended or invalid driver's licenses. Regarding time of day, younger males make up a greater percentage of red light runners in nighttime crashes than in daytime crashes.

In another study by Porter and England [64], a forward stepwise logistic regression model was calibrated, based on trained human observer data collected at six intersections located in three cities in Virginia, in order to test explanatory variables of yellow-light versus red-light runners. The recorder variables were time to green change; signal indication when last vehicle crossed the stop bar, driver sex, use of safe belt, estimated driver age, ethnicity group, direction traveled, and estimated model year; with a total of 5,112 last drivers were collected, of which only 3,785 were observed entering on yellow or red. The model showed that city, time, safety belt use and ethnicity were the most significant variables; i.e. unbuckled and non-Caucasian drivers were more likely to run red lights.

Another paper by Bonneson and Son [65] calibrated a statistical model that can be used to project the red light running frequency for any given intersection, based on 6-hr traffic follow data on approaches of five different intersections. The authors categorized the red light running behavior based on three criteria; traffic movement type, entry time after onset of red, and motivation of driver's decision to run the red light, and they focused only on the through moving drivers who run the red light unavoidably during the first few seconds after the onset of red, because the fact that this group of drivers is the most treatable by the enforcement and the engineering countermeasures. The variables included in the analysis were approach flow rate, cycle length, yellow interval duration, percentage of heavy vehicle, running speed, clearance path length, platoon ratio, approach grade, number of approach lanes, use of LED signal indication instead of bulb indication, use of signal head back plates, use of advance detection, and signal head mounting. The analysis revealed that significant relationships exist between red light running frequency and yellow interval duration, use of signal head back plates, speed,

clearance path length, and platoon ratio. The calibrated model with the estimated variables coefficients is as presented as

$$E[R] = \frac{Q}{C}\frac{1}{0.927}\ln\left[1+e^{\left(2.30-0.927T-0.334B_p+0.0435V-0.0180L_p+0.220R_p\right)}\right] \quad (7)$$

where $E[R]$ is expected red-light-running frequency (veh/h)

Q is approach flow rate (veh/ h)

C is cycle length (sec)

T is average travel time before red-light running can occur (sec)

$= p_x Y + (1-p_x)\max\left[Y, \frac{D}{V}\right]$

p_x is probability of phase termination by max-out

= 1.0 if pre-timed or actuated without advance detection

Y is yellow interval duration (sec)

D is distance between stop line and most distant upstream detector (ft)

V is average running speed (mph)

B_p is presence of signal head back plates (1 if present, 0 if not)

L_p is clearance path length (ft)

R_p is platoon ratio = Q_e/Q

Q_e is phase end flow rate (veh/h)

The paper suggested that the model can be used to evaluate the effectiveness of different countermeasures addressing the red light running problem, before introducing these measures to an intersection. These measures include increasing the cycle length, increasing the yellow duration, adding advance detection, adding back plates, changing the speed limit, and adjusting platoon arrival time and concentration. In addition, the authors concluded that higher frequencies of red light running are associated with approaches with higher approach speeds as well as those with platoons concentrations near the phase end, and also less red light running is associated with intersections with wider cross streets as well as those with signal heads back plates.

Furthermore, in 2003, Lum and Wong [47] tried to address the results of a before/after study in order to evaluate the impacts of installing and operating RLCs at three intersections in Singapore. The collected data included red running violations and their after-red times, volumes, speeds, and the timings and status of each signal phase, beside the geometry, traffic characteristics, and signal control. The results indicated a drop in the number of daily red running violations at approaches installed with RLC while there were mostly increases at the non-camera approaches. The red runners were grouped according to after-red time into three

levels; Type I (after-red times up to 2 s), those caught in the dilemma zone whose right-angle collisions risk is fairly low, Type II (after-red times between 2 and 5 s), those deliberately beat the red signal, whose collisions risk is reasonably low, and Type III (after-red times more than 5 s), those unconsciously cross the intersection and whose actions are potentially hazardous to other road users. The presence of the RLC reduced the share of Type II and III violations. It was found also that drivers were more inclined to run the red at weekends as they crossed the stop line at a much later after-red time.

One more paper that investigated the effect of installing RLC systems on 15 signalized four-legged intersections in Singapore was presented by Huang et al. [4]. The paper argued that although the use of RLCs reduces the right-angle collisions, there would be potential increase in the rear-end collisions. The variables included in the analysis were intersection width, presence of RLC, cycle time, ratio of green to cycle time, time of day, distance to stop line, estimated time to stop line, estimated time to cross intersection, and being leader or follower. A multinomial logit model was calibrated and showed that the presence of RLC reduces the number of would-be red runners as well as reduces the time that red runners cross into the red, whereas the presence of RLC increases the rear-end collision probability, at intersections with speed higher than 40 km/h.

Recently in 2008, Retting et al. [61] evaluated two methods used to reduce red light running violations at six approaches of two intersections in Philadelphia, PA; first, extending yellow duration by one second, and introducing red light cameras several weeks later. The results showed that the yellow duration extension reduced the red light violation rates between 21 to 63% at all sites, while the RLC enforcement reduced the violation rates additional 87 to 100%. Nevertheless, it was argued that extending yellow time may not eliminate the need for red light camera enforcement.

One last study by Yang and Najm [66] presented an interesting comprehensive review of the different factors affecting the red light violation across the literature as summarized in Table 2.

Table 2: Review Summary of Factors Affecting Red Light Violation [66]

Group	Factor	Key Findings
Driver	**Age**	• The older age groups accounted for a relatively small portion of red light running crashes compared to the young age group. • Younger drivers between the ages of 18 to 25 years old are more likely to run red lights compared to other age groups. • Red light runners tend to be drivers under 30 years old.
	Gender	• Red light runners are more likely than non-runners to be male.
	Occupancy	• Drivers have a higher probability of running red lights when driving alone compared to when passengers are in their vehicles.
	Seat-Belt	• Red light runners are less likely to wear seat belts.
	Driving Record	• Red light runners are more likely than non-runners to be driving with suspended or revoked driver's licenses. • Drivers with poor driving records and driving smaller and older cars have a higher tendency to run red lights.
Intersection	**Signal Timing**	• The frequency of red light running increases when the yellow interval < 3.5 s. • Longer yellow intervals will cause drivers to enter the intersection later and lengthening the all-red intervals caters to red light violators.
	Stopping Distance	• Probability of a vehicle stopping for a traffic light decreases as its distance from the intersection decreases.
	Approach Speed	• Probability of a driver stopping for a traffic light decreases as the approach speed to the intersection increases.
	Intersection Width	• Drivers tend to stop for traffic lights more at wider intersections than at narrower intersections.
Traffic and Environment	**Approach Volume**	• Higher red light running rates were observed in cities with wider intersections and higher traffic volumes. • The red light running frequency increases as the approach traffic volume at intersections increases.
	Time of Day	• Higher red light violations occur during the time period of 3 PM to 5 PM.
	Day of Week	• There are more red light violations on weekdays compared to weekends.
	Weather	• The influence of rainfall on red light running behavior is insignificant.

2.4 SUMMARY AND CONCLUSIONS

This chapter presented a review of the literature relevant to the different driver behavior topics. The reviewed literature showed that there are many research efforts that address the driver behavior at the onset of yellow indication. Nevertheless, there are still some gaps that have not been thoroughly investigated yet. Examples of the areas that have these gaps are the stochastic nature of the driver-related attributes; namely PRT and deceleration behavior, and how to incorporate this stochastic nature within the characterization and the modeling of driver behavior, as well as into the design of the clearance intervals. In addition, there is a need to have a novel framework that is able to simulate the driver behavior within the dilemma/option zones, while considering the stochastic nature of that behavior. Accordingly, this dissertation attempts

to fill some of these gaps, by fulfilling the objectives listed in Chapter 1, for the sake of better understanding of the driver behavior.

CHAPTER 3 ANALYSIS APPROACH

As mentioned earlier in Chapter 1, the goal of this research initiative is to develop a better understanding of driver behavior while traveling on high-speed signalized approaches at the onset of a yellow indication. This goal includes a number of specific objectives in order to develop statistical and behavioral modeling frameworks of driver behavior at the onset of yellow indication at high-speed signalized intersections. This chapter describes the analysis approach adopted in order to achieve these specific objectives and describes the overall research plan. The adopted analysis approach is outlined in the flowchart shown in Figure 7. This research plan is divided into several tasks. The description of the different tasks is presented hereinafter.

3.1 CONDUCT LITERATURE REVIEW

A literature review is conducted to determine previous research efforts the different topics addressed in the present research. Those topics are first, driver-related parameters, including PRT and deceleration behavior; second, driver behavior at the yellow onset, including dilemma zone and option zone, dilemma zone mitigation strategies, driver stop-run decision, and red-light running. This task is already presented in Chapter 2.

3.2 EXPERIMENTAL DESIGN AND DATA COLLECTION

An experimental effort is designed in order to collect intersection field data in order to serve as the main data source for the analyses carried out in this research. The experiment is carried out on the Virginia Smart Road facility. It is worth mentioning here that this study is considered as phase II of an earlier study that collected similar data and was sponsored by Federal Highway Administration (FHWA). The experimental design task consists of some sub-tasks that are listed below. Detailed description of this task and its subtasks is presented in Chapter 4.

3.2.1 Institutional Review Board Approvals

In order to be able to conduct an experiment that includes human subjects, it is mandatory to comply with the human subject protection guidelines. This requires obtaining detailed approvals from the Institutional Review Board (IRB), before recruiting participants.

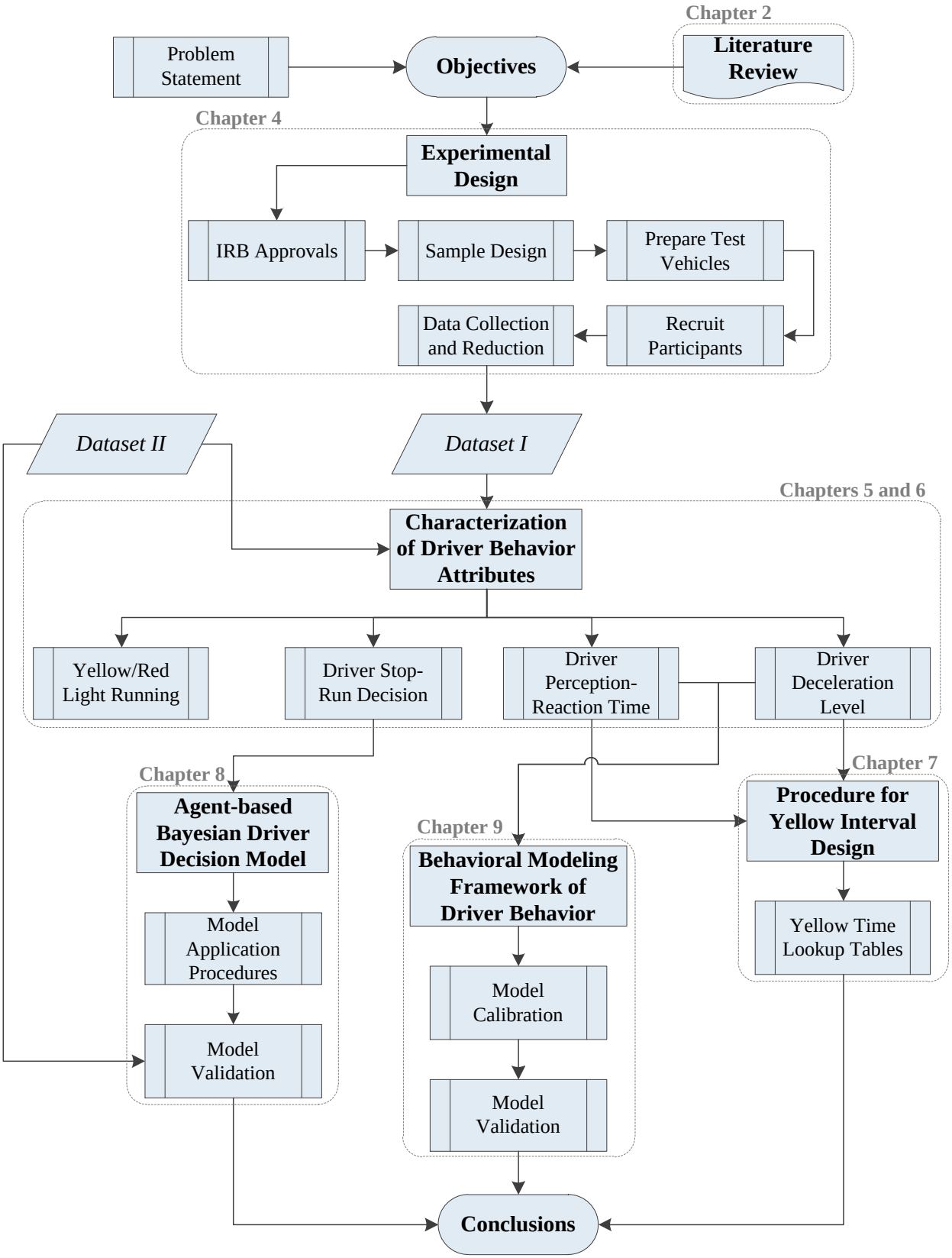

Figure 7: Flowchart of the Adopted Analysis Approach

3.2.2 Sample Design

In this task, the structure of the experiment sample is designed in order to fulfill two objectives. First is to include most variables of interest, such as driver's demographics. Second is to match the sample structure adopted in the phase I study to enable extending the results and comparisons from it.

3.2.3 Prepare Test Vehicles and Equipment

After obtaining the IRB approvals, the next task is to equip the vehicles that are used for the experiment with a Data Acquisition System (DAS) and to develop a program for coding and storing the collected data, as well as for enabling communication between the test vehicles and the intersection infrastructure.

3.2.4 Recruit Participants and Collect Data

After having everything ready, the next step is to recruit the experiment subject according to the designed sample criteria and in compliance with the IRB approvals. The recruited test subjects are then scheduled for different driving sessions on the Smart Road and their driving data is collected beside their demographics.

3.2.5 Data Reduction and Preparation

The last subtask in the experimental design is to transfer the collected data from the DAS and store it securely on a data server. The stored data then is decoded and reduced to eliminate excessive redundancy and to focus on the variables of interest to the research. Finally, the reduced data is exported into different data format and become ready for analysis.

3.3 CHARACTERIZATION OF DRIVER BEHAVIOR ATTRIBUTES

After having the available datasets from both experiments ready for analysis, the first step in modeling the driver behavior at the onset of yellow is to characterize the different attributes associated with it. This characterization is carried out in order to serve as an input for the next tasks. The various attributes to be characterized are summarized in the following list. The detailed results of the characterization of driver behavior attributes are presented in Chapter 5 and Chapter 6.

3.3.1 Yellow/Red Light Running Behavior

In this task, the distribution of the stopping probabilities of the different drivers in the datasets is investigated, and then the analysis investigates the running behavior of the drivers who decided to proceed through the intersection at the onset of yellow. Some of these drivers were able to hit the stop line before the end of the yellow and those are the yellow time runners, whereas those drivers who failed to cross the stop line before the start of red indication are the red light runners.

3.3.2 Driver Stop-Run Decision

In this step, logistic linear regression models are calibrated to the driver stopping probability versus the different surrounding variables. The logistic regression models are then used to carry out sensitivity analysis of the different explanatory variables.

3.3.3 Driver Perception-Reaction Time

The PRTs of those drivers who decided to stop at the onset of yellow is characterized at this point. First, the distribution of the PRTs is investigated versus the different variables and the corresponding statistical tests were conducted to measure the significance of these variables. Then, a stepwise linear regression model is calibrated for estimating the PRT as a function of the independent variables.

3.3.4 Driver Deceleration Level

Similar to the analysis made to the PRTs, the distribution of deceleration levels of those drivers who decided to stop at the onset of yellow is investigated versus the different variables and the corresponding statistical tests that were conducted to measure the significance of these variables. Subsequently, a stepwise linear regression model is calibrated to estimate the deceleration levels as a function of the independent variables.

3.4 DEVELOPMENT OF NEW YELLOW INTERVAL DESIGN PROCEDURE

Based on the results of the characterized variables from the previous task, a need for a new procedure for the design of the yellow interval is argued, in order to account for the variations among different drivers. The corresponding subtasks summarized below utilize the Monte Carlo simulation techniques in developing the new procedure. Furthermore, the details of the new yellow timing procedure are presented in Chapter 7.

3.4.1 Impacts of PRT and Deceleration on Yellow Interval

The impact of the variations in the PRT and the deceleration levels among different drivers on the computation of the required yellow duration is investigated versus the currently used constant values.

3.4.2 Impacts of Gender and Age on Yellow Interval Design

Having different PRTs and deceleration levels among different drivers' age and gender groups directly affects the calculation of the required yellow time. Accordingly, the effect of the different age and gender groups is analyzed and the technique to incorporate age and gender into the yellow design procedure is addressed.

3.4.3 Development of Lookup Tables for Yellow Clearance Intervals

A set of lookup tables is developed in this subtask, in order to provide an example application of the new proposed yellow time design procedure. These tables are developed based on the impacts of the surrounding variables addressed in the previous subtasks.

3.5 AGENT-BASED STOCHASTIC MODELING OF STOP-RUN DECISION USING BAYESIAN STATISTICS

In this task, the concept of Bayesian statistics is adopted in order to develop an agent-based stochastic approach for the modeling of driver stop-run decision and to compare the stochastic modeling behavior. The proposed approach can capture the parameter correlations without the need to store all parameter combinations. This task is presented in-detail in Chapter 8, and the corresponding subtasks are listed hereinafter.

3.5.1 Calibration of an Agent-Based Bayesian Driver Decision Model

In this subtask, the Bayesian statistics approach is used to calibrate an agent-based driver stop-run decision model. The Markov Chain Monte Carlo (MCMC) slice algorithm built in the MATLAB® software is used to calibrate the Bayesian model parameter realizations.

3.5.2 Application and Validation of the Agent-Based Bayesian Driver Decision Model

Two mathematical approaches are adopted in order to simplify the application of the Bayesian model to capture the stochastic nature of the driver decision. The proposed application approaches are Cascaded regression and Cholesky decomposition and enable applying the Bayesian model without the need for intensive storage capabilities to store the model parameter

realizations. Furthermore, the Bayesian model is validated using the available datasets from the two experiments.

3.6 BEHAVIORAL MODELING FRAMEWORK OF DRIVER BEHAVIOR

This task introduces a novel state-of-the-art behavioral model that can be used as a tool to simulate driver behavior after the onset of a yellow indication until he/she reaches the intersection stop line. This tool can be used for testing new signal timings and dilemma zone mitigation strategies before actual implementation, and could be also implemented in traffic simulation software to enhance its modeling capability. The model framework and its details are presented in Chapter 9.

3.6.1 Development of the Behavioral Model Framework

The overall framework of the proposed behavioral model and the logic behind that framework are presented. The different components of the model are illustrated and the ability of the model to simulate and track the dilemma zone drivers until they reach a final decision is discussed.

3.6.2 Calibration and Validation of the Behavioral Model

An effort to characterize the behavioral model components and to validate the model using different Monte Carlo (MC) simulation scenarios is made. The validation results then is discussed and compared to the results of the statistical model calibrated earlier.

CHAPTER 4 EXPERIMENTAL DESIGN AND AVAILABLE DATA

4.1 INTRODUCTION

As mentioned earlier, the data required to fulfill the objectives of the present research is provided by two field experiments that was conducted on Virginia Smart Road with designed samples of drivers. One experiment was conducted earlier in the spring of 2005. Alternatively, the other experiment was conducted in the summer of 2008, and was considered an extension to the dataset. This new dataset includes more variables and more runs encountering a green indication. Nevertheless, it should be noted here that conducting the new experiment is intended to be a part of the analysis methodology of this dissertation. Accordingly, most of the analyses made in this dissertation are based mainly on the results of the new experiment. The present chapter gives an overview of the different details of the new experiment, with a brief overview on the old experiment. The details include the sample structure, the experiment procedures, as well as the resulting available datasets for the analysis.

4.2 DEVELOPMENT OF A FRAMEWORK FOR EVALUATING YELLOW TIMING AT SIGNALIZED INTERSECTIONS STUDY

As mentioned earlier, this new experiment was conducted in the summer of 2008 as part of the "Development of a Framework for Evaluating Yellow Timing at Signalized Intersections" study [67]. The design of this experiment, including test facility, test vehicles, and the test subjects, is presented hereinafter.

4.2.1 Roadway Layout

The VDOT's Virginia Smart Road at the Virginia Tech Transportation Institute (VTTI) was the site of the field test. The Smart Road is a unique, state-of-the-art, full-scale research facility for pavement research and evaluation of Intelligent Transportation System (ITS) concepts, technologies, and products. The Smart Road is a 3.5 km (2.2 miles) two-lane road with one four-way signalized intersection and a high-speed banked turnaround at one end and a medium-speed flat turnaround at the other end. Access to the Smart Road is controlled by electronic gateways, making the test facility a safe location to conduct field tests.

The section of the Smart Road used for the data collection includes only the section between the high-speed turnaround and marker 108 (where a second turnaround is located) with

a four-way signalized intersection, as shown in Figure 8 and Figure 9. The horizontal layout of the test section is fairly straight with some minor horizontal curvature which does not impact vehicle speeds. The vertical layout of the test section has a substantial grade of 3%. The details of how the vertical profile was generated are described by Rakha et al. [68]. Because participants turned around at the end of each run, half the trials were on a 3% upgrade and the other half were on a 3% downgrade.

Figure 8: Layout of the Testing Site on Virginia Smart Road (Source: Google Earth)

Figure 9: Signalized Intersection at Testing Site

4.2.2 IRB Procedures

In order to start recruiting participants to run the designed experiment, approvals must be obtained from the IRB office at Virginia Tech. The process of obtaining these approvals requires the following steps:

1. Obtain conditional approval for initial project activities.
2. Receive the IRB Initial Review template approval (VTTI IRB Coordinator).
3. Submit the IRB Initial Review application.
4. Supply necessary forms and applications, including:
   - Sample Flyer and Newspaper Advertisement
   - Driver Screening Questionnaire
   - Informed Consent Form
   - On-Site Health Screening Questionnaire
5. Make revisions requested by the IRB

After going through all these procedures, the IRB approval was obtained in April 2008 for one year and was renewed again in 2009 and 2010. In addition, the IRB required that the entire research team attend a human subject training course and receive a completion certificate.

4.2.3 Intersection and Test Vehicles Equipment

The designed experiment required communication between the intersection control cabinet and the subject car through a programmed wireless communication interface (Figure 10). In addition, three vehicles were used in the study, one was driven by test participants (accompanied by the in-vehicle experimenter) and the other two vehicles were driven by two research assistants. A 2004 Chevrolet Impala (Figure 11) was driven by the test participants as the subject car. The vehicle was instrumented with additional equipment that included a Differential GPS (DGPS), a real-time Data Acquisition System (DAS), and a computer to run the different experimental scenarios. The data recording equipment had a communications link to the intersection signal control box that synchronized the vehicle data stream with changes in the traffic signal controller. The DAS contained within the vehicle was custom built by the Center for Technology Development at VTTI. The DAS was located inside the trunk in a custom durable mounting case for accurate measurement and out of the view of the test subject (Figure 11). One of the other two vehicles leads or follows the subject car as a confederate car

(1997 Ford Taurus; Figure 12), whereas the other car services as the side-street traffic. All three vehicles were equipped with a communications system between vehicles, operated by the research assistants.

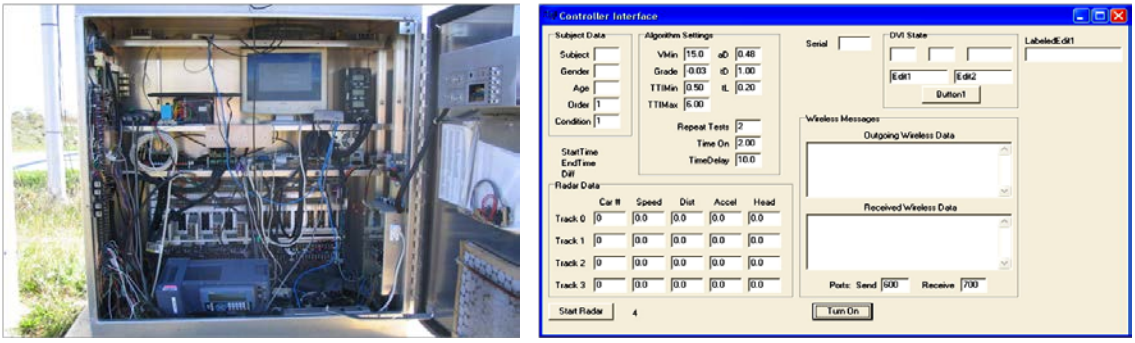

Figure 10: Wireless Communication Interface in the Intersection Signal Cabinet

Figure 11: DAS and Communication Interface in the Subject Car

Figure 12: Communication Interface in the Confederate Car

4.2.4 Participants

Participants were licensed drivers recruited from the VTTI participant database, word-of-mouth, posters, and through ads in the local Blacksburg, VA newspaper. Participants were screened through a verbal telephone questionnaire to determine if they were licensed drivers and if they had any health concerns that would exclude them from participating in the study. Six pilot participants were recruited to run pilot sessions for the purpose of training research team, testing vehicle equipment, validating collected data, and adjusting the most appropriate yellow trigger distances. After finishing the pilot sessions and having the yellow distances chosen, twenty-four drivers were recruited in three equal age groups (under 40-years-old, 40 to 59-years-old, and 60 years of age or older); equal numbers of males and females were assigned to each group.

4.2.5 Procedures

There were two main steps to the makeup of this study. The first step involved determining eligibility and obtaining an informed consent from the participant. The second step involved the Smart Road test-track driving portion of the study, which required six sessions, once per day, where each participant was assigned to six different test conditions. The different test conditions were based on two instructed vehicle speeds of 72.4 km/h (45 mi/h) and 88.5 km/h (55 mi/h) and three platoon conditions (leading, following, and no other vehicle). The various conditions were run in predetermined randomized orders, with a different order for each participant. Each participant was assigned to the entire six test conditions (sessions), one test condition per day, taking approximately 1.5 hours per session to complete.

Participants drove loops on the Smart Road, crossing a four-way signalized intersection where the data were collected. Exclusive of practice trials, the participant drove the entire test course 24 times for a total of 48 trials, where a trial consists of one approach to the intersection.

Each participant was tested individually. Among the 48 trials, there were 24 trials in which each yellow trigger time to stop-line occurred four times. On the remaining 24 trials the signal indication remained green. This scheme would result in yellow/red signals being presented on 50 percent of the 48 trials; conversely, 50 percent of intersection approaches would consist solely of a green indication. To examine whether willingness to stop varies with speed, the onset of yellow was based on the time-to-stop line (between 2.0 s and 4.6 s) at the instructed speed rather than on distance from the stop line. Radar was used to determine vehicle distance from the intersection. Outputs from the radar triggered the phase change events.

Upon arrival at VTTI, each participant was asked to review and sign an informed consent form. In addition, each participant was asked to complete a medical questionnaire to verify that he/she was not under the influence of any drugs or alcohol and did not have medical conditions that would impair his/her ability to drive. Subsequently, the participant was escorted to the test vehicle. After familiarizing himself/herself with the test vehicle (e.g., adjusting mirrors, seat, fastening seat belt), the participant drove to the Smart Road with the in-vehicle experimenter (who was present at all times during the study to provide instructions, supervise the operation of the computer system, and answer questions as necessary). Before the first trial, the participant drove two loops (four intersection passes or four trials) to allow the participant to familiarize himself/herself with the vehicle and the Smart Road. During the drive to the first turn-around, the participant was asked to accelerate and brake several times to ensure that he/she was familiar with the vehicle's handling characteristics under hard braking. On each of the four practice trials, the participant was asked to cruise the road at the instructed speed of 72.4 km/h (45 mi/h) or 88.5 km/h (55 mi/h). If a participant drove more than 8 km/h (5 mi/h) above or below the instructed speed he/she was asked to drive at the instructed speed. The participant was told that maintenance vehicles will occasionally be entering and leaving the road via a standard signalized intersection. These maintenance vehicles were the confederate vehicles driven by trained experimenters who were involved in the study. The participant was asked to follow all normal traffic rules and to obey all traffic laws. After each trial run the participant was reminded of the instructed speed at the turnaround that followed the trial if they exceeded or failed to reach the instructed speed.

Three vehicles were used, one was driven by test participants (accompanied by the in-vehicle experimenter) and the other two vehicles were driven by two researchers. The first

confederate vehicle was either leading or following the test vehicle to investigate the effect of the presence of a lead or following vehicle on the participant's driving behavior. The second confederate vehicle (this vehicle was felt to be a necessary addition to the scenario to simulate real-world conditions) crossed the intersection from the conflicting approach when the traffic light was green. All three vehicles were equipped with a communications system, operated by the research assistants and the Smart Road control tower.

During each session the participant was assigned to one of the platoon conditions (leading, following, or no other vehicle). In the leading platoon condition, the participant's vehicle was followed by the first confederate vehicle. The confederate vehicle maintained a 2-second headway which is equivalent to a 40 m (130 ft) spacing at a speed of 72.4 km/h (45 mi/h) and a 50-meter (163 ft) spacing at the 88.5 km/h (55 mi/h) instructed speed. In the following platoon condition, the participant driver followed the first confederate vehicle. The participant was asked to follow the confederate vehicle at a 2-second headway which is equivalent to 8 car lengths at the 72.4 km/h (45 mi/h) instructed speed and 10 car lengths at the 88.5 km/h (55 mi/h) instructed speed. In the *no other vehicle present* condition, there was no leading or following confederate vehicle traveling in the same direction as the participant or approaching the participant in the opposing lane. Only the second confederate vehicle was crossing the intersection from the conflicting approach when the traffic signal was red for the test vehicle.

During the test runs the participants drove a distance of 1.6 km (1 mile) going downhill to approach the intersection followed by a 0.5-kilometer (0.3 mile) leg to a high-speed turnaround, and another 0.5-kilometer (0.3 mile) approach going back to the intersection. The yellow interval used for the 72.4 km/h (45 mi/h) instructed speed is 4 s, whereas for the 88.5 km/h (55 mi/h) instructed speed is 4.5 s. Those yellow intervals were triggered for a total of 24 times (four repetitions at six distances). The yellow indications were triggered when the front of the test vehicle was 40.2, 54.3, 62.5, 70.4, 76.5, and 82.6 m (132, 178, 205, 231, 251, and 271 ft) from the intersection for the 72.4 km/h (45 mi/h) instructed speed and 56.7, 76.2, 86, 93.6, 101, and 113 m (186, 250, 282, 307, 331, and 371 ft) for the 88.5 km/h (55 mi/h) instructed speed to ensure that the entire dilemma zone was within the range. An additional 24 green trials were randomly introduced into the 24 yellow trials to introduce an element of surprise into the experiment. The run sequence was generated randomly and thus was different from one trial to another. As was mentioned earlier, the phase change events were controlled by the test vehicle

through the use of a wireless communication system between the vehicle and the custom-built signal controller.

4.2.6 Available Datasets

After conducting the field experiment, the data were reduced and tested for correctness and logicality. The data format was exported to different data types (e.g. Txt, Excel, and MATLAB). The available datasets include two instructed approach speeds with two major datasets; 72 km/h (45 mi/h) and 88 km/h (55 mi/h). Each dataset includes a complete tracking data every deci-second of the subject vehicle within about 150 m (500 ft) before and after the intersection. This tracking data includes stop-run decision, driver's age and gender, platoon scenario (leading, following, or no other), approach grade (uphill or downhill), remaining yellow time, traveling speed, DTI, PRT and accepted deceleration rate if stopped and accepted acceleration rate and maximum speed if ran. The 72 km/h dataset includes 1658 valid record (687 running records and 971 stopping records), whereas the 88 km/h dataset includes 1670 valid record (625 running records and 1045 stopping records), those yield a total of 3328 valid records.

4.3 INTERSECTION COLLISION WARNING FIELD STUDY

As mentioned earlier, this experiment was conducted in the spring of 2005 as part of the "Intersection Collision Warning Field Study" that was funded by Federal Highway Administration (FHWA), Mid-Atlantic Universities Transportation Center (MAUTC), and Virginia Department of Transportation (VDOT).

This experiment collected data on 60 subjects approaching the signalized intersection at VDOT's Smart Road facility. In the experiment, participants were instructed to drive the car at 72.4 km/h (45 mph) except in the turnarounds or when stopping at the intersection. Participants were instructed to behave normally when faced with a yellow light, making the decision whether to stop or to go as they usually would do. Not counting the initial practice run, participants drove along the entire test course (2.1 km downhill, low-speed turnaround, 2.1 km uphill, high-speed turnaround) 12 times, passing through the traffic lights 24 times (12 times uphill, 12 times downhill), resulting in 24 trials. At the beginning of each trial run, the signal displayed a green light. As the car approached the intersection, the on-board computer decided whether or not to trigger the yellow and, if so, at what distance from the stop line.

The yellow duration was fixed at 4 s and was initiated when the front of the car was at the following distances from the stop line: 32 m (105 ft), 55 m (180 ft), 66 m (215 ft), 88 m (290 ft), or 111 m (365 ft). This corresponds to TTIs of 1.6 s, 2.7 s, 3.3 s, 4.4 s, and 5.6 s, respectively, assuming a speed of 72.4 km/h (45 mph). Each participant faced phase changes from green to yellow four times for each TTI. These 24 trial conditions (20 yellow lights and 4 green lights) ran in a predetermined, randomized sequence, with a different order for each participant. In this study no vehicles other than that driven by the participants were present on the Smart Road. Had the drivers in the previous studies been following other vehicles that ran the yellow, they too might have proceeded. Furthermore, had there been vehicles following the subject drivers in the preceding studies, the drivers might have decided differently because of a perceived risk of a rear-end collision. Furthermore, this study only considered a single speed of 45 mph.

Based on this field experiment, the final complementary dataset included a total of 1186 valid yellow time approaching trials; out of which 745 trials was for drivers who decided to stop, whereas 441 trials was for running drivers.

4.4 SUMMARY AND CONCLUSIONS

This chapter sheds light on the two experimental studies that serve as sources for the data available for the analysis in this dissertation. Both experiments were conducted on the Virginia Smart Road in 2005 and 2008. The old experiment comprised 60 drivers equally divided by gender and age. Each driver was involved in one driving session was 20 yellow approaching trials at 72.4 km/h (45 mi/h) instructed speed limit. On the other hand, the new experiment comprised 24 drivers equally divided by gender and age. Each driver was involved in six driving sessions with 2 different instructed speed limits (72.4 km/h (45 mi/h) and 88.5 km/h (55 mi/h)) and 3 different platoon conditions (leading, following, and driving alone). Each session included 24 yellow approaching trials. Both experiments resulted in three main datasets: two datasets from the new experiment (Dataset Ia and b) for the 72.4 km/h (45 mi/h) and the 88.5 km/h (55 mi/h) speed limits, and one dataset from the first experiment (Dataset II) for the 72.4 km/h (45 mi/h) speed limit. Table 3 summarizes the number of valid records (running, stopping and all) from each dataset.

Table 3: Breakdown of Number of Trials in Available Datasets

Experiment	Dataset		Speed km/h (mi/h)	Running Trials	Stopping Trials	All Trials
New (2008)	**(I)**	**a**	**72.4 (45)**	687	1040	1727
		b	**88.5 (55)**	625	1102	1727
Old (2005)	**(II)**		**72.4 (45)**	441	745	1186

CHAPTER 5 CHARACTERIZATION OF YELLOW/RED LIGHT RUNNING BEHAVIOR AND DRIVER STOP-RUN DECISION

5.1 INTRODUCTION

In order to model the driver behavior at the onset of yellow indication at high-speed signalized intersection approaches, it is required first to characterize the different attributes associated with it. This characterization will serve as the input for the statistical and behavioral modeling objectives. Both present and next chapters are assigned to present the details of the characterization of the driver behavior attributes. In this chapter, two driver behavior attributes are characterized; the driver yellow/red light running behavior and the driver stop-run decision. The driver yellow/red light running behavior is characterized first by comparing the distributions of the stopping/running probabilities based on different surrounding variables, and then by empirical investigations of the running behavior of the different drivers either before or after the end of the yellow indication. The driver stop-run decision is characterized then by modeling the stopping probability using traditional statistical models. It is worth mentioning here that the analysis in this chapter is published in four references [67, 69, 70, 71].

5.2 CHARACTERIZATION OF YELLOW/RED LIGHT RUNNING BEHAVIOR

In this section, the distribution of the running/stopping probabilities of the different drivers in dataset I is investigated. Then, based on the same dataset I, the behavior of the yellow/red light running at the onset of a yellow indication is characterized.

5.2.1 Distribution of Driver Stopping/Running Probabilities

As described earlier, the data were gathered for two instructed approach speeds; 72.4 km/h and 88.5 km/h. Each data set included a complete tracking of the subject vehicle with a binary (0 or 1) stop-run decision, The data were sorted based on the driver's TTI, at the onset of the yellow indication, into equal-sized bins (equal number of observations) and the average TTI and probability of stopping for each bin was computed for illustration purposes only given the large number of observations. The stopping/running probabilities versus the TTI at the onset of the yellow signal indication for the two instructed speeds are presented in Figure 13. The 0.9/0.1 probability of stopping/running was between 3.6 and 3.8 s from the stop line at the onset of yellow for the 72.4 km/h instructed speed, while the 50 percent stopping/running decision

point occurred when the yellow indication was triggered while the vehicle was 3.1 s from the stop line. For the 88.5 km/h instructed speed, the 0.9/0.1 probability of stopping/running was between 4.1 and 4.3 s from the stop line at the onset of the yellow indication and the 50 percent stopping/running decision point occurred when the yellow indication was triggered when the vehicle was 3.2 s from the stop line.

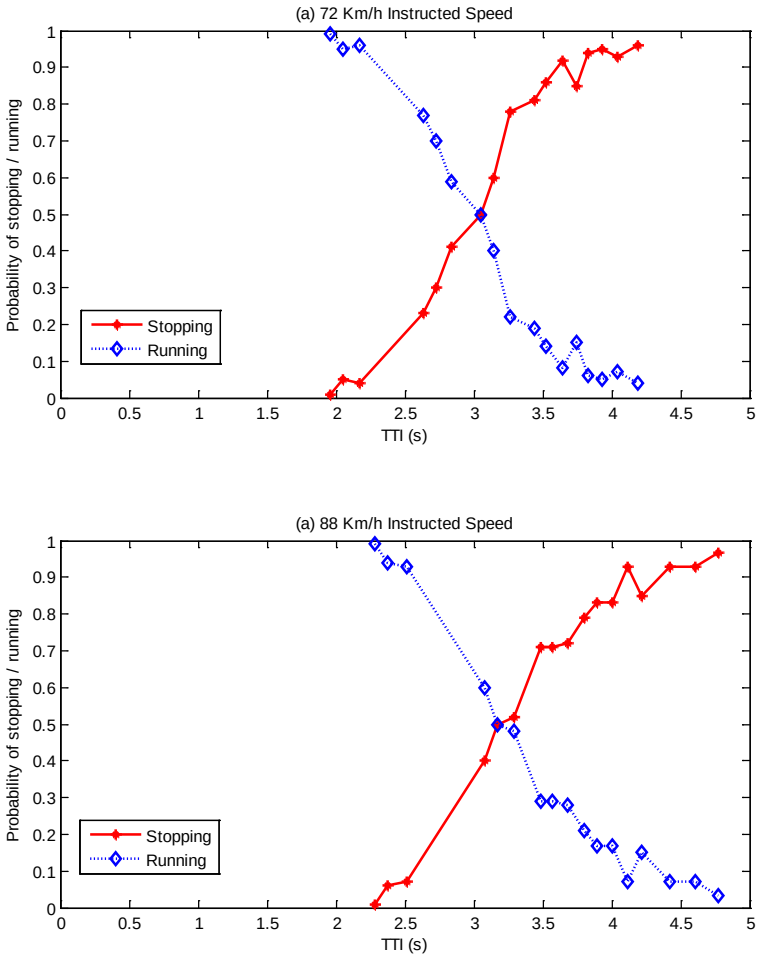

Figure 13: Probability Distributions of Stopping/Running

5.2.2 Analysis of Yellow/Red Light Running Behavior

After analyzing the driver stopping/running probabilities, the analysis investigates both the yellow and red light running behavior based on dataset I. As mentioned earlier in Chapter 4, the 72.4 km/h dataset Ia includes 687 valid running records, whereas the 88.5 km/h dataset Ib includes 625 valid running records. This yields a total of 1312 running records. Based on these records, the average acceleration levels when the yellow indication was triggered at the signalized intersection can be estimated using Equation (8).

$$a_{avg} = \frac{v - v_o}{t \times 3.6} \quad (8)$$

where a_{avg} is the average acceleration level (m/s^2),
v is the vehicle speed at the onset of the yellow indication (km/h),
v_o is the final vehicle speed while crossing the stop line (km/h), and
t is the acceleration time (s).

The histogram for the observed acceleration levels of the 1312 running events for the two approach speeds are shown in Figure 14. These figures demonstrate that the driver acceleration levels were very similar for both instructed speeds.

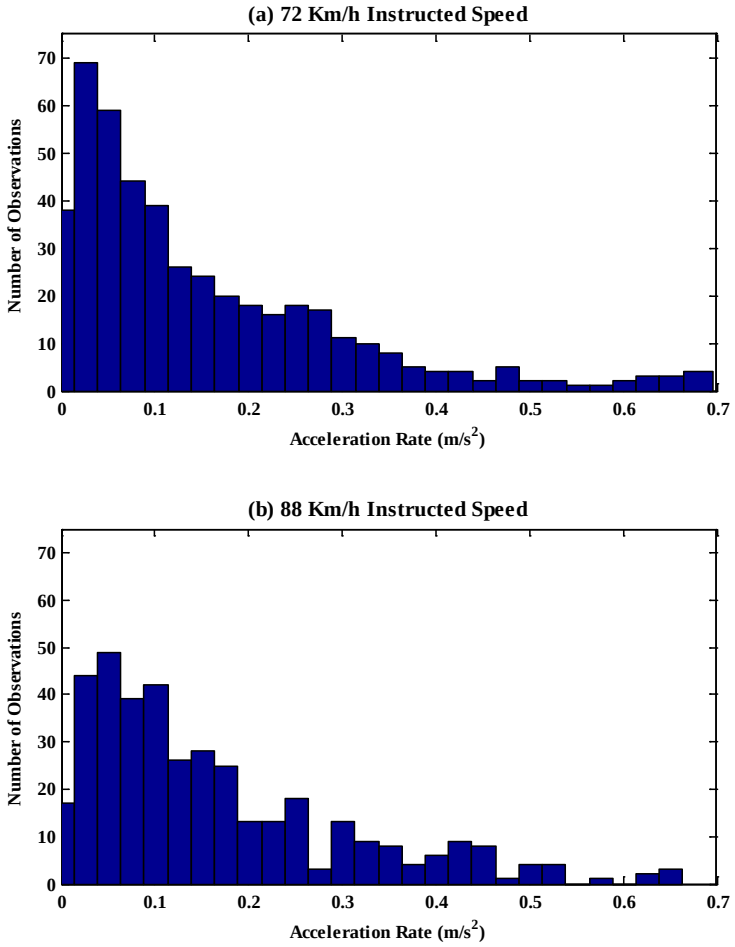

Figure 14: Histogram of Acceleration Levels

The acceleration level ranged from a minimum of 0.0015 m/s^2 (0.005 ft/s^2) to a maximum of 0.6959 m/s^2 (2.283 ft/s^2) with a mean of 0.1492 m/s^2 (0.490 ft/s^2) for the participants who were instructed to drive at 72.4 km/h (45 mph). Alternatively, the acceleration level ranged between 0.0012 m/s^2 (0.004 ft/s^2) and 0.6568 m/s^2 (2.155 ft/s^2) with a mean equal to 0.1623 m/s^2

(0.532 ft/s^2) for those who were instructed to drive at 88.5 km/h (55 mph), as demonstrated in Table 4.

Table 4: Descriptive Statistical Results of Acceleration Level

Instructed Speed	N	Min	Max	Mean	15%	50%	85%	StD
72 Km/h	687	0.0015	0.6959	0.1492	0.0262	0.0978	0.2852	0.1461
88 Km/h	625	0.0012	0.6568	0.1623	0.0372	0.1161	0.3176	0.1399
Overall	1312	0.0012	0.6959	0.1553	0.0300	0.1065	0.3030	0.1433

Furthermore, Figure 15 presents the scatter diagrams between the vehicles' TTIs at the onset of the yellow indication and the time elapsed after the onset of the yellow indication at the instant the vehicle enters the intersection (i.e., when the vehicle hits the intersection stop line). It can be seen from the figure that for both instructed speeds, the scatter plots follow a line with a slope of 1 and zero intercept (i.e., a 45° line). This trend implies that the running drivers maintain their approach speed after the onset of the yellow and do not accelerate in order to ensure that they cross the intersection safely before the onset of red. In other words, the approaching speed at the onset of yellow can be reasonably considered representative for the driver's speed at the intersection entry instant. This is valid for both drivers running during yellow, who hit the intersection stop line before the end of yellow time (4 s for 72.4 km/h instructed speed and 4.5 s for 88.5 km/h instructed speed), and those running during red, who hit the intersection stop line after the end of yellow time. Accordingly, it appears that the red-light runners did not violate the red light intentionally; instead they appeared to misjudge their stop-run decision. It is worth noting here that in a real situation, drivers would intentionally violate the traffic signal at only light traffic volumes (e.g., late night traffic), where they can secure that there will be no movement conflicting them when they run the red light. On the other hand, in the present study, side street traffic was always present as a conflicting movement, which minimizes the number of those intentional violators.

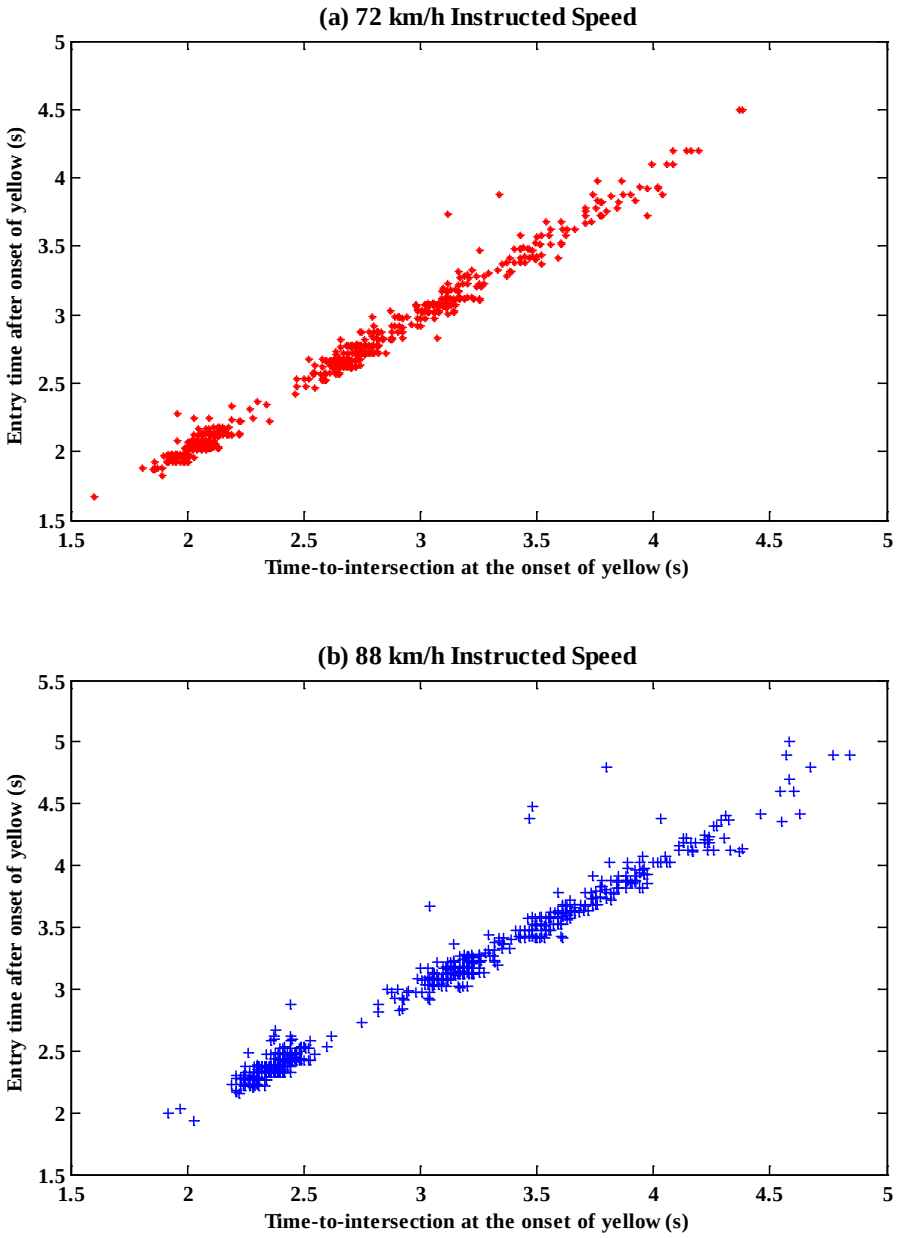

Figure 15: Relation between Yellow Entry Time and TTI at Yellow Onset

In terms of the number of running drivers as a function of the entry time after the yellow onset, Figure 16 shows histograms of yellow/red-light runners as a function of the time elapsed after the onset of the yellow indication until reaching the stop line. According to the figure, it can be seen that, for both instructed speeds, the number of running drivers is inversely proportional with the entry times after the onset of yellow indication; i.e., the longer the elapsed time after the yellow onset at the intersection entry, the fewer number of drivers decide to run. Furthermore, it is obvious from Figure 16 that, for both instructed speeds, the last bin in the histograms (with

entry time more than 4 s for the 72.4 km/h instructed speed and more than 4.5 s for the 88.5 km/h instructed speed) represents the red-light runners, those who entered the intersection after the onset of the red indication.

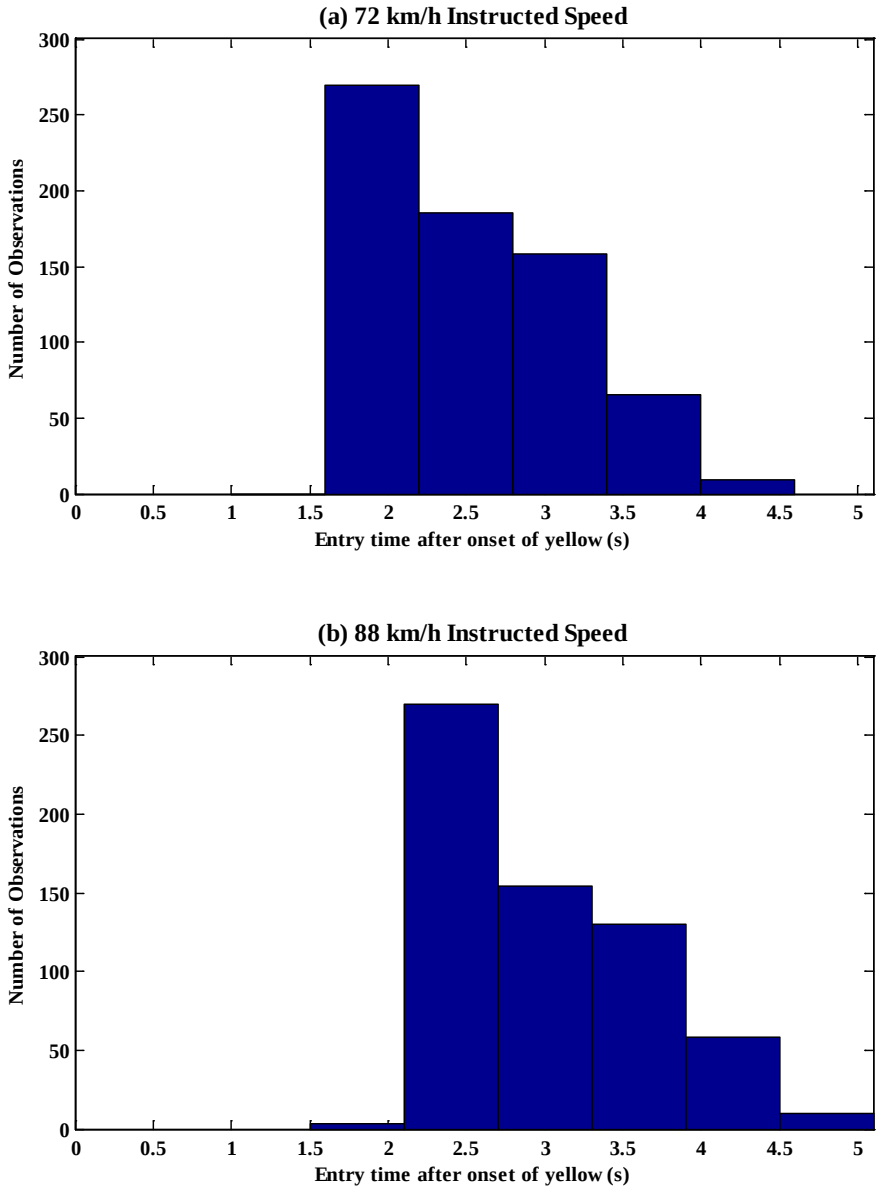

Figure 16: Histograms of Yellow/Red-Light Runners' Entry Times after Yellow Onset

Another illustration for the yellow/red-light running behavior is shown in Figure 17, which presents the relation between the vehicle's TTI at the onset of yellow and its position at the end of the yellow indication with reference to the stop line. The interesting point in this figure is that it combines both the potential red-light runners versus the actual red-light runners. Throughout the figure, the potential red-light runners can be recognized for both instructed

speeds by those points laying at TTI more than the yellow time (4 s for the 72.4 km/h instructed speed and 4.5 s for the 88.5 km/h instructed speed), whereas the actual red-light runners can be easily distinguished as those points upstream of the intersection stop line (i.e., positive DTI). Accordingly, it can be seen that a small number of the potential red light runners, who faced the onset of yellow at a TTI more than the yellow time, were able to pass the intersection stop line legally before the end of the yellow time by accelerating to a speed higher than their approaching speed. Those drivers appear to be intentionally deciding to run and are able to avoid the dilemma zone by increasing their speed.

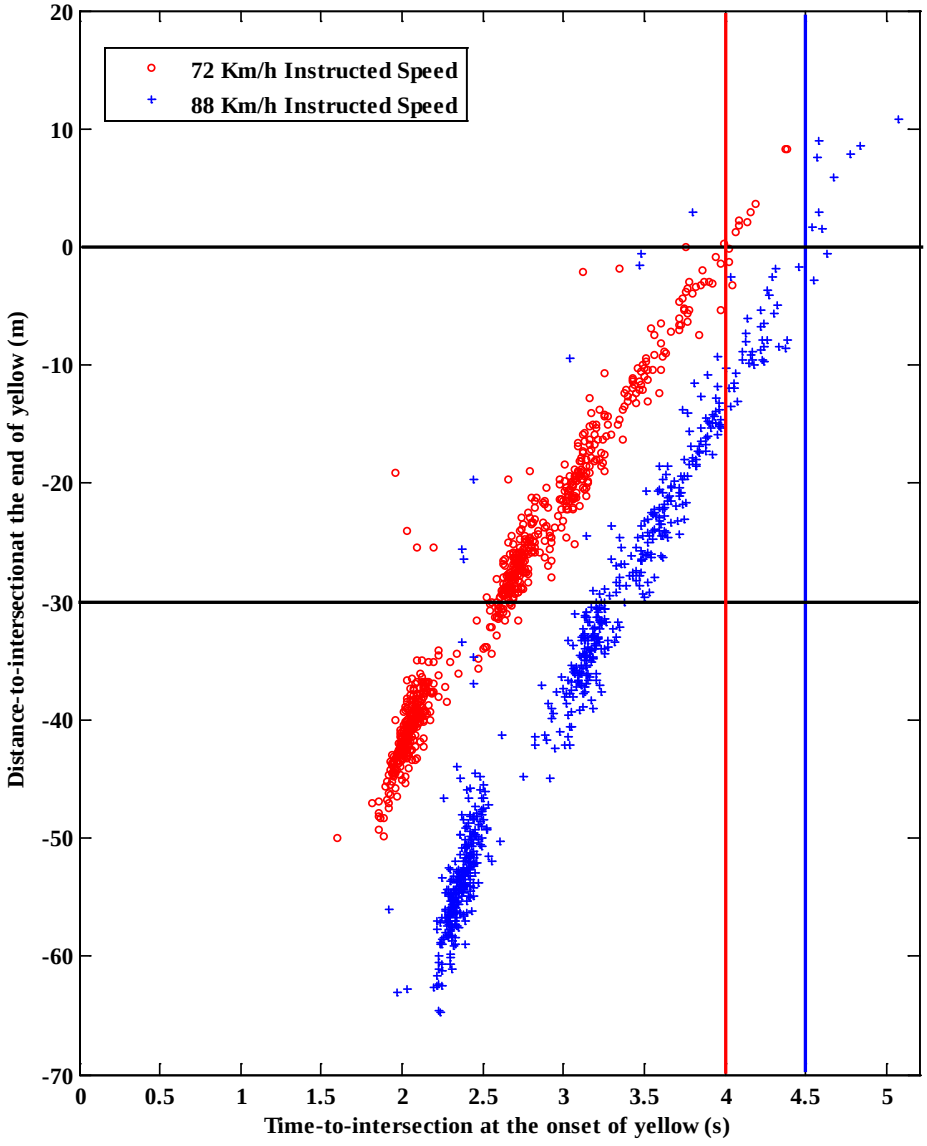

Figure 17: Relation between DTI at End of Yellow and TTI at Yellow Onset

Furthermore, although the number of actual red-light runners, who were behind the stop line at the onset of the red light indication, is not large (1.4 percent) as shown in Table 5, a substantial number (43 percent) of the drivers, who crossed the stop line during the yellow time, were not able to completely clear the intersection width, which equals 30 meters, at the onset of red indication. In order for the driver to be able to clear the 30-meter intersection width, approximately 1.5 s for the 72.4 km/h instructed speed or 1.2 s for the 88.5 km/h instructed speed is needed. Accordingly, if the adopted all-red interval is the minimum conventional 1 s, then there is a potential risk that the legal yellow-light runners would not be able to completely clear the intersection at the instant the side-street traffic gains the right-of-way (Table 5). This conclusion assumes that there is no start-up lost time for the side-street traffic in order to consider the worst case scenario, while considering a side-street start-up lost time or applying fairly longer all-red times could then minimize this risk.

Table 5: Number of Yellow/Red-Light Runners with Potential Crash Risk

		Instructed Speed		
		72 km/h	**88 km/h**	**All**
No. of Yellow/Red Light Runners	**Behind Stop Line at Onset of Red**	9 (1.3%)	10 (1.6%)	19 (1.4%)
	Inside Intersection at Onset of Red	368 (53.6%)	194 (31.0%)	562 (42.8%)
	Inside Intersection at End of 1-s All-Red	51 (7.4%)	22 (3.5%)	73 (5.6%)
	Outside Intersection at Onset of Red	259 (37.7%)	399 (63.9%)	658 (50.2%)
Sample Size		**687 (100%)**	**625 (100%)**	**1312 (100%)**

A comparison of driver running probabilities at the onset of the yellow indication for both males and females was performed in order to characterize the effect of age on driver behavior. Male drivers appeared to be less likely to run when compared to female drivers for the two instructed speed levels as shown in Figure 18. The figure demonstrates that the probability of running for male drivers is shifted to the left when compared to female drivers; this shift correlates to a decrease in the probability of running for male drivers relative to female drivers. The F-statistic generated from the GLMM revealed that these differences are statistically significant at the 0.05 level ($P < 0.0001$) for the 72.4 km/h and for the 88.5 km/h instructed speeds.

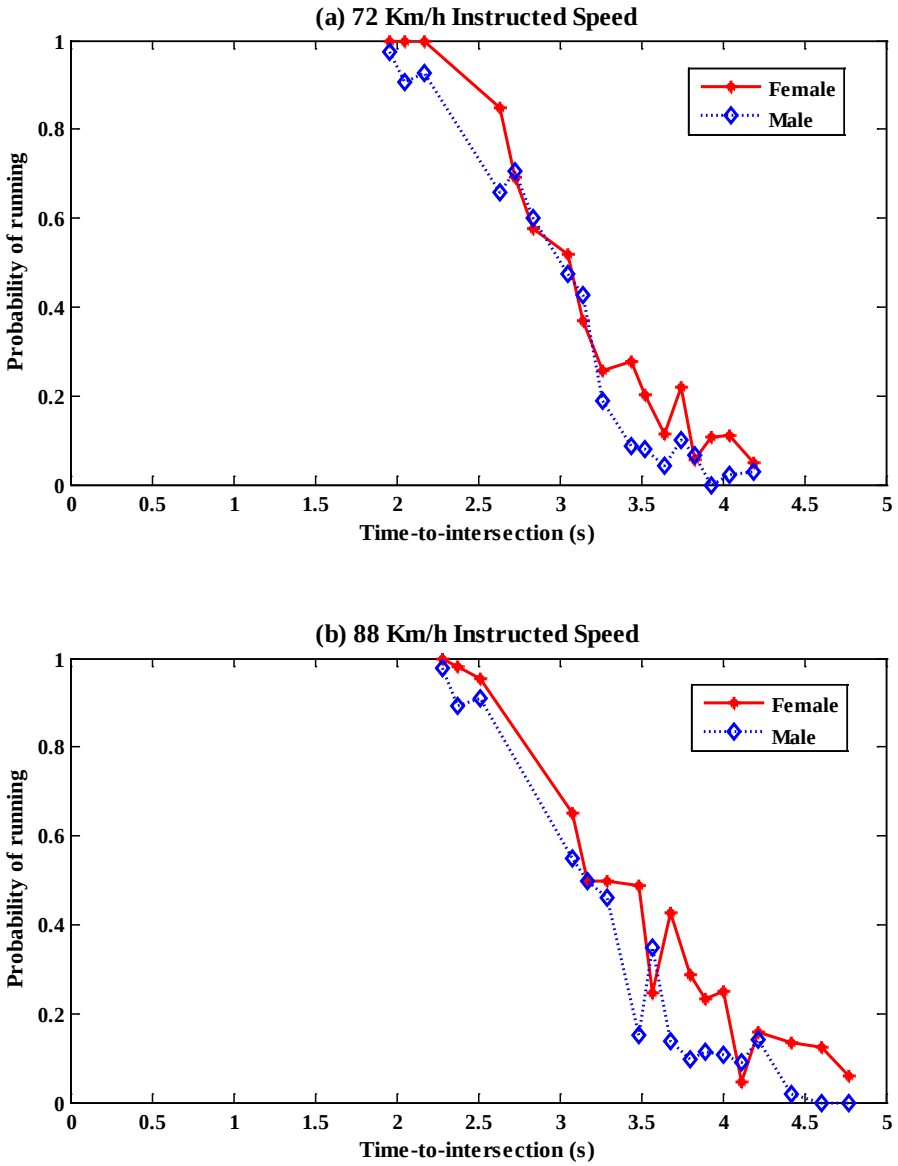

Figure 18: Probability of Running as a Function of Gender.

In addition, the data were utilized to derive the stopping/running probabilities at the onset of the yellow indication for the three different age groups (under 40-years-old, 40 to 59-years-old, and 60 years of age or older) to characterize the effect of age on driver behavior. Figure 19 demonstrates that the percentage of older drivers (60 years of age and older) who elected to run at the short yellow trigger times was less than the younger drivers for both the 72.4 km/h and 88.5 km/h instructed speeds. Older drivers were less likely to run for average TTIs, at the onset of the yellow indication, ranging between 2 to 3.1 s when compared to younger drivers for the 72.4 km/h instructed speed and ranging from 2.3 to 3.7 s for the 88.5 km/h instructed speed. The

F-statistic generated from the GLMM for the three age groups demonstrated that, there are statistically significant differences, with P-value=0.041 for the younger and the middle age groups and with P-value=0.015 for the younger and the older age groups. While there is no significance difference between the middle and the older age groups with P-value=0.6289.

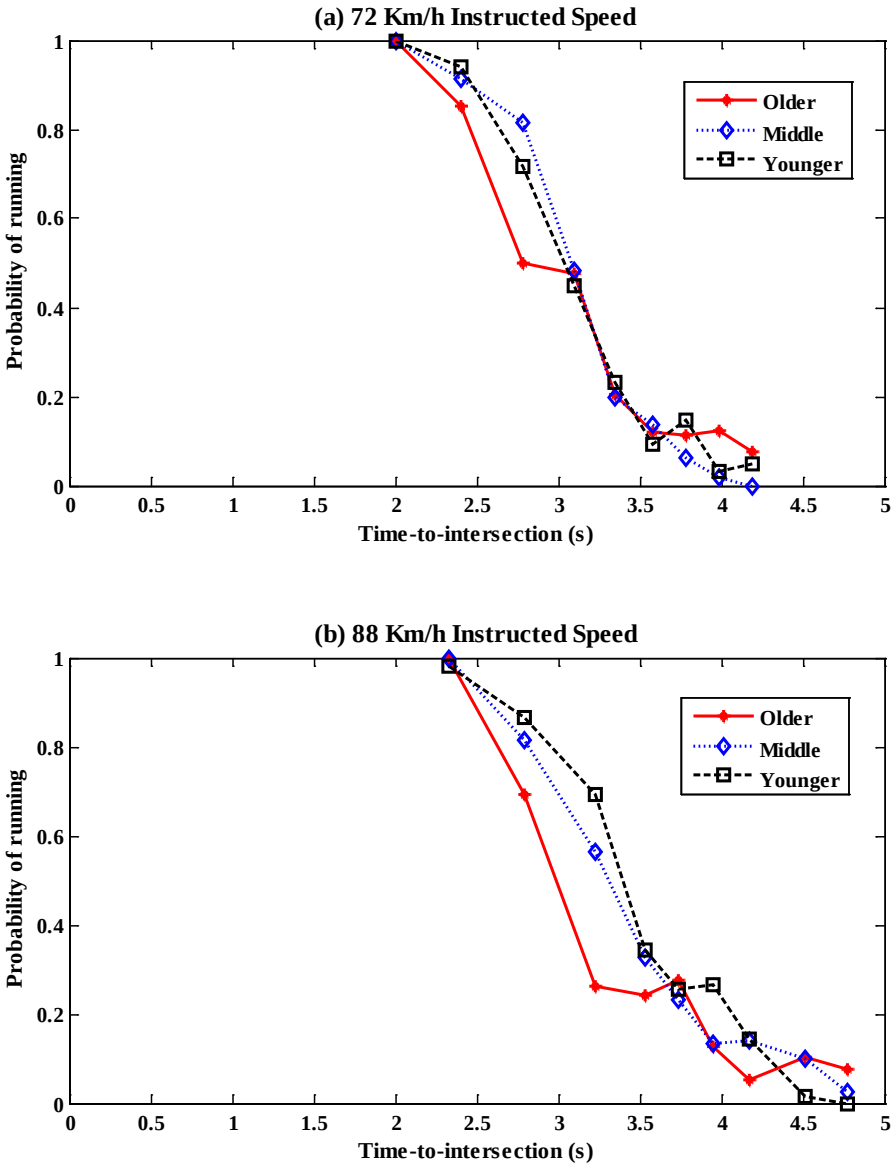

Figure 19: Probability of Running as a Function of Different Age Groups

5.3 STATISTICAL MODELING OF DRIVER STOP-RUN DECISION

In this section, the two datasets I and II are utilized in order calibrate traditional statistical choice models based on the classical frequentist approach in order to model the driver stopping probability as function of the different surrounding variables.

5.3.1 Modeling driver stop-run decision from dataset II

As mentioned earlier, a total of 1186 stop-run decisions were available from dataset II. The data included, the driver age, gender, TTI, vehicle speed at the onset of yellow, and a binary (0 or 1) driver stop decision variable to indicate whether a driver stopped or proceeded through the intersection. Using the data a Generalized Linear Model (GLM) of the logistic type was fit to the data considering a binomial distribution. Different forms of the model were tried with the different variables and it was found that the TTI is the most significant explanatory variable. The final model form is illustrated in Equation (9).

$$\ln\left(\frac{P_r}{P_s}\right) = \ln\left(\frac{1-P_s}{P_s}\right) = c_0 + c_1 TTI \tag{9}$$

where P_r is the probability of running,
P_s is the probability of stopping,
c_0 and c_1 are model constants, and
TTI is the time-to-intersection (s).

The model calibrated parameters were 4.486 and -1.806 for parameters c_0 and c_1, respectively ($p<<0.0005$). The model produced 86.34% success rate (a total of 1024 correct decisions out of the 1186 trials). The field observed data and model fit are illustrated graphically in Figure 20. In order to illustrate the field data graphically, the probability of stopping (P_s) was computed considering a bin size of 20 observations sorted by TTI (P_s was computed as the number of stopped trials divided by the 20 total trials within the bin). The field data, as is the case with previous field studies, clearly demonstrates a decrease in the probability of stopping as the TTI decreases. The figure also demonstrates a good match between the VT model estimates and field observations with some outlier field observations at the 5.5 and 6.1 TTIs.

Because drivers experienced more yellow than green indications (20 yellows versus 4 greens), it appeared that drivers were more willing to stop at shorter TTIs when compared to uncontrolled field test results reported in the literature, as illustrated in Figure 20 (comparing the controlled smart road VT Model to uncontrolled field test UWn Model). As mentioned earlier in Chapter 2, a study conducted by the University of Wisconsin reported a model with c_0 and c_1 coefficient values of 6.34 and -1.69, respectively [28].

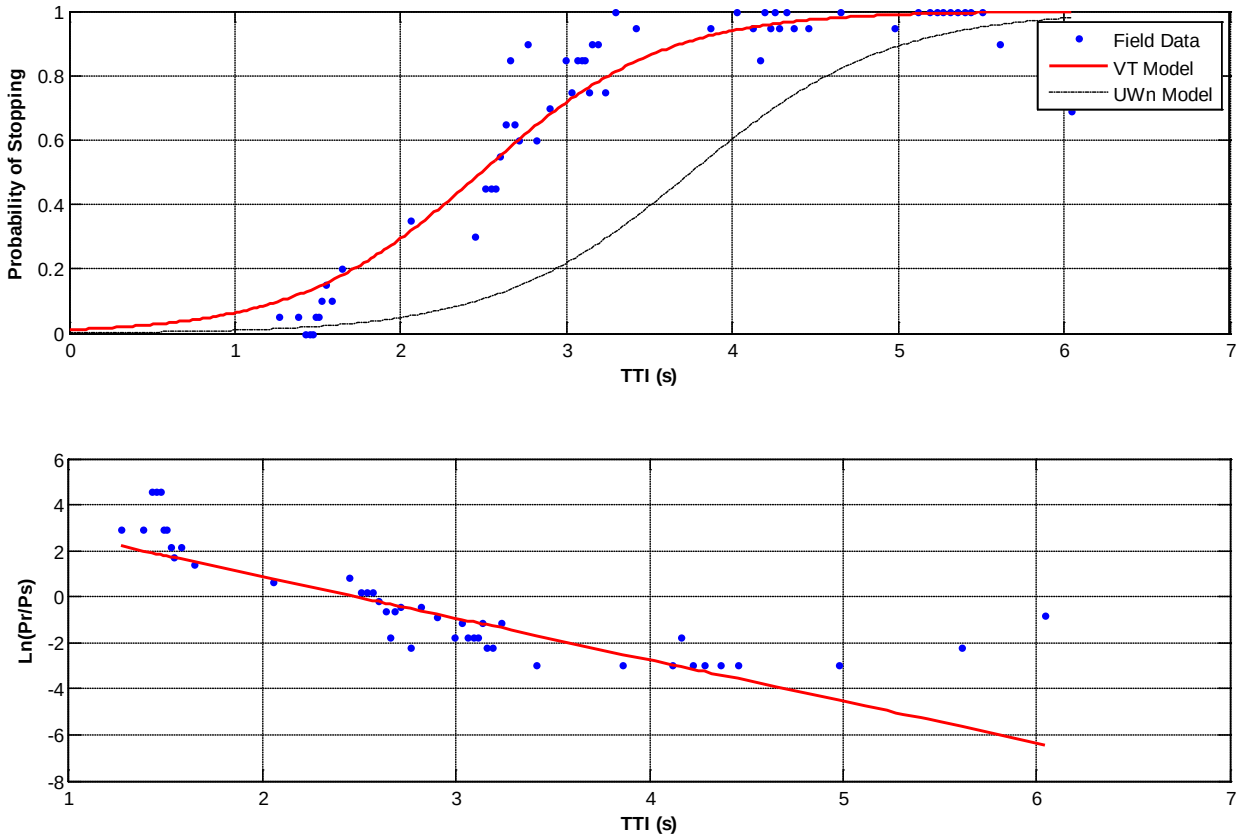

Figure 20: Smart Road Field Data and Model Predictions of Probability of Stopping

Consequently, a data transformation of the Smart Road TTI observations was applied to adjust for the higher propensity for vehicle stopping in the controlled field test versus uncontrolled field test; while maintaining the advantage of tracking the subject driver in the controlled test versus an uncontrolled field test. The computation of the data transformation parameters can be derived considering the adjusted TTI (TTI') as

$$TTI' = a_0 + \left(1 + a_1\right) TTI \tag{10}$$

A data transformation from the VT model to the UWn model parameters can be computed considering that

$$c_0 + c_1 TTI' = c'_0 + c'_1 TTI \tag{11}$$

where c'_0 and c'_1 are the desired model parameters (6.34 and -1.69, respectively).

Solving Equation (11), the TTI adjustment factors a_0 and a_1 can be computed as

$$a_0 = \frac{c_0' - c_0}{c_1} \text{ and } a_1 = \frac{c_1' - c_1}{c_1} \quad (12)$$

After deriving the data transformation parameters, the Smart Road field data were transformed and the logistic model was fit to the transformed data to produce a model similar to the UWn model, as illustrated in Figure 21. The optimized model parameters are estimated at 5.82 and -1.62 ($p<<0.0005$) with a prediction error rate of 12.8% and a dispersion parameter of 1.01. This model is statistically equivalent to the UWn model given that the parameter standard errors are 0.41 and 0.10, respectively.

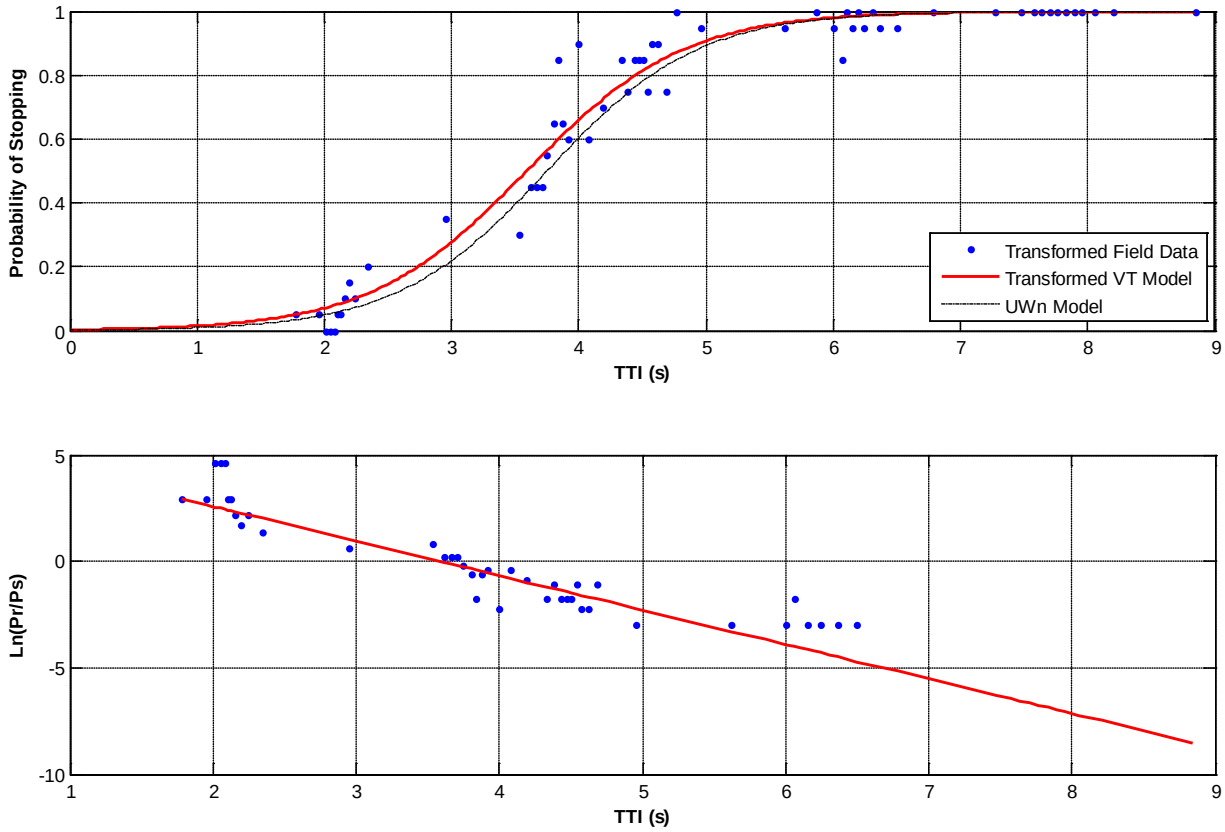

Figure 21: Transformed Smart Road Field Data and Model Predictions of Probability of Stopping

5.3.2 Modeling driver stop-run decision from dataset I

One of the objectives of this dissertation is to develop an agent-based Bayesian modeling framework that can capture the stochastic nature of the driver stop-run decision. In addition, dataset I will be used in developing the agent-based model, whereas dataset II will be used to validate the model transferability. However, before getting into using the Bayesian approach, it would be useful first to develop a traditional statistical model based on the classical frequentist

approach from dataset I. This would help in better understanding of the driver behavior based on the available data, and besides it would serve as the initial solution needed for the Bayesian approach, as will be explained later.

A total of 3328 stop-run decisions are available from dataset I, including the driver age, gender, TTI, vehicle speed at the onset of yellow, roadway grade (uphill or downhill), platoon scenario (leading, following, or no other), and a binary (0 or 1) driver stop-run decision variable to indicate whether a driver stopped or proceeded through the intersection. Given that the driver decision is a discrete variable (stop or run) while the independent variables are continuous, a Generalized Linear Model (GLM) of the logistic type was fit to the data considering a binomial distribution of the form in Equation (13).

$$\ln\left(\frac{P_s}{P_r}\right) = \ln\left(\frac{P_s}{1-P_s}\right) = \text{logit}\left(P_s\right) = \beta_0 + \beta_1 r + \beta_2 A + \beta_3 \frac{TTI}{y} + \beta_4 \frac{v}{v_f} \quad (13)$$

where P_s is the probability of stopping,
P_r is the probability of running,
β_i's are model constants,
r is the gender (0 = female, 1 = male),
A *is* the age (years),
TTI is the time-to-intersection (s),
y is the yellow time (s),
v and v_f are the approaching speed and the speed limit (m/s).

Different multivariate model forms were evaluated and compared and the above form is selected as the best model. The model calibrated coefficients and their corresponding P-values are summarized in Table 6 and show a good statistical fit. Furthermore, in order to validate the calibrated model, it is used to replicate the dataset and it produced an 82.03% success rate (a total of 2730 correctly estimated decisions out of the 3328 total decisions).

Furthermore, the calibrated statistical model is used to carry out a sensitivity analysis for the impact of the different independent variables included in the model. Figure 22 shows the sole impact of changing four different variables (gender, age, yellow time, ratio of speed to speed limit) separately while keeping other variables unchanged. It can be inferred from Figure 22 that female drivers and younger drivers are more willing to run the intersection for the same TTI value. In addition, those drivers facing longer yellow time are more encouraged to run and those

traveling at speed higher than the speed limit are also running the intersection more than those traveling at lower speeds.

Table 6: Statistical Model Calibration Results

Coefficients	Coefficient Values	P-value
β_0	- 6.1773	0.0003
β_1	0.5745	0.0000
β_2	0.0185	0.0000
β_3	12.4665	0.0000
β_4	- 4.2307	0.0088

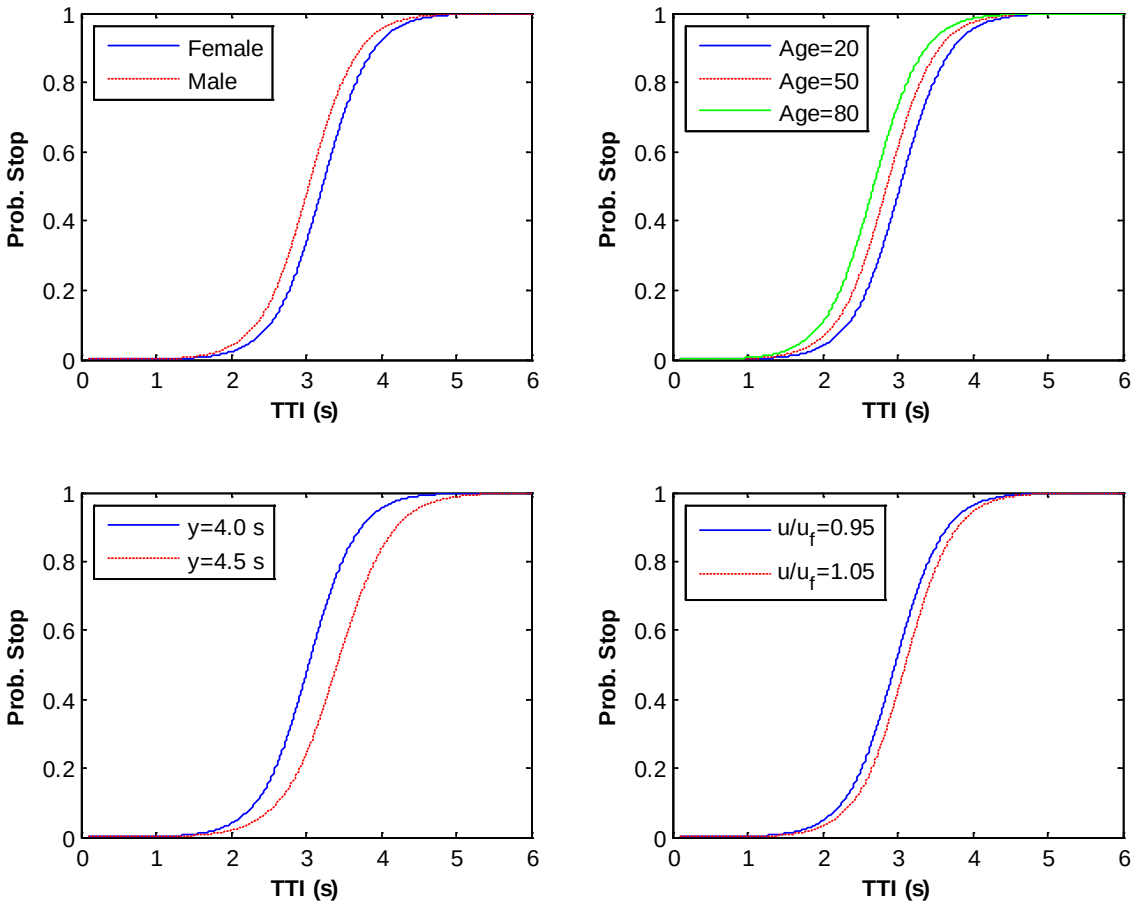

Figure 22: Sensitivity Analysis of the Statistical Model Independent Variables

Furthermore, it is worth mentioning that general linear mixed model (GLMM) can introduce the idea that an individual's pattern of responses is likely to depend on many characteristics of the subject, including some that are unobserved. These unobserved variables are then included in the model as random variables (i.e. random effects). Accordingly, a GLMM

model is calibrated on the data [71]. The results from the model are found equivalent to the GLM model presented here.

5.4 SUMMARY AND CONCLUSIONS

In this chapter, two driver behavior attributes were characterized; namely driver yellow/red light running behavior and driver stop-run decision. The evaluation of drivers' yellow/red light running behavior showed that driver drivers are more likely to run at the onset of the yellow indication at shorter distances. It was demonstrated that the running drivers maintain their approach speed after the onset of the yellow and do not accelerate in order to ensure that they cross the intersection safely before the onset of red, and hence the red-light runners appeared not to violate the red light intentionally; instead they appeared to misjudge their stop-run decision. In addition, it was found that the number of running drivers is inversely proportional with the intersection entry times after the onset of yellow indication. Moreover, it was concluded that although the number of actual red-light runners, who were behind the stop line at the onset of red indication, is not large, if the adopted all-red interval is the minimum conventional 1 s, there is a potential risk that the legal yellow-light runners would not be able to completely clear the intersection at the instant the side-street traffic gains the right-of-way. Finally, the observed running probability of younger and female drivers under the same TTI was significantly higher compared to older and male drivers.

Furthermore, the statistical modeling of the stopping probability based on dataset II demonstrated that the TTI is the most significant explanatory variable, whereas the model of dataset I showed other variables to be significant beside the TTI, including gender, age, yellow time, and ratio of approaching speed to speed limit. A data transformation technique was applied to the model of dataset II to adjust for the higher propensity for vehicle stopping in the controlled field test versus uncontrolled field test. In addition, a sensitivity analysis based on the model of dataset I confirmed the results obtained from the empirical testing of the frequency distributions of the stopping/ running probability.

CHAPTER 6 CHARACTERIZATION OF DRIVER PERCEPTION-REACTION TIME AND DECELERATION LEVEL

6.1 INTRODUCTION

As mentioned earlier in Chapter 5, characterization of the different driver behavior attributes will serve as the input for the statistical and behavioral modeling frameworks. In this chapter, the characterization of the driver behavior attributes continues. After having the driver yellow/red light running behavior and the driver stop-run decision characterized in the preceding chapter, another two driver attributes are characterized in the present chapter; the driver PRT and the driver deceleration level. Both variables are characterized by comparing the distributions of each variable based on different surrounding variables. It is worth mentioning here that the analysis in this chapter is published in four references [67, 72, 73, 74].

6.2 CHARACTERIZATION OF DRIVER PERCEPTION-REACTION TIME

As mention earlier in Chapter 2, the PRT in the context of this dissertation is defined as the time elapsed between the onset of the yellow indication and the instant the driver started to press the brake pedal. In this section, the driver PRT is characterized by analyzing its distributions, with respect to the different surrounding variables. First, the PRT from dataset II of the first experiment is analyzed as the cruising and overall PRTs. Thereafter, the overall PRT from dataset I is analyzed based on further investigation of the impact of the different surrounding variables on it.

6.2.1 Distribution of Driver Perception-Reaction Time from Dataset II

The total PRT can be split into a mental processing time (the time required for the driver to perceive the sensory input and to decide on a response) and a movement time (the time used to perform the programmed movement, such as lifting the foot from the accelerator and touching the brake) [22]. In the case of a driver arriving at a signalized intersection when the phase changes from green to yellow, the processing time (time interval from the onset of the yellow light to the instant the accelerator released) is called the perception time while the movement time (time interval when the accelerator released to the instant the brake pedal pressed) is called the reaction time.

A total of 745 data records were available from dataset II for this analysis, for all drivers who stopped at the onset of the yellow-indication, ranging from a minimum TTI of 1.34 s to a maximum of 6.19 s with a mean equal to 3.96 s, a median of 4.14 s, and a standard deviation of 1.08 s. Only 482 data records (of the 745 data records) were for those who were cruising at the onset of the yellow-indication ranging from a minimum TTI of 1.34 s to a maximum of 6.19 s with a mean equal to 3.97 s, a median of 4.15 s, and a standard deviation of 1.09 s. The data were sorted based on the driver's TTI, at the yellow-indication onset, into equal sized bins (equal number of observations) and the average of the cruising PRT and the overall PRT for each bin was computed. Furthermore, a four-factor analysis of variance (ANOVA) was conducted using the general linear model procedure (GLM) of the SAS® software to investigate the effects of the TTI, grade, age group, and gender on each PRT.

In general, PRT measurements (which is the time interval from the yellow-indication onset to the instant the brake pedal is pressed) from driving simulator and controlled-road studies can also be computed as the summation of both the perception and reaction times. However, in naturalistic studies, it is not possible to measure the perception and reaction times separately and also to differentiate between the drivers who were pressing the accelerator from those who had their foot lifted off the accelerator in advance of the yellow-indication onset.

Based on dataset II, cruising PRT and overall PRT were only calculated for those who stopped. Cruising PRT will be considered only for those drivers with their foot already on the accelerator pedal at the yellow-indication onset, while overall PRT will be considered for all stopping drivers. Observed PRT for each driver was calculated, which provided a sample of 482 cruising PRT in the range of 0.38 to 2.4 s, with a mean equal to 0.76 s, a median of 0.69 s, and a standard deviation of 0.21 s. Overall PRT (745 observations) ranged between 0.14 to 2.4 s, with a mean equal to 0.73 s, a median of 0.69 s, and a standard deviation of 0.22 s.

The ANOVA model for both the cruising PRT and overall PRT was significant ($P < 0.0001$) at the 0.05 level and the ANOVA analysis confirmed the trend that cruising PRT ($F(9,482) = 13$, $p < 0.0001$) and overall PRT ($F(9,745) = 12$, $p < 0.0001$) increase as the TTI increases.

Figure 23 shows the mean cruising PRT and overall PRT from both approaches (uphill and downhill). Mean cruising PRT and overall PRT for drivers going downhill (0.71 and 0.66

respectively) were shorter than going uphill (0.77 and 0.78 respectively). The F-statistic generated from the ANOVA test demonstrated that roadway grade had a significant effect on both cruising PRT ($F(2,482) = 12.4$, $p = 0.0005$) and overall PRT ($F(2,745) = 74.3$, $p < 0.0001$). No significant differences were found in the mean cruising PRT ($F(2,482) = 2.9$, $p = 0.06$) and overall PRT ($F(2,745) = 2.09$, $p = 0.12$) for the driver age groups, and also no significant differences ($F(1,482) = 0.04$, $p = 0.84$ for cruising PRT and $F(1,745) = 0.54$, $p = 0.46$ for overall PRT) exist between male and female drivers.

Mean PRTs in both cases (cruising PRT and overall PRT) were compared as shown in Figure 24. The figure demonstrates that the mean cruising PRT curve was shifted up compared to the overall PRT over the entire TTI range except for less than 2.75 s. This shift correlates to a lower PRT for those drivers who have their foot lifted off the accelerator at the onset of the yellow interval. The results, however, indicate a similar trend and thus the gathering of PRT data when driver foot information is not available should be valid.

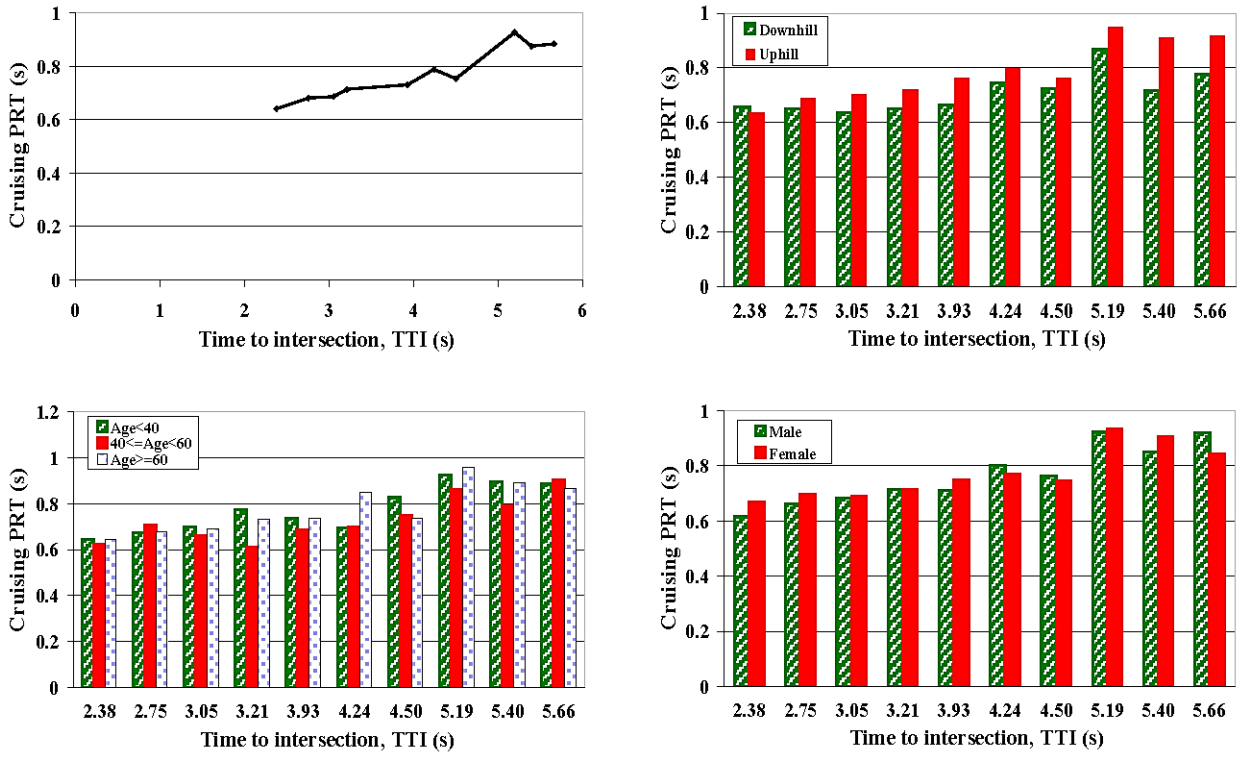

(a) Cruising PRT

Figure 23: Mean Perception-Reaction Time as a Function of TTI, Age, and Gender

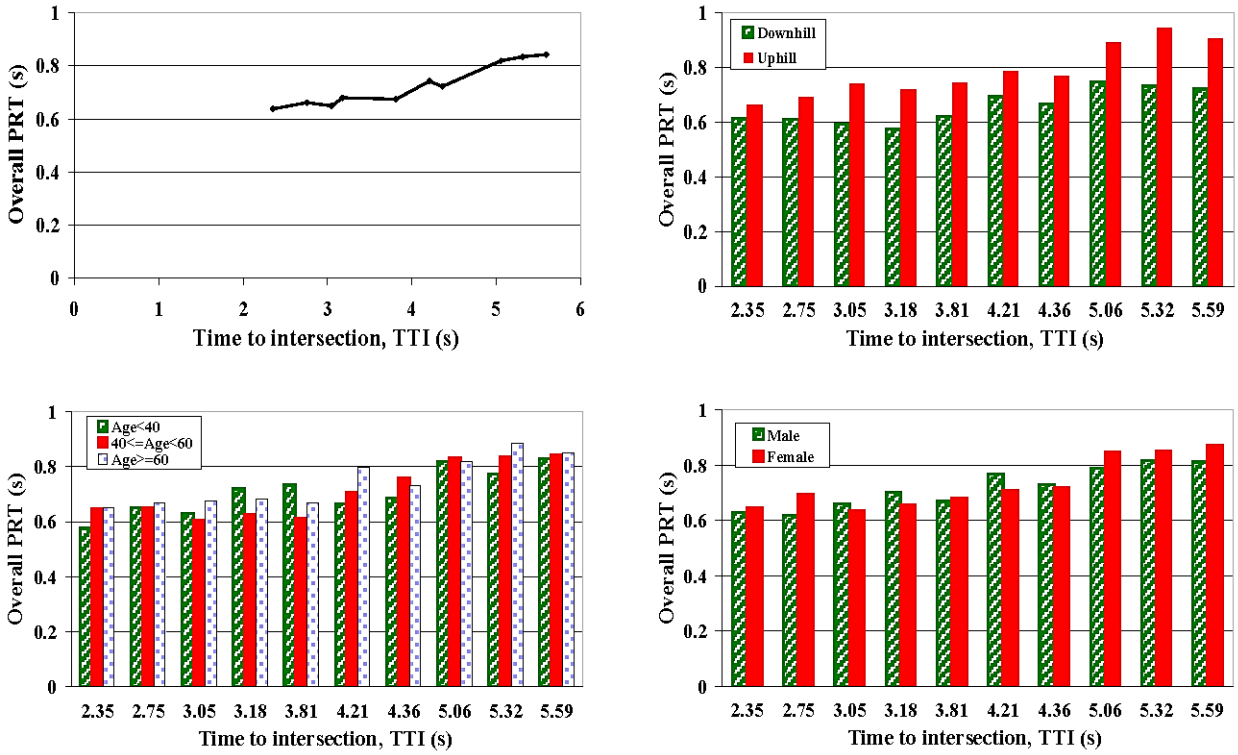

(b) Overall PRT

Figure 23: Mean Perception-Reaction Time as a Function of TTI, Age, and Gender (Cont'd)

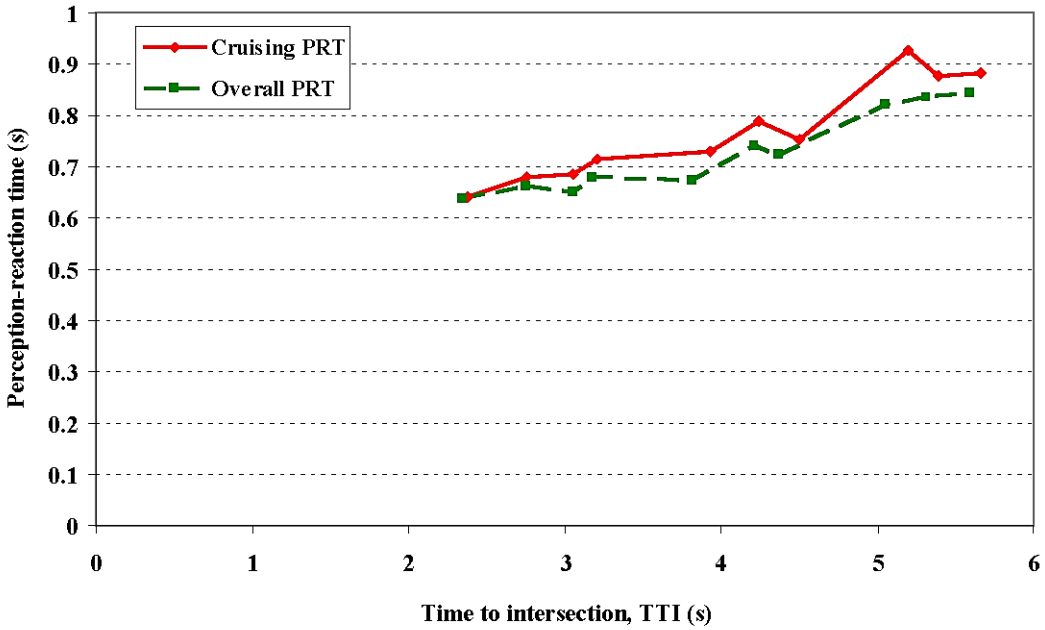

Figure 24: Cruising PRT and Overall PRT as a Function of TTI

6.2.2 Distribution of Driver Perception-Reaction Time from Dataset I

A total of 2016 valid data records were available for analysis from dataset I, of which 971 valid data records were for those who were instructed to drive at 72.4 km/h (45 mph) and 1045 valid observations were for a speed of 88.5 km/h (55 mph). The TTI for the 72.4 km/h instructed speed ranged from a minimum of 1.93 s to a maximum of 4.69 s with a mean equal to 3.59 s, a median of 3.66 s, and a standard deviation of 0.45 s. The remaining 1045 data records for an instructed speed of 88.5 km/h (55 mph) included TTIs ranging between 2.31 s to 5.33 s with a mean equal to 3.98 s, a median of 3.99 s, and a standard deviation of 0.53 s. In other words, drivers decelerated at farther distances when they traveled at higher speeds.

6.2.2.1 Frequency distributions of perception-reaction time

A study of driver PRTs at the onset of the yellow indication was performed considering all stopping events. As was noted earlier, it was possible to determine the approach speed of the vehicle, the TTI, and the brake application of the stopping vehicles from the data files. Using this information, PRT characteristics and profiles were examined. PRT was defined as the time elapsed between the onset of the yellow indication and the instant the driver started to press the brake pedal. The PRT ranged from a minimum of 0.22 s to a maximum of 1.52 s with a mean of 0.73 s, a median of 0.72 s, and a standard deviation of 0.18 s for the participants who were instructed to drive at 72.4 km/h (45 mph). Alternatively, the PRT ranged between 0.18 s and 1.53 s with a mean of 0.74 s, a median of 0.72 s, and a standard deviation of 0.18 s for those who were instructed to drive at 88.5 km/h (55 mph). The histogram for the observed PRTs of the 2016 stopping events for the two approach speeds is shown in Figure 25. These figures demonstrate that the driver PRTs were very similar for both instructed speeds.

The observed 15^{th}, 50^{th}, and 85^{th} percentile PRTs were 0.57, 0.72, and 0.92 s, respectively, in the case of the 72.4 km/h instructed speed; and were 0.58, 0.72, and 0.92 s, respectively, in the case of the 88.5 km/h instructed speed. The 85^{th} percentile is consistent with earlier studies which showed that the 85^{th} percentile PRT on high-speed intersection approaches (greater than 64 km/h or 40 mph) is in the range of 1.1 to 1.3 s. The lower value of PRTs in the current study may be attributed to the fact that the PRT was defined from the instant the signal indication changed to yellow until the driver touched the brake pedal, and not when the brake light was activated as in most studies; thus the PRT did not include the time lag from the instant the driver presses the brake pedal until the brake lights activate. Consequently, the results appear

to be consistent with other naturalistic field study findings. The data were sorted based on the driver's TTI, at the yellow-indication onset, into equal-sized bins (equal number of observations) and the average TTI and PRT for each bin was computed (for illustration purposes only) given the large number of observations.

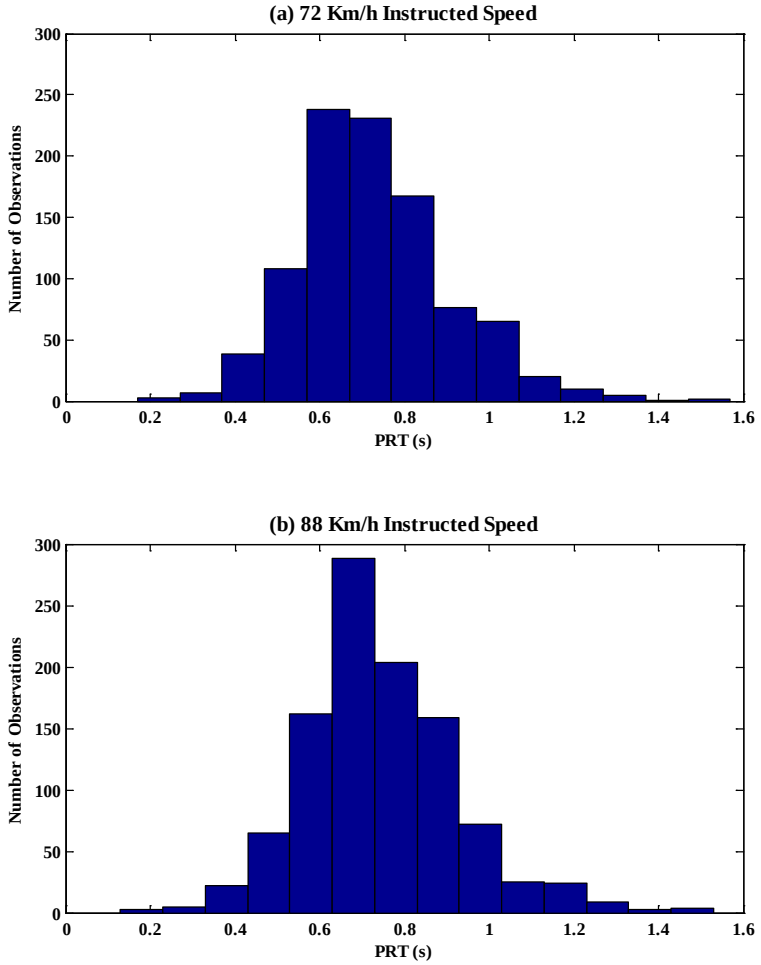

Figure 25: Histogram of Perception–Reaction Times

6.2.2.2 Effects of other variables on perception-reaction time

The experimental design accounts for the effects of the various factors on the driver PRT. These factors include: TTI; grade (uphill and downhill); age group (under 40-years-old, between 40 and 59-years-old, and 60 years of age or older); gender (male and female); and platoon (leading, following, and no other vehicle), for the two instructed speed levels (72.4 and 88.5 km/h). The design also includes repeated measurements for each driver and thus should be assessed relative to the average response made by the subject for all conditions and/or occasions.

In essence, each subject serves as his/her own control, and accordingly, the variability caused by differences in the average response is eliminated from the extraneous error variance. A consequence of this is that the power to detect the effects of within-subject experimental factors is increased compared to a standard between-subject design. The response variable (PRT) is likely correlated rather than independent even after conditioning on the explanatory variable. Consequently, the models need to include parameters linking the explanatory variables to the repeated response values in order to calibrate the parameters by explicitly accounting for the correlation structure of the repeated measurements.

A linear mixed model (LMM) introduces the needed correlations by formalizing the idea that an individual's pattern of responses is likely to depend on many characteristics of the subject, including some that are unobserved. These unobserved variables are then included in the model as random variables (i.e. random effects). The chi-square test statistic is used to test the null hypothesis. The chi-square statistic is 311.45, which is significant at the 5% level (P-value <0.0001). The random effect in the model has a variance that differs significantly from zero with a P-value <0.0001. The LMM analysis shows that all the experimental factors have a statistical significant effect on the PRT (p-values <0.001) except for the platoon factor although there is a statistical significant interaction with the TTI effect (p-value=0.004).

The mean PRT estimates at each TTI for the two instructed speed levels and approaches (uphill and downhill) were used to illustrate various trends and effects, as demonstrated in Figure 26. The results show that the PRT on either approach (i.e., on upgrade or downgrade) exhibit similar trends, with slightly higher PRTs in the case of the uphill approach. This difference, which is significant, demonstrates that drivers traveling uphill might be pressing harder on the accelerator and take longer to release their push and move their feet to press the brake pedal while drivers traveling downhill might not be pressing the accelerator in order to maintain some desired speed and are more alert because they realize that the deceleration level needed to stop the vehicle is greater. For TTIs in the range of 1.93 to 4.69 s, for the 72.4 kph instructed speed, the PRT ranged from 0.22 to 1.67 s for the uphill approach, and from 0.23 to 1.27 s for the downhill approach. Similarly, for the 88.5 km/h instructed speed, the PRT ranged from 0.22 to 1.53 s and from 0.18 to 1.43 s for the uphill and downhill approaches, respectively. These results occurred for TTIs ranging from 2.31 to 5.33 s, as shown in Table 7. There is statistical significant differences in PRTs was observed for the grade, t-value = -13.79, P < 0.0001, the

uphill (M = 0.78 s) and downhill (M = 0.68 s) conditions for the 72.4 km/h instructed speed, and also for the uphill (M = 0.77 s) and downhill (M = 0.71 s) conditions for the 88.5 km/h instructed speed.

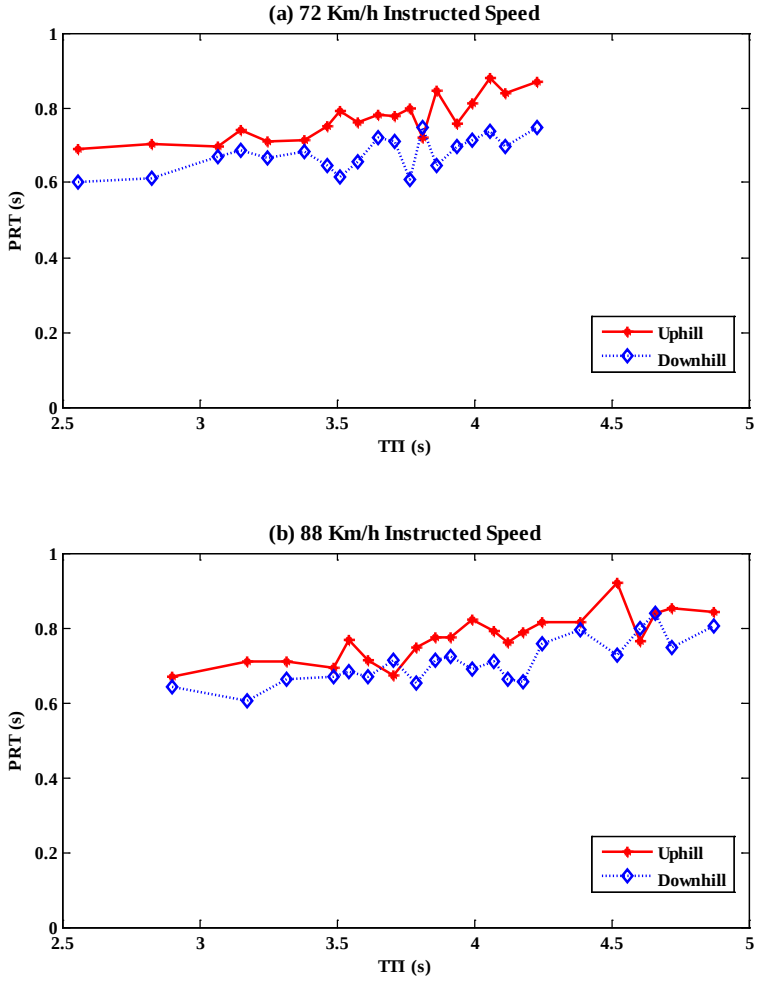

Figure 26: Effect of Roadway Grade on Perception–Reaction Times

Female drivers appeared to have slightly longer PRTs when compared to male drivers for both the 72.4 km/h (45 mph) and 88.5 km/h (55 mph) instructed speeds, as shown in Figure 27. For the 72.4 km/h instructed speed, the mean PRT was found to be 0.75 s for the female drivers and 0.71 s for the male drivers (as shown in Table 7); for the 88.5 km/h instructed speed, the mean PRT was found to be 0.76 s and 0.73 s for the female and male drivers, respectively. Although the difference in PRT between male and female drivers seems small, the t-statistic generated from the "Differences of Least Squares Means (DLSM)" of the SAS® software demonstrated that these differences are statistically significant with a p-value <0.001.

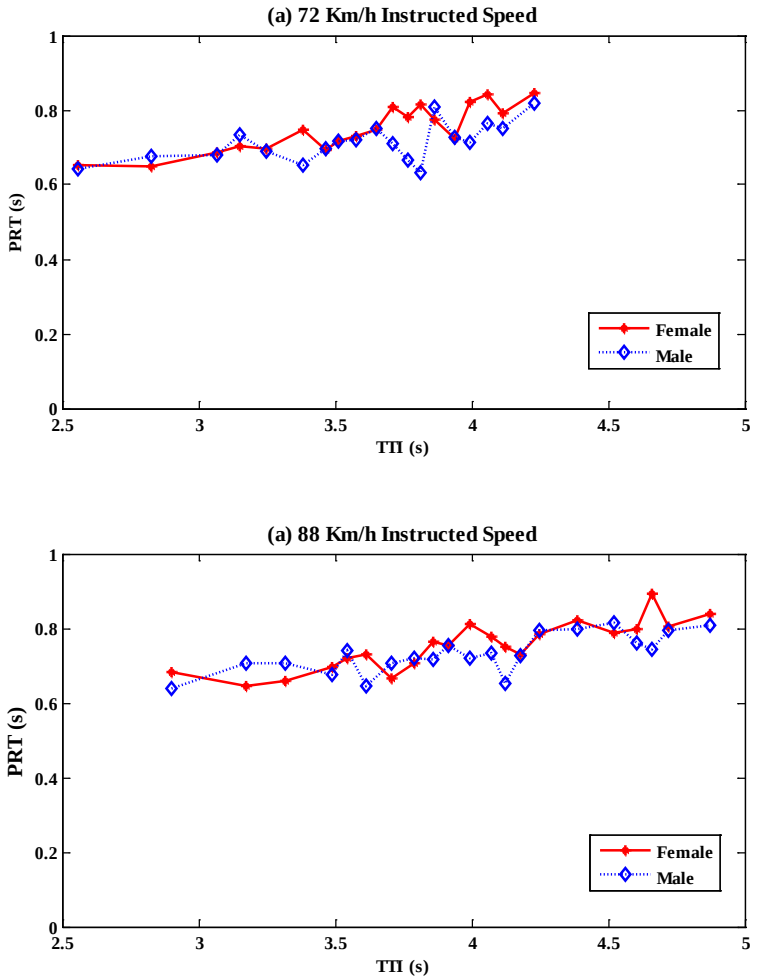

Figure 27: Effect of Gender on Perception–Reaction Times

The data were utilized to analyze differences in driver PRTs associated with driver age. The PRT for drivers 60 years of age and older (M = 0.79 s for the 72.4 km/h instructed speed and 0.81 s for the 88.5 km/h instructed speed) were found to be significantly higher than those for the 40 to 59 age group (M = 0.71 s for the 72.4 km/h and 0.72 s for the 88.5 km/h) and those for the under 40-years-old age group (M = 0.70 s for the 72.4 km/h and 0.69 s for the 88.5 km/h), as shown in Table 7 and Figure 28. The t-statistic generated from the DLSM for the three age groups demonstrated that statistical significant differences (P-values less than 0.0001) exist between all the driver age groups except for the under 40-years-old age group and the 40 to 59 age group (p-value=0.061).

Table 7: Descriptive Statistical Results of PRT for Grade, Age, Gender, and Platoon.

Variable		N	PRT (s)						
			Min	Max	Mean	15%	50%	85%	StD
Grade	Uphill	532	0.22	1.67	0.78	0.62	0.74	0.96	0.18
	Downhill	440	0.23	1.27	0.68	0.53	0.67	0.83	0.16
Gender	Female	462	0.23	1.42	0.75	0.58	0.73	0.93	0.18
	Male	510	0.22	1.67	0.71	0.57	0.68	0.88	0.17
Age	Older	317	0.42	1.42	0.79	0.63	0.78	0.93	0.15
	Middle	345	0.37	1.31	0.71	0.57	0.67	0.88	0.17
	Younger	310	0.22	1.67	0.70	0.53	0.67	0.88	0.20
Platoon	Following	309	0.22	1.47	0.74	0.58	0.72	0.92	0.18
	Leading	325	0.23	1.42	0.73	0.57	0.71	0.92	0.18
	Single	338	0.37	1.67	0.73	0.57	0.72	0.91	0.17
Overall		972	0.22	1.52	0.73	0.57	0.72	0.92	0.18

(a) 72 km/h instructed speeds

Variable		N	PRT (s)						
			Min	Max	Mean	15%	50%	85%	StD
Grade	Uphill	544	0.22	1.53	0.77	0.62	0.73	0.93	0.18
	Downhill	501	0.18	1.43	0.71	0.53	0.68	0.87	0.18
Gender	Female	489	0.22	1.53	0.76	0.61	0.73	0.92	0.18
	Male	556	0.18	1.48	0.73	0.57	0.68	0.92	0.18
Age	Older	360	0.51	1.48	0.81	0.66	0.78	0.97	0.16
	Middle	366	0.22	1.53	0.72	0.57	0.68	0.88	0.18
	Younger	319	0.18	1.32	0.69	0.57	0.68	0.85	0.17
Platoon	Following	336	0.22	1.48	0.78	0.62	0.77	0.93	0.18
	Leading	351	0.18	1.27	0.71	0.57	0.68	0.88	0.17
	Single	358	0.32	1.53	0.74	0.58	0.72	0.90	0.18
Overall		1045	0.18	1.53	0.74	0.58	0.72	0.92	0.18

(b) 88 km/h instructed speeds

A comparison of driver PRTs for the three different platooning scenarios (following, leading, or alone) was performed in order to characterize the effect of surrounding traffic on driver behavior. This behavior is important in designing traffic signal timing plans within the IntelliDrive^{SM} initiative. The analysis showed that there is no statistical significance in the mean PRT especially for platooning scenarios (Single and Leading) with P-value=0.29, while there are statistical significance differences between the other scenarios, as shown in TABLE 2. In addition, the results showed that the PRT was not impacted by the platooning scenario in the case of the 72.4 km/h instructed speed (M= 0.74, 0.73, and 0.73 s for the leading, following, and alone scenarios, respectively), as shown in Table 7 and Figure 29. Alternatively, in the case of the 88.5 km/h (55 mph) instructed speed, the mean PRTs for the following, leading, or single vehicle scenarios were 0.78, 0.71, and 0.74 s, respectively. Figure 29 shows that in the following platoon scenario, where the test vehicle was following another vehicle that proceeded through

the intersection without slowing or stopping, the mean PRT was higher compared to the other two scenarios. A potential explanation for the higher PRT values could be that because the lead vehicle ran through the intersection, the subject driver was also inclined to proceed. This initial inclination to run increased the deliberation time for the drivers that eventually elected to stop. In the case of the leading platoon condition, a shorter mean PRT was observed (compared to the other two scenarios) as the driver may have been forced to decide faster in order to provide the following vehicle with sufficient braking time to avoid a rear-end collision.

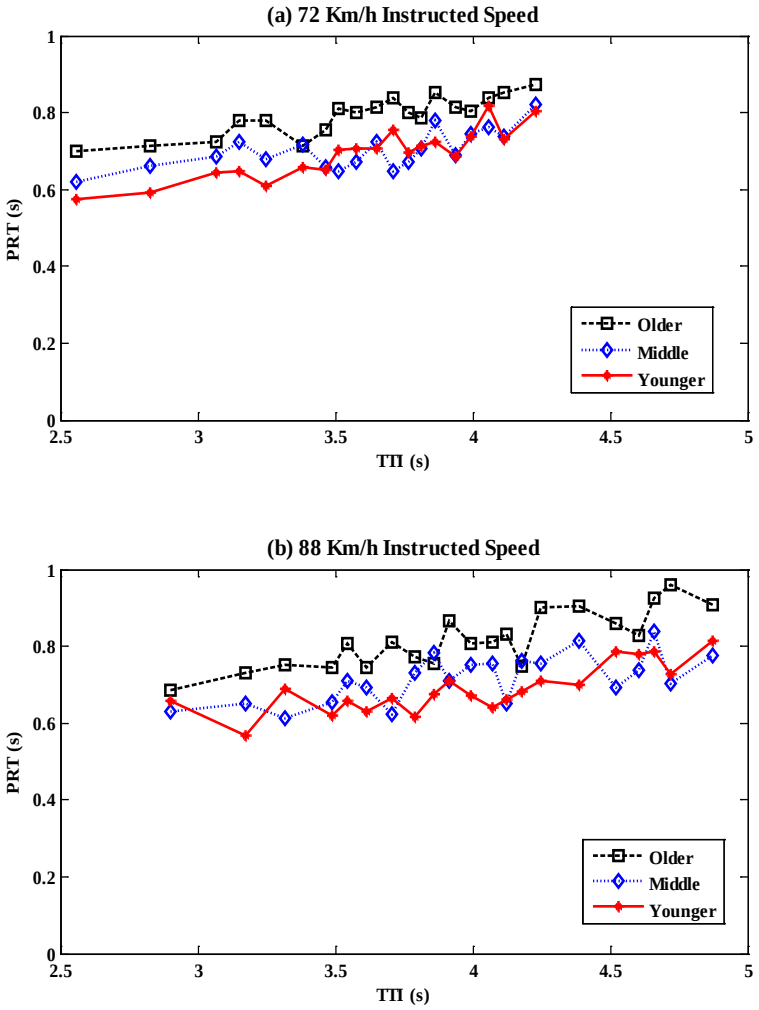

Figure 28: Effect of Age on Perception–Reaction Times

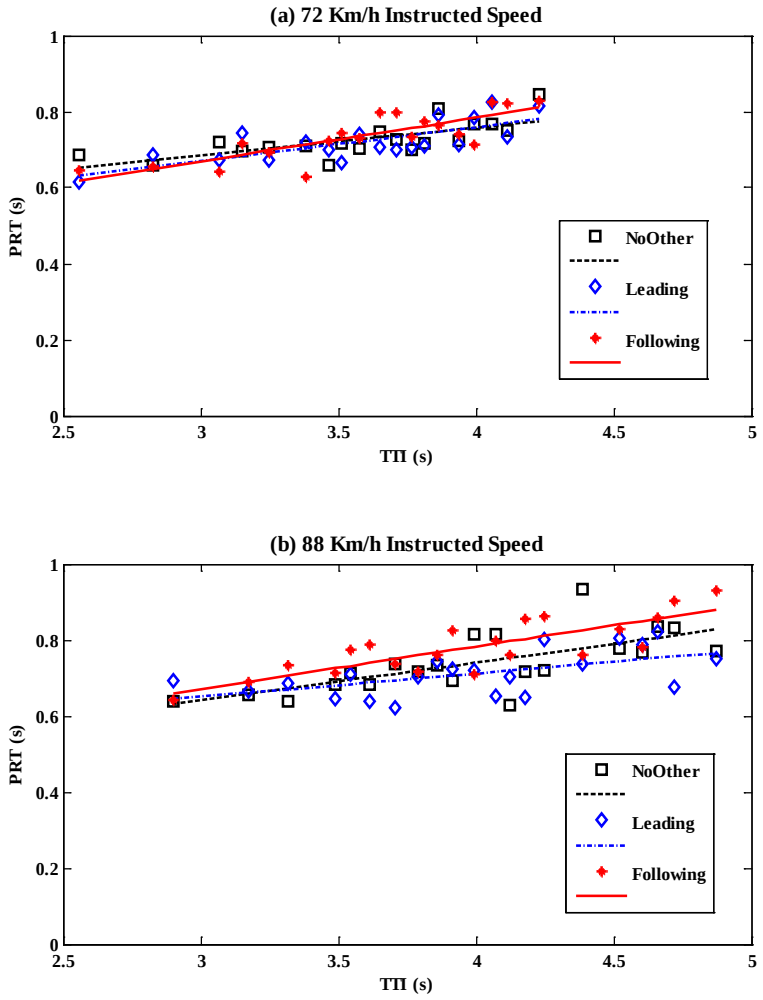

Figure 29: Effect of Surrounding Traffic on Perception–Reaction Times

The mean PRTs for the 4-second (72.4 km/h instructed speed) and 4.5-second (88.5 km/h instructed speed) yellow intervals were plotted against the TTI at the yellow interval change time, as shown in Figure 30. The results show that the PRT tends to increase as the TTI increases. For the range of TTIs from 4.69 to 1.93 s for the 72.4 km/h (45 mph) instructed speed, the PRT decreased from 1.53 to 0.22 s with a mean of 0.73s, while for the range of TTIs from 5.33 to 2.31 s for the 88.5 km/h (55 mph) instructed speed, the PRT decreased from 1.53 to 0.18 s with a mean of 0.74s. The figure demonstrates that the mean PRT curve for the 72.4 km/h (45 mph) instructed speed was higher than the 88.5 km/h (55 mph) instructed speed over the entire TTI range. This shift correlates to a lower PRT for those drivers traveling at higher speeds on the onset of the yellow interval. The results indicate a similar PRT trend at different speeds. The

results generated using the DLSM showed that the approach speed had no significant effect, with P-values equal to 0.059, on the average PRT.

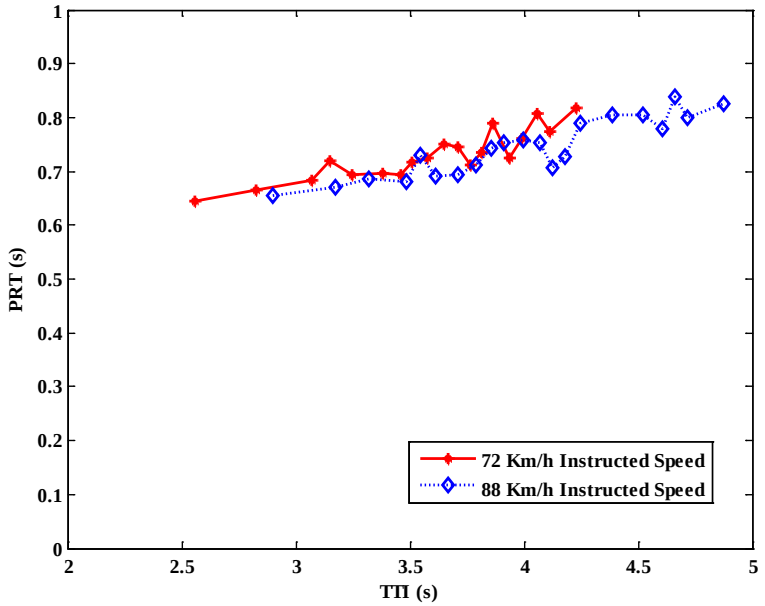

Figure 30: Effect of Vehicle Speed on PRTs

6.2.2.3 Statistical modeling of perception-reaction time

As previously mentioned, a total of 2016 stopping data records were available for the analysis. Using these observations, a stepwise linear regression model was fit to the data. After experimenting with different model forms, including absolute and normalized variables, the selected form is shown in Equation (14). The equation shows that the significant variables are driver's gender and age, roadway grade, TTI, yellow time, approaching speed and speed limit; whereas the platoon is not found to be significant.

$$t = \beta_0 + \beta_1 r + \beta_2 A + \beta_3 G + \beta_4 \frac{TTI}{y} + \beta_5 \frac{v}{v_f} + e_t \qquad (14)$$

where t is the perception-reaction time (s),
β_i's are model constants,
r is the gender (0 female and 1 male),
A is the age (years),
G is the roadway grade (percent/100),
TTI is the time-to-intersection (s),
y is the yellow time (s), and
v and v_f are the approaching speed and the speed limit (m/s).

The model calibrated coefficients and their corresponding P-values are summarized in Table 8, showing a good statistical fit. Although the model has a low adjusted-R^2 of 18 percent, there is a good relation between the PRT and each of the explanatory variables. Figure 31 shows histograms of the model residuals and the calibrated PRT values.

Table 8: Statistical PRT Model Calibration Results

Coefficients	Coefficient Values	P-value
β_0	0.7775	
β_1	-0.0415	0.0000
β_2	0.0025	0.0000
β_3	1.1966	0.0000
β_4	0.3980	0.0000
β_5	-0.4897	0.0000

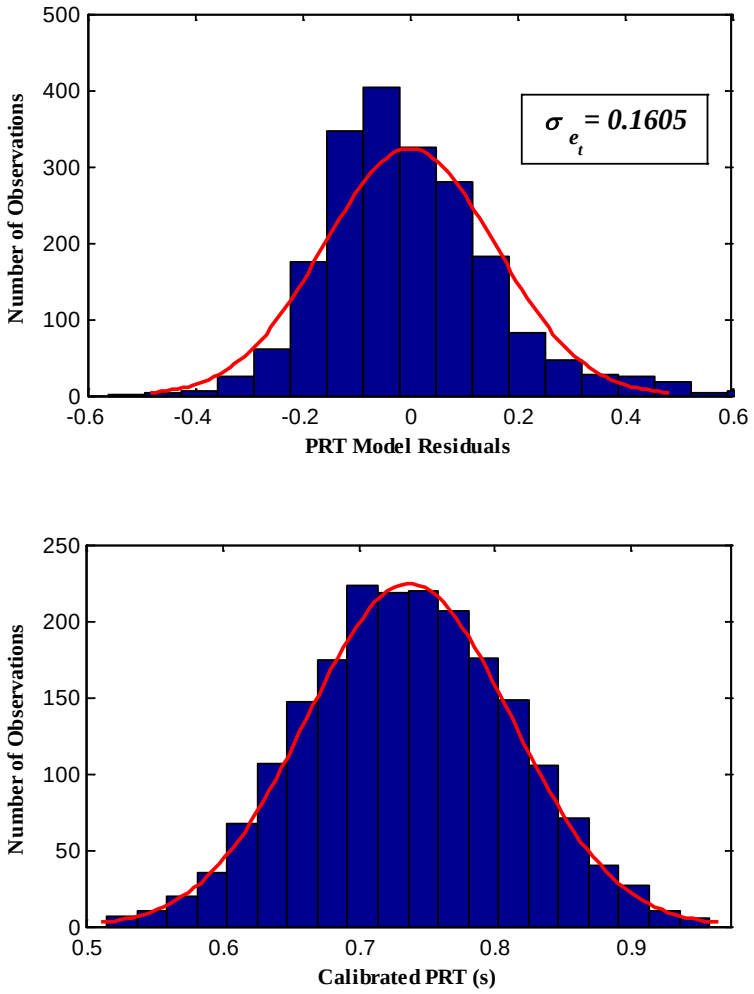

Figure 31: Histograms of Model Residuals and the Calibrated PRT

6.3 CHARACTERIZATION OF DRIVER DECELERATION LEVELS

In the case of PRT, it was interesting to investigate its different types of PRT separately (cruising and overall PRTs), from dataset II. However, this is not the case for the deceleration level. Therefore, the analysis of the deceleration levels is conducted only based on dataset I, in order to serve as an input for the upcoming tasks in this dissertation.

6.3.1 Distribution of Driver Deceleration Level from Dataset I

Similar to PRT analysis, a total of 2016 valid data records were available for analysis from dataset I, of which 971 valid data records were for those who were instructed to drive at 72.4 km/h (45 mph) and 1045 valid observations were for a speed of 88.5 km/h (55 mph).

6.3.1.1 Distribution of deceleration level

The deceleration levels at the onset of a yellow indication were found to vary considerably. As has been noted, it was possible to determine the approach speed to the intersection, the deceleration distance, and the deceleration time of the stopping vehicles from the field data. With this information, the effect of the approach speed and surrounding vehicles on the deceleration level characteristics and profiles was examined. Average deceleration levels were calculated in m/s^2 from the time the driver started to press the brake pedal after the onset of the yellow indication until the final speed of the deceleration event (this was less than 3.6 km/h [2.2 mph], which is the speed of a pedestrian).

The second-by-second speed profile data collected by the in-vehicle GPS unit in this study provides more accurate measurements of driver deceleration behavior such as the approach speed to the intersection, TTI, and the brake application of the stopping vehicles. The average deceleration levels for the deceleration event when the yellow indication was triggered at the signalized intersection can be estimated using Equation (15).

$$d_{avg} = \frac{v - v_o}{t \times 3.6} \tag{15}$$

where d_{avg} is the average deceleration level (m/s^2),
v is the vehicle speed at the instant the driver started to press the brake pedal after the onset of the yellow indication (km/h),
v_o is the final vehicle speed for the deceleration event (less than 3.6 km/h), and
t is the braking time (s).

The deceleration level ranged from a minimum of 2.31 m/s^2 (7.6 ft/s^2) to a maximum of 7.31 m/s^2 (24 ft/s^2) with a mean of 3.7 m/s^2 (12.1 ft/s^2) for the participants who were instructed to drive at 72.4 km/h (45 mph). These results are consistent with field experiments that were conducted for similar speeds. Alternatively, the deceleration level ranged between 2.3 m/s^2 (7.5 ft/s^2) and 7.28 m/s^2 (23.9 ft/s^2) with a mean equal to 3.91 m/s^2 (12.8 ft/s^2) for those who were instructed to drive at 88.5 km/h (55 mph), as demonstrated in Table 9.

Table 9: Descriptive Statistical Results of Deceleration Level for Grade, Age, Gender and Platoon

Variable		N	Min	Max	Mean	15%	50%	85%	StD
Grade	**Uphill**	532	2.31	7.31	3.65	3.00	3.54	4.37	0.71
	Downhill	440	2.31	7.25	3.75	3.12	3.58	4.48	0.71
Gender	**Female**	462	2.42	5.52	3.65	3.05	3.55	4.34	0.61
	Male	510	2.31	7.31	3.74	3.06	3.56	4.45	0.79
Age	**Older**	317	2.51	6.31	3.77	3.15	3.61	4.51	0.68
	Middle	345	2.31	7.31	3.69	2.98	3.50	4.46	0.83
	Younger	310	2.42	5.40	3.63	3.04	3.56	4.24	0.58
Platoon	**Following**	309	2.42	7.31	3.74	3.11	3.60	4.46	0.70
	Leading	325	2.31	7.25	3.71	3.10	3.55	4.38	0.71
	Single	338	2.42	7.20	3.65	2.98	3.50	4.40	0.72
Overall		971	2.31	7.31	3.70	3.05	3.55	4.39	0.71

(a) 72 km/h instructed speeds

Variable		N	Min	Max	Mean	15%	50%	85%	StD
Grade	**Uphill**	544	2.43	7.28	3.87	3.19	3.82	4.55	0.72
	Downhill	501	2.30	7.28	3.94	3.17	3.80	4.73	0.76
Gender	**Female**	489	2.30	6.47	3.84	3.15	3.75	4.58	0.69
	Male	556	2.43	7.28	3.96	3.20	3.88	4.64	0.78
Age	**Older**	360	2.30	5.89	4.08	3.33	3.98	4.86	0.69
	Middle	366	2.43	7.28	3.88	3.07	3.76	4.59	0.85
	Younger	319	2.51	5.81	3.75	3.15	3.70	4.39	0.61
Platoon	**Following**	336	2.51	7.28	3.96	3.19	3.88	4.78	0.72
	Leading	351	2.52	7.28	3.89	3.16	3.80	4.59	0.75
	Single	358	2.30	7.18	3.87	3.18	3.78	4.57	0.75
Overall		1045	2.30	7.28	3.91	3.17	3.82	4.61	0.74

(b) 88 km/h instructed speeds

The histogram for the observed deceleration levels of the 2016 stopping events for the two approach speeds are shown in Figure 32. These figures demonstrate that the driver deceleration levels were very similar for both instructed speeds. The data were then sorted based on the driver's TTI at the yellow-indication onset into equal-sized bins (i.e., equal number of observations); and the average TTI and deceleration levels for each bin were computed for illustration purposes only given the large number of observations.

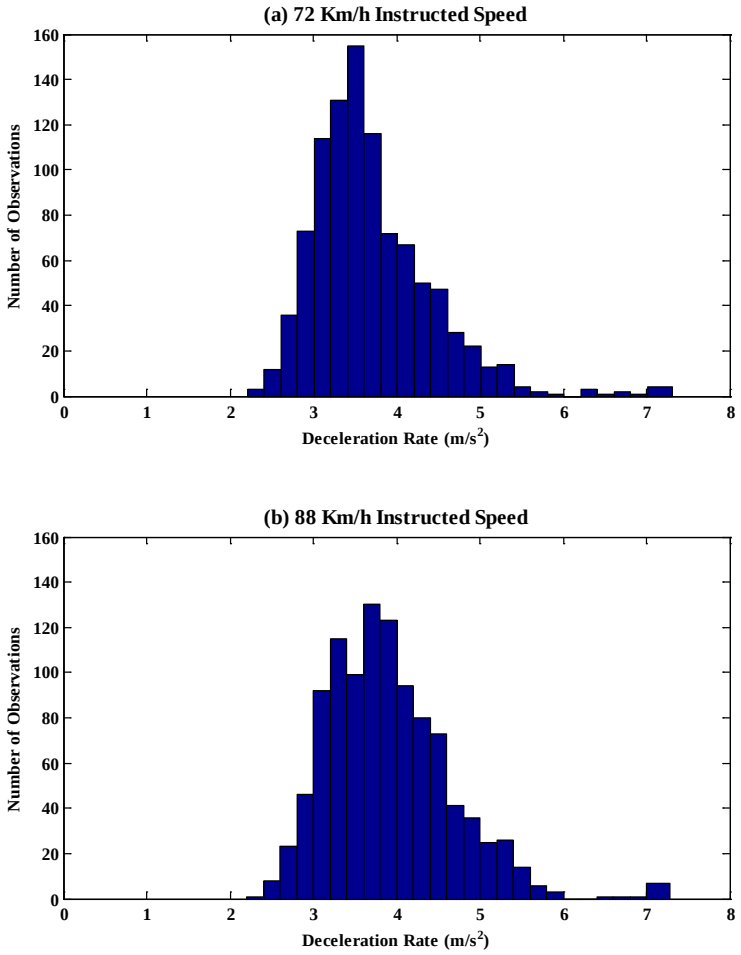

Figure 32: Histogram of Deceleration Levels

6.3.1.2 Effects of other variables on driver deceleration behavior

A linear mixed model (LMM) was conducted using the SAS® software to investigate the effects of the TTI, grade (uphill and downhill), age group (under 40-years-old, between 40 and 59-years-old, and 60 years of age or older), gender (male and female), platoon (leading, following, and no other vehicle), and approach speed (72.4 km/h and 88.5 km/h) on the average deceleration level. The effects of the various factors at each TTI on the driver deceleration levels for the two instructed speeds were used to illustrate various trends and effects, as demonstrated in Table 9. The chi-square test statistic is used to test the null hypothesis. The chi-square statistic is 227.73, which is significant at the 5 percent level (P-value <0.0001). The random effect in the model has a variance that differs significantly from zero with a P-value <0.0001. The LMM analysis shows that all the experimental factors have a statistical significant effect on the deceleration levels (P-values <0.001) except for the gender and platoon factors.

The mean deceleration level estimates at each TTI for the two instructed speed levels and approaches (uphill and downhill) were used to illustrate various trends and effects, as demonstrated in Figure 33. The results show that the deceleration level on either approach (i.e., on upgrade or downgrade) exhibit similar trends, with slightly higher deceleration levels in the case of the downhill approach. This difference, which is significant, demonstrates that the deceleration needed to stop the car when driving downhill would be greater than when traveling uphill, as would be expected. For TTIs in the range of 1.93 to 4.69 s, for the 72.4 km/h (45 mph) instructed speed, the deceleration level ranged from 2.31 m/s^2 (7.6 ft/s^2) to 7.31 m/s^2 (24 ft/s^2) for the uphill approach, and from 2.31 m/s^2 (7.6 ft/s^2) to 7.25 m/s^2 (23.8 ft/s^2) for the downhill approach. Similarly, for the 88.5 km/h (55 mph) instructed speed, the deceleration level ranged from 2.43 m/s^2 (8 ft/s^2) to 7.28 m/s^2 (23.9 ft/s^2) and 2.3 m/s^2 (7.5 ft/s^2) to 7.28 m/s^2 (23.9 ft/s^2) for the uphill and downhill approaches, respectively. These results occurred for a mean TTI from 2.31 to 5.33 s, as shown in Table 9. The t-statistic generated from the "Differences of Least Squares Means (DLSM)" demonstrated that these differences are statistically significant (t-value = 5.28, P-value < 0.0001).

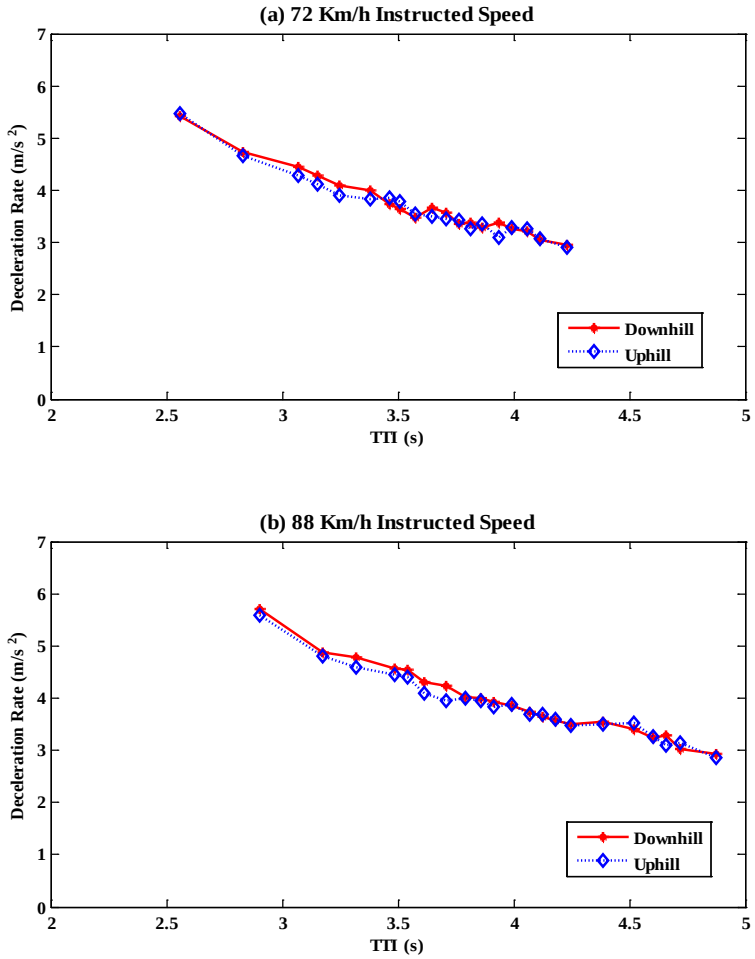

Figure 33: Effect of Roadway Grade on Deceleration Levels

Male drivers appeared to show slightly higher levels of deceleration when compared to female drivers for both the 72.4 km/h (45 mph) and 88.5 km/h (55 mph) instructed speeds, as shown in Figure 34. For the 72.4 km/h (45 mph) instructed speed, the mean deceleration level was found to be 3.65 m/s^2 (12 ft/s^2) for the female drivers and 3.74 m/s^2 (12.3 ft/s^2) for the male drivers as shown in Table 9; for the 88.5 km/h (55 mph) instructed speed, the mean deceleration level was found to be 3.84 m/s^2 (12.6 ft/s^2) and 3.96 m/s^2 (13 ft/s^2) for the female and male drivers, respectively. The figure demonstrates that the mean deceleration level curve for male drivers was shifted to the right when compared to female drivers in the range between the 2.6 to 3.5 s yellow-indication trigger times for the 72.4 km/h (45 mph) instructed speed, and from 2.9 to 3.9 s for the 88.5 km/h (55 mph) instructed speed. This shift correlates to an increase in the deceleration level for male drivers relative to female drivers at short trigger times. The t-statistic

generated from the DLSM demonstrates that these differences are not statistically significant with a p-value=0.08.

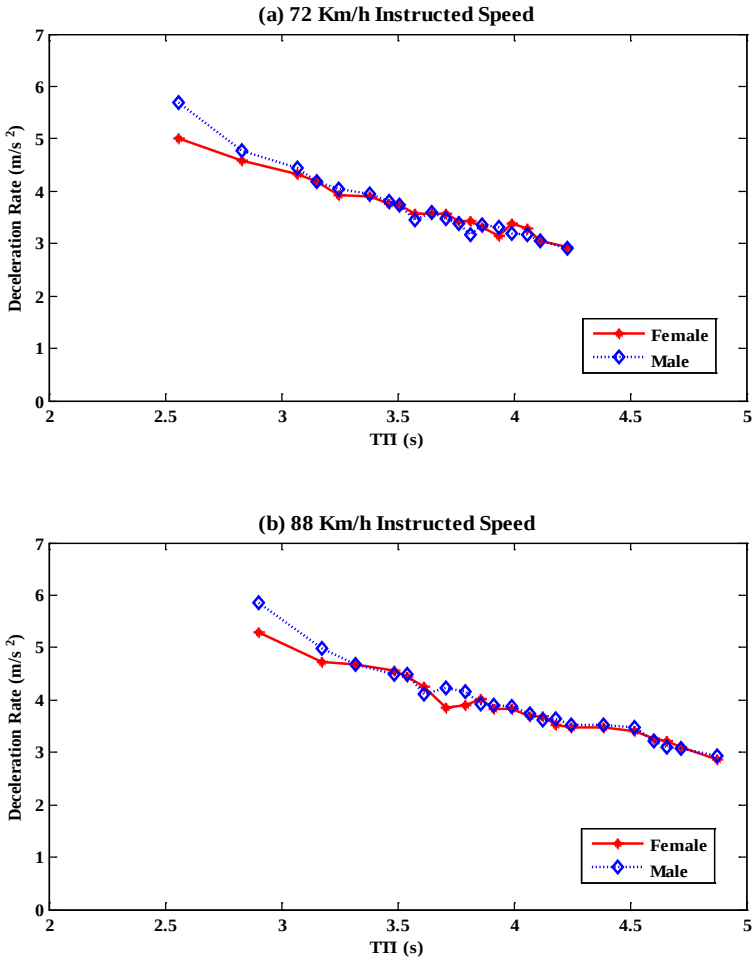

Figure 34: Effect of Gender on Deceleration Levels

In addition, the data were utilized to analyze the deceleration levels associated with different driver age groups (under 40-years-old, between 40 and 59-years-old, and 60 years of age or older). The analysis of the deceleration levels for both instructed speeds showed that the deceleration levels chosen by drivers 60 years of age or older (M = 3.61 m/s^2 for the 72.4 km/h and 3.98 m/s^2 for the 88.5 km/h) were significantly higher than those of the age group between 40 and 59 years old (M = 3.5 m/s^2 for the 72.4 km/h and 3.76 m/s^2 for the 88.5 km/h) and those under 40 years old (M = 3.56 m/s^2 for the 72.4 km/h and 3.7 m/s^2 for the 88.5 km/h) as shown in Table 9 and Figure 35.

The t-statistic generated from the DLSM for the three age groups demonstrated that statistically significant differences (P-values less than 0.0005) exist between all the driver age groups except for those under 40 years old and the 40 to 59 age group (p-value=0.92). These findings are consistent with the conclusions of the earlier study [40]. It is found that older drivers (60 years of age or older) applied greater deceleration levels when compared to mid-age drivers in the 40 to 59 age group. It is hypothesized that the higher deceleration levels for the older driver population (60 years of age or older) could be because they are typically more cautious and thus apply higher deceleration levels in order to ensure that they stop prior to the stop line.

A comparison of driver deceleration levels for the three different platoon scenarios (following, leading, or alone) was performed in order to characterize the effect of surrounding traffic on driver behavior. This behavior is important in designing traffic signal timing plans within the IntelliDrive^{SM} initiative in order to improve the safety of signalized intersections. The observed 15th, 50th, and 85th percentile deceleration levels in the following platoon scenario, where the test vehicle was following another vehicle that proceeded through the intersection without slowing or stopping, were higher compared to the other two scenarios as shown in Table 9 and Figure 36. The observed 15th, 50th, and 85th percentile deceleration levels in the following platoon scenario were 3.11 m/s^2 (10.2 ft/s^2), 3.6 m/s^2 (11.8 ft/s^2), and 4.46 m/s^2 (14.6 ft/s^2), respectively, in the case of the 72.4 km/h (45 mph) instructed speed compared to 3.1 m/s^2 (10.2 ft/s^2), 3.55 m/s^2 (11.6 ft/s^2), and 4.38 m/s^2 (14.4 ft/s^2) in the leading platoon scenario and 2.98 m/s^2 (9.8 ft/s^2), 3.5 m/s^2 (11.5 ft/s^2), and 4.4 m/s^2 (14.4 ft/s^2) in the single vehicle scenario. Also, in the 88.5 km/h (55 mph) instructed speed case, the observed deceleration levels for the 15th (3.19 m/s^2), 50th (3.88 m/s^2), and 85th (4.78 m/s^2) percentile in the following platoon scenario were higher compared to the leading platoon (3.16 m/s^2, 3.8 m/s^2, and 4.59 m/s^2) and the single vehicle (3.18 m/s^2, 3.78 m/s^2, and 4.57 m/s^2) scenarios. A potential explanation for the higher deceleration level values could be that because the lead vehicle ran through the intersection the subject driver was also inclined to proceed. This initial inclination to run resulted in the driver reacting later and thus forced the drivers to apply higher deceleration levels in order to ensure that they stop prior to the stop line.

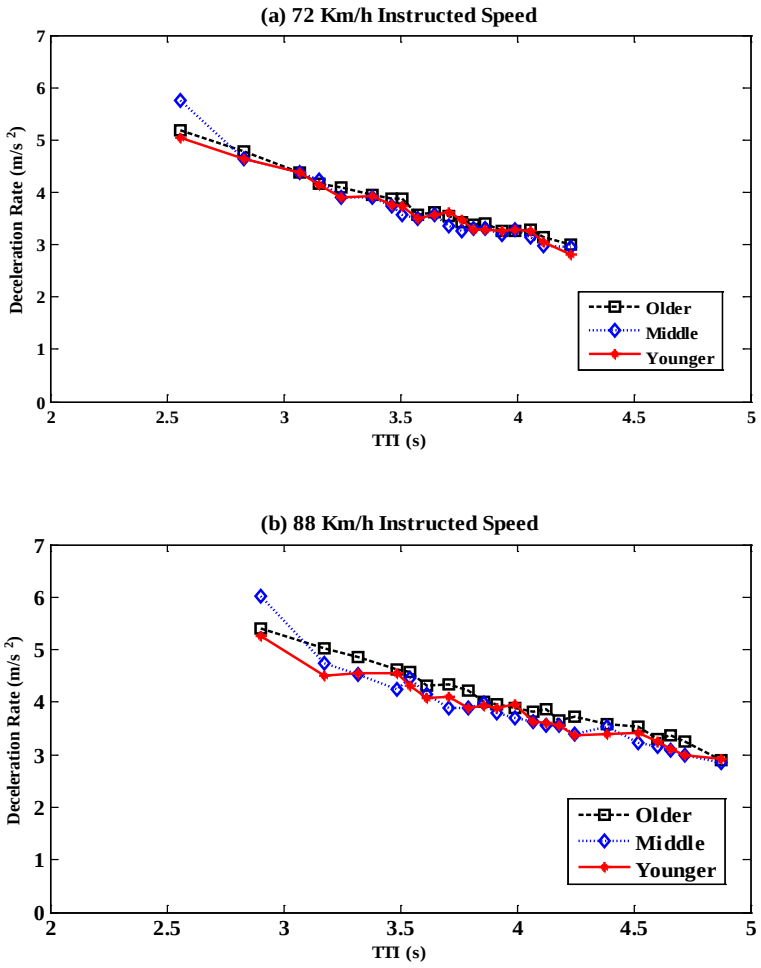

Figure 35: Effect of Age on Deceleration Levels.

The DLSM analysis showed that there is no statistically significant difference in the deceleration levels for the single and leading platooning scenarios with a P-value of 0.66, while there are statistically significant differences between the other scenarios. Another hypothesis that is common is the assumption that drivers who lead another vehicle (leading case) exert lesser deceleration levels in order to ensure that the vehicle behind them has sufficient time to stop without colliding with them. The results of the experiment clearly indicate that this hypothesis is not true and that there is no difference between a single vehicle on the roadway and a leading vehicle in terms of vehicle deceleration behavior at the onset of a yellow indication.

The mean deceleration levels for the 4-second (72.4 km/h instructed speed) and 4.5-second (88.5 km/h instructed speed) yellow intervals were plotted against the TTI at the yellow interval change time, as shown in Figure 37. The figure demonstrates that the mean deceleration level curve for the 88.5 km/h (55 mph) instructed speed was higher than the 72.4 km/h (45 mph)

instructed speed over the entire TTI range. This shift correlates to a higher deceleration level for those drivers traveling at higher speeds at the onset of the yellow interval. The results, however, indicate a similar deceleration level trend at different speeds. The results generated using the DLSM showed that the approach speed had a significant effect on the average deceleration level, with P-values less than 0.0001.

The results show that the deceleration level tends to increase as the TTI decreases. For the range of mean TTIs from 4.23 to 2.56 s for the 72.4 km/h (45 mph) instructed speed, the deceleration level increased from 2.31 to 7.31 m/s^2 (7.6–24 ft/s^2) with a mean of 3.7 m/s^2 (12.1 ft/s^2), while for the range of mean TTIs from 4.87 to 2.9 s for the 88.5 km/h (55 mph) instructed speed, the deceleration level increased from 2.3 to 7.28 m/s^2 (7.5–23.9 ft/s^2) with a mean of 3.91 m/s^2 (12.8 ft/s^2).The observed 15^{th}, 50^{th}, and 85^{th} percentile deceleration levels were 3.05 m/s^2 (10 ft/s^2), 3.55 m/s^2 (11.6 ft/s^2), and 4.39 m/s^2 (14.4 ft/s^2), respectively, in the case of the 72.4 km/h (45 mph) instructed speed compared to 3.17 m/s^2 (10.4 ft/s^2), 3.82 m/s^2 (12.5 ft/s^2), and 4.61 m/s^2 (15.1 ft/s^2) for the 88.5 km/h (55 mph) instructed speed case.

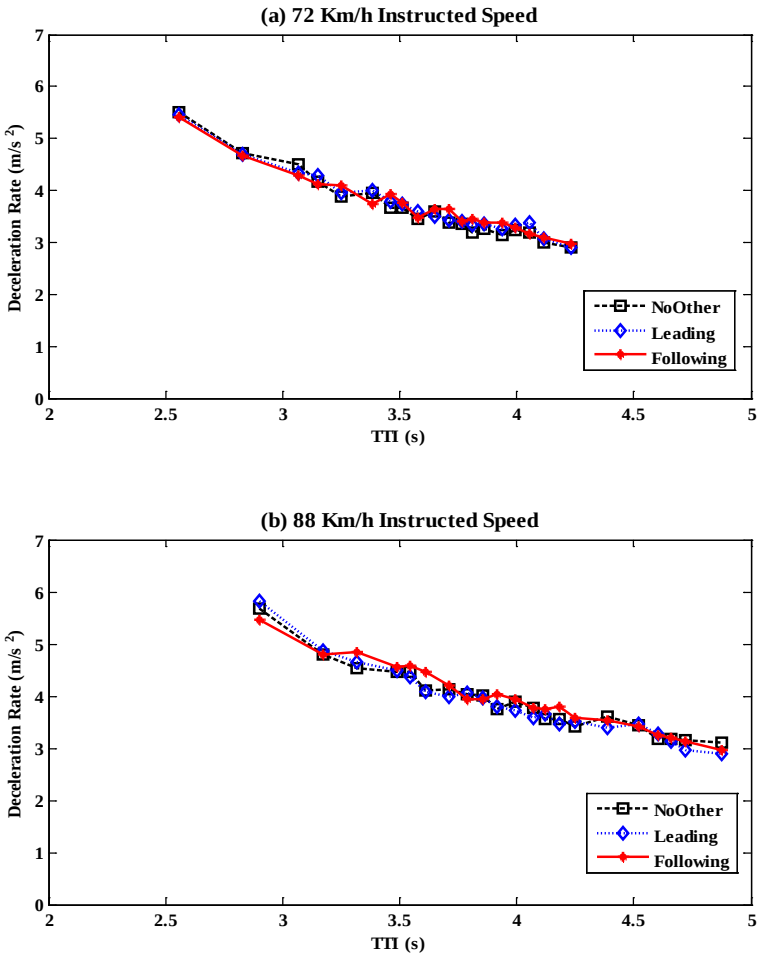

Figure 36: Effect of Surrounding Traffic on Deceleration Levels

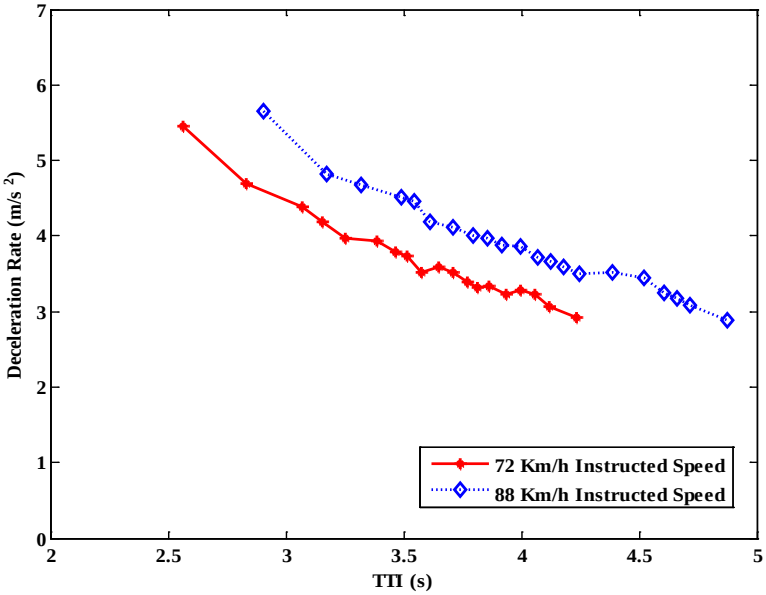

Figure 37: Effect of Vehicle Speed on Deceleration Levels

6.3.1.3 Statistical modeling of driver deceleration behavior

As previously mentioned, a total of 2016 stopping data records were available for the analysis. Using the data, a stepwise linear regression model was tested. After trying many model forms, including absolute and normalized variables, the final form that was selected is shown in Equation (16). The equation shows that the significant variables are driver's gender and age, roadway grade, TTI, yellow time, approaching speed, speed limit, and PRT; whereas the platoon is not found to be significant.

$$d = \beta_0 + \beta_1 r + \beta_2 A + \beta_3 G + \beta_4 \frac{TTI}{y} + \beta_5 \frac{v}{v_f} + \beta_6 t + e_d \quad (16)$$

where d is the deceleration level (m/s^2),
β_i's are model constants,
r is the driver gender (0 female and 1 male),
A is the driver age (years),
G is the roadway grade (percent/100),
TTI is the time-to-intersection (s),
y is the yellow time (s),
v and v_f are the approaching speed and the speed limit (m/s), and
t is the perception-reaction time (s).

The model calibrated coefficients and their corresponding P-values are summarized in Table 10, showing a good statistical fit. Contrary to the PRT model, the deceleration model has a good adjusted-R^2 of 85.6 percent. Figure 38 shows histograms of the model residuals and the calibrated deceleration levels' values.

Table 10: Statistical Deceleration Level Model Calibration Results

Coefficients	Coefficient Values	P-value
β_0	6.1048	
β_1	0.0977	0.0000
β_2	-0.0008	0.0289
β_3	-2.8531	0.0000
β_4	-6.0033	0.0000
β_5	1.9372	0.0000
β_6	1.4575	0.0000

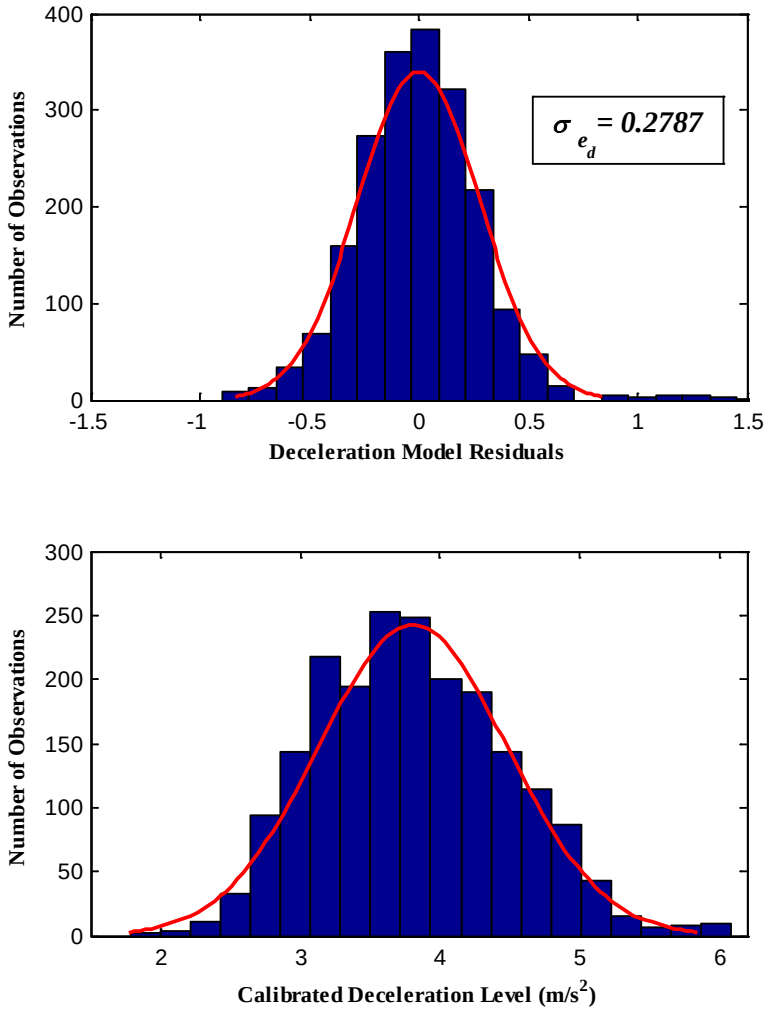

Figure 38: Histograms of Model Residuals and the Calibrated Deceleration Level

6.4 CONCLUSIONS AND RECOMMENDATIONS

The driver PRT and the deceleration behavior are characterized in this chapter as the major driver stopping behavior attributes. First, the different components of the PRTs form dataset II were analyzed separately as cruising PRT and overall PRT. Both cruising and overall PRTs from dataset II were not dependent on driver age and gender, whereas both increase when the TTI increases. With respect to the PRT distributions from dataset I, it was demonstrated that the driver PRT is higher for female and older drivers compared to younger male drivers. The PRT is also larger for vehicles traveling uphill given that the driver is typically accelerating when the yellow indication is initiated. Driver PRTs are typically higher if they are following a vehicle that runs a yellow light, whereas driver PRTs decrease when they are followed by another vehicle. In general, the PRT values from both datasets are found consistent with earlier

studies, which demonstrates that the driver behavior observed in the controlled field experiment appear to be consistent with naturalistic and non-obtrusive field-observed driver behavior.

The characterization of the deceleration level from dataset I indicated that driver deceleration levels are significantly higher than the 3 m/s^2 deceleration level used in the state-of-the-practice traffic signal design guidelines. The results demonstrate that driver deceleration levels are higher at shorter TTIs at the onset of yellow. Furthermore, younger (less than 40 years old) and older (60+ years old) drivers employ greater deceleration levels compared to middle-aged drivers (40 to 59 years old). A driver following another vehicle that proceeds legally through the intersection without stopping exerts higher deceleration levels compared to drivers driving alone or leading another vehicle. Drivers leading a platoon of vehicles are not affected by the vehicles behind them with regards to their deceleration behavior.

Finally, the statistical modeling of both attributes (PRT and deceleration) based on dataset I showed that gender, age, TTI, yellow time, and ratio of approaching speed to speed limit; are significant explanatory variables, and that the deceleration level depends on the PRT.

CHAPTER 7 STOCHASTIC PROCEDURE FOR COMPUTING THE DURATION OF THE YELLOW INTERVAL AT SIGNALIZED INTERSECTIONS

7.1 INTRODUCTION

After fulfilling the first two objectives of this dissertation by having the different driver behavior attributes characterized in Chapter 5 and Chapter 6, the third objective of this dissertation is fulfilled in this chapter. A novel approach for computing the clearance interval duration is developed in this chapter. The proposed procedure accounts for the reliability of the yellow time design (probability that drivers do not encounter a dilemma zone). Using this approach lookup tables are developed to assist practitioners in the design of yellow timings, based on the variation between different driver populations at different intersections. Furthermore, the concept is extended to utilize the drivers persona attributes (age and gender) in order to develop customized clearance warnings for each individual driver. Such extension could be integrated as part of the IntelliDrive^{SM} initiative. It is worth mentioning here that the analysis in this chapter is published in [67].

7.2 PROPOSED PROCEDURE FOR YELLOW INTERVAL DESIGN

After characterizing the driver stopping behavior attributes, including PRT and deceleration level, the analysis moves to the yellow-time design. As mentioned earlier, the current guidelines for computing the traffic signal clearance interval consider a fixed 1.0 s PRT and 3.0 m/s^2 (10.0 ft/s^2) deceleration level. The use of constant deterministic values for the PRT and the deceleration level is simplistic and does not allow the practitioner to make trade-off decisions between safety and operational considerations. Furthermore, the current approach fails to account for variations between different drivers approaching the same intersection at the onset of yellow. These variations include variations in each driver's PRT and deceleration level. Such variations are confirmed based on the above analyses made on both PRT and deceleration levels. Due to these variations, the standard yellow interval (based on a 1.0 s PRT and a 3.0 m/s^2 deceleration level) may be insufficient for some drivers when their PRT is longer than 1.0 s and/or their deceleration rate is less than 3.0 m/s^2. On the other hand, the standard yellow interval may be more than sufficient for drivers with PRTs shorter than 1.0 s and/or deceleration

rates greater than 3.0 m/s^2. Accordingly, it is more appropriate to consider: first, the differences in average PRT and deceleration levels between different driver populations at different intersections, and second, the differences in individual PRT and deceleration levels between different drivers within a driver population at a specific intersection. In this section, the yellow clearance interval calculation formula, presented earlier in Equation (3), is used to conduct a Monte Carlo (MC) simulation exercise to model the required yellow time based on the actual mean values and the statistical models calibrated earlier in Chapter 6 for the PRT and the deceleration level. The yellow time formula and the two models are listed again in Equations (17), (18) and (19) for the reader's convenience.

$$y = t + \frac{v}{2\left(d \pm g G\right)} \tag{17}$$

$$t = 0.7775 - 0.0415\, r + 0.0025\, A + 1.1966\, G + 0.3980\, \frac{TTI}{y} - 0.4897\, \frac{v}{v_f} + e_t \tag{18}$$

$$d = 6.1048 + 0.0977\, r - 0.0008\, A - 2.8531\, G - 6.0033\, \frac{TTI}{y} + 1.9372\, \frac{v}{v_f} + 1.4575\, t + e_d \tag{19}$$

where y is the duration of the yellow interval (s),
t is the perception-reaction time (s),
v is the approaching speed (m/s),
d is the deceleration level (m/s^2),
g is the gravitational acceleration (9.81 m/s^2),
G is the roadway grade (percent/100),
r is the gender (0 female and 1 male),
A is the age (years),
TTI is the time-to-intersection (s), and
v_f is the speed limit (km/h).

The purpose of the Monte Carlo simulation of the yellow time computation is twofold: first is to compare the yellow timings derived using the field-observed mean PRT and/or deceleration level versus the current guideline values, and second is to develop a yellow time lookup table as an example illustration for the proposed procedure.

In order to model the required yellow time, a Monte Carlo simulation considering a sample of 100,000 drivers is simulated by randomly generating the independent variables affecting the PRT and the deceleration level with the corresponding yellow time. These variables listed above include the driver's gender and age, roadway grade, TTI, and approach speed. In

order to generate a TTI distribution, a uniform random number generator is used to produce TTI values from a range that is slightly larger than the option zone boundaries corresponding to the posted speed limit. On the other hand, the approach speed is generated using the empirical distribution of the speed observations. However, in order to generalize the approach speed distribution to be able to generate a speed distribution for any posted speed limit, the actual speed distribution for the 88.5 km/h (55 mph) instructed speed is shifted left by the difference between its mean and the mean of the 72.4 km/h (45 mph) instructed speed, and then both distributions are combined resulting in one generalized empirical distribution for the 72.4 km/h (45 mph) speed limit. Accordingly, in order to generate a speed distribution for any speed limit other than 72.4 km/h (45 mph), the generalized empirical distribution is shifted by the difference between the 72.4 km/h (45 mph) and the desired speed limit.

7.3 IMPACTS OF PRT AND DECELERATION LEVEL ON YELLOW TIME COMPUTATION

In order to examine the impacts of PRT and deceleration level, a posted speed limit of 45 mph (72.4 km/h) and a level roadway (G = 0%) are considered. Four MC sample realizations of the yellow times are generated. The first sample is constructed using the current guideline deterministic values for PRT (1 s) and deceleration level (3 m/s^2). Subsequently, two samples are generated by replacing the deterministic PRT value by the actual PRT mean value that was observed in the study (0.74 s) while using the guideline deceleration level and vice versa with the field-observed mean deceleration level (3.81 m/s^2). One last sample is made using the actual mean values for both PRT and deceleration levels. The histograms and the cumulative distributions of the four realizations and their corresponding statistics are presented in Figure 39. Traditionally, the recommended yellow time for the 72.4 km/h (45 mph) speed limit is 4.3 s. In order to compare the simulated yellow time distribution to the deterministic guideline yellow time; the percentile corresponding to the 4.3-second yellow time is determined and compared to the 85th percentile yellow time.

It can be seen from Figure 39 that using the proposed 1-second PRT and 3 m/s^2 deceleration level requires an 85th-percentile yellow time of approximately 4.53 s, which is longer than the 4.3-second recommended yellow time. The recommended yellow time corresponds to only a 12.6 percentile, which means that most of the drivers will encounter a yellow time that is shorter than what is needed; i.e., they will be trapped in a dilemma zone. In

order for these drivers to be able to avoid being in a dilemma zone, they either need to react faster (have short PRTs) and/or brake harder (have higher deceleration levels). It is interesting that this conclusion is consistent with the actual data, where the mean PRT is 0.74 s and the mean deceleration level is 3.81 m/s^2. It can be seen from the figure that when the PRT is equal to 0.74s while maintaining the 3 m/s^2 deceleration, the recommended yellow time of 4.3 s is found to be sufficient for 91.3 percent of the drivers. On the other hand, increasing the deceleration level to 3.81 m/s^2, with a 1-second PRT, makes the maximum required yellow time (~4.23 s) even less than the recommended yellow time. Almost the same findings are observed when adopting both adjustments: a short PRT and a higher deceleration level.

7.4 LOOKUP TABLE FOR YELLOW CLEARANCE INTERVALS

A lookup table is developed that computes the yellow time duration based on different posted speed limits, different roadway grades, and a reliability factor (percentage of drivers that are not trapped in the dilemma zone [percentile]). As an example illustration, three posted speed limits are presented here: 35 mph (56.3 km/h), 45 mph (72.4 km/h), and 55 mph (88.5 km/h). Also, three roadway grades are presented ranging from -4% downhill to +4% uphill. Table 11 summarizes the different yellow times corresponding to each speed limit, grade, and reliability level.

This table serves as a simple lookup table to compute the required yellow time for a specific intersection at the desired reliability level depending on the importance of the intersection and the traffic volumes on its approaches.

The potential benefits from using the reliability measure in computing the yellow time can be either savings in the number of potential crashes (safety benefits) or enhancements in the approach capacity. In order to illustrate both types of benefits, the zero-percent roadway grade situation in the lookup table (Table 11) is considered for illustration purposes. Based on the current yellow timing guidelines, the required yellow time for each speed limit would be 3.5, 4.3, and 5.0 seconds for the 35, 45, and 55 mi/h, respectively. It can be seen from Table 11 that these yellow times correspond to reliability factors of 90%, 97%, and 99% for the three speed limits. These can be translated into savings in the potential dilemma zone crashes of 10%, 3%, and 1%, if the maximum yellow times (corresponding to 99.9% reliability) were adopted. According to the General Estimates System (GES) of the NHTSA, the number of signalized intersection

crashes in 2000 nationwide was 545,000 [2]. Accordingly, the crash savings from the proposed yellow time lookup table ranging between 1% and 10% are equivalent to total potential savings from 5,450 to 54,500 in signalized intersection crashes. Furthermore, with respect to the efficiency benefits, it can be concluded from Table 11 that adopting the yellow times corresponding to the nominal 85% reliability yields yellow times of 3.3, 3.8, and 4.2 seconds for the three speed limits, respectively. These can be translated into savings in the yellow times of 0.2, 0.5, and 0.8 seconds from the current guidelines yellow times.

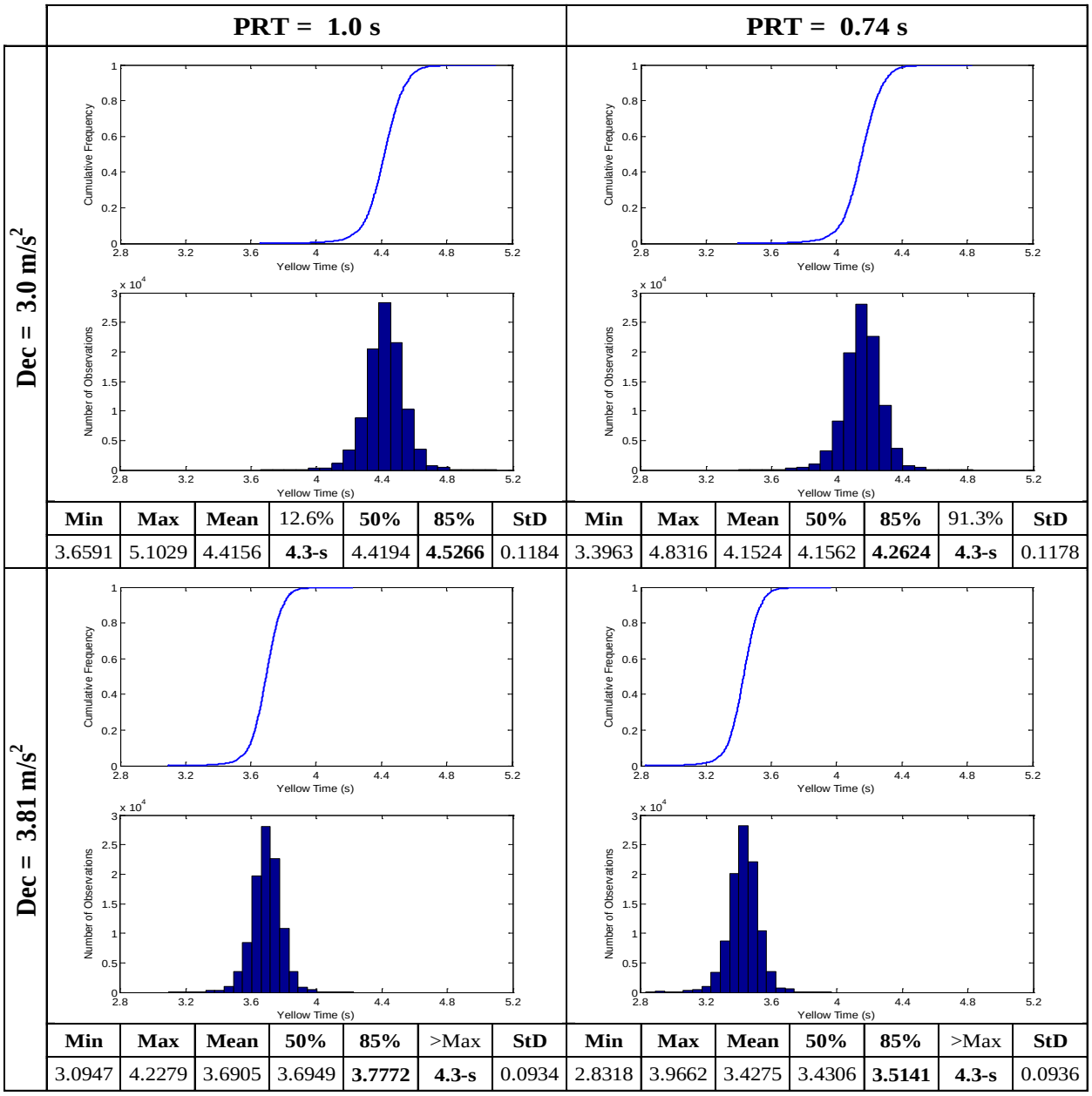

	Min	Max	Mean	12.6%	50%	85%	StD	Min	Max	Mean	50%	85%	91.3%	StD
Dec = 3.0 m/s²	3.6591	5.1029	4.4156	**4.3-s**	4.4194	**4.5266**	0.1184	3.3963	4.8316	4.1524	4.1562	**4.2624**	**4.3-s**	0.1178
Dec = 3.81 m/s²	3.0947	4.2279	3.6905	3.6949	**3.7772**	**4.3-s**	0.0934	2.8318	3.9662	3.4275	3.4306	**3.5141**	**4.3-s**	0.0936

Figure 39: Yellow Time Distributions for Different PRT and Deceleration Levels

Table 11: Yellow Clearance Interval Lookup Table

G	-4%			-3%			-2%			*G*
v_f *(mi/h)*	35	45	55	35	45	55	35	45	55	v_f *(mi/h)*
50%	2.6	3.1	3.6	2.5	3.1	3.6	2.5	3.0	3.5	50%
60%	2.8	3.3	3.8	2.8	3.3	3.8	2.7	3.2	3.7	60%
70%	3.1	3.6	4.1	3.0	3.5	4.0	3.0	3.5	3.9	70%
80%	3.4	3.9	4.4	3.3	3.8	4.3	3.3	3.7	4.2	80%
85%	3.6	4.0	4.5	3.5	4.0	4.5	3.4	3.9	4.4	85%
90%	3.8	4.3	4.7	3.7	4.2	4.6	3.6	4.1	4.6	90%
95%	4.1	4.5	5.0	4.0	4.4	4.9	3.9	4.3	4.8	95%
96%	4.2	4.6	5.1	4.1	4.5	5.0	4.0	4.4	4.9	96%
97%	4.3	4.7	5.2	4.2	4.6	5.1	4.1	4.5	5.0	97%
98%	4.5	4.9	5.4	4.3	4.8	5.2	4.2	4.6	5.1	98%
99%	4.7	5.1	5.6	4.5	5.0	5.4	4.4	4.8	5.3	99%
99.9%	5.6	5.9	6.4	5.3	5.7	6.1	5.1	5.5	5.9	99.9%

Reliability Factor

G	-1%			0%			1%			*G*
v_f *(mi/h)*	35	45	55	35	45	55	35	45	55	v_f *(mi/h)*
50%	2.5	3.0	3.5	2.5	2.9	3.4	2.5	2.9	3.4	50%
60%	2.7	3.2	3.7	2.7	3.1	3.6	2.6	3.1	3.6	60%
70%	2.9	3.4	3.9	2.9	3.4	3.8	2.8	3.3	3.8	70%
80%	3.2	3.7	4.1	3.1	3.6	4.1	3.1	3.6	4.0	80%
85%	3.4	3.8	4.3	3.3	3.8	4.2	3.3	3.7	4.1	85%
90%	3.6	4.0	4.5	3.5	3.9	4.4	3.4	3.9	4.3	90%
95%	3.8	4.2	4.7	3.7	4.2	4.6	3.7	4.1	4.5	95%
96%	3.9	4.3	4.8	3.8	4.2	4.7	3.7	4.1	4.6	96%
97%	4.0	4.4	4.9	3.9	4.3	4.8	3.8	4.2	4.7	97%
98%	4.1	4.5	5.0	4.0	4.4	4.9	3.9	4.3	4.8	98%
99%	4.3	4.7	5.2	4.2	4.6	5.0	4.1	4.5	4.9	99%
99.9%	4.9	5.3	5.8	4.7	5.1	5.6	4.6	4.9	5.4	99.9%

Reliability Factor

G	2%			3%			4%			*G*
v_f *(mi/h)*	35	45	55	35	45	55	35	45	55	v_f *(mi/h)*
50%	2.4	2.9	3.3	2.4	2.9	3.3	2.4	2.8	3.3	50%
60%	2.6	3.1	3.5	2.6	3.0	3.5	2.6	3.0	3.4	60%
70%	2.8	3.3	3.7	2.8	3.2	3.7	2.8	3.2	3.6	70%
80%	3.1	3.5	4.0	3.0	3.5	3.9	3.0	3.4	3.8	80%
85%	3.2	3.6	4.1	3.1	3.6	4.0	3.1	3.5	4.0	85%
90%	3.4	3.8	4.2	3.3	3.7	4.2	3.3	3.7	4.1	90%
95%	3.6	4.0	4.4	3.5	3.9	4.4	3.4	3.9	4.3	95%
96%	3.6	4.0	4.5	3.6	4.0	4.4	3.5	3.9	4.3	96%
97%	3.7	4.1	4.6	3.6	4.0	4.5	3.6	4.0	4.4	97%
98%	3.8	4.2	4.7	3.7	4.1	4.6	3.6	4.1	4.5	98%
99%	3.9	4.4	4.8	3.8	4.3	4.7	3.8	4.2	4.6	99%
99.9%	4.4	4.8	5.3	4.3	4.7	5.2	4.2	4.6	5.1	99.9%

Reliability Factor

7.5 EXTENSION OF THE PROPOSED PROCEDURE BASED ON GENDER AND AGE

It can be concluded from the above results that determining the required yellow time as a probabilistic distribution would be better than having a single deterministic value. This is because generating a distribution of yellow time realizations provides a measure of the level of dilemma zone risk associated with each yellow time value. One potential add-on to the proposed procedure is to utilize the availability of information about age and gender of driver population at a certain intersection to compute overall average yellow interval durations for the subject intersection. Furthermore, customized clearance intervals can be provided to each driver, based on his/her specific attributes, and hence can be integrated as part of the deployment of the IntelliDrive^{SM} safety/mobility initiatives, where the information about socioeconomic attributes can be easily communicated with the intersection hardware.

In addition to the MC simulations conducted earlier for the different PRT and deceleration values, the yellow time realizations can also be generated for different gender and age groups. This can be done by cross-classifying the population of drivers by gender and age, and determining the yellow time distribution for each gender and age group. Such group distributions would enable obtaining the overall yellow time distribution for a certain intersection by adding up the distributions of gender and age groups by the percentage of each group at that intersection. In order to illustrate this procedure, the population of stopped drivers in the available data, which includes 2016 records, is stratified by gender (female and male) and age (younger < 40 years, $40 \leq$ mid-age < 60, older ≥ 60 years). For each of the six cross-classes, a realization of the yellow-time distribution is generated. Figure 40 shows the cumulative distribution function (CDF) and the corresponding statistics for each of the six groups.

The figure demonstrates that, in general, female drivers need longer yellow times compared to male drivers. In addition, the age slightly affects the required yellow time, where older drivers need slightly longer yellow times when compared to younger drivers. The extreme comparison here could arise from comparing an intersection with a majority of old female drivers to another intersection with majority of young male drivers.

After generating the realizations for all groups, the overall distribution for all drivers can be obtained by weighting each realization by its ratio in the population. In other words, if n is the total number of drivers and n_i is the number of drivers in each gender/age group, the overall

cumulative distribution function can be obtained by weighting each value within each group by the ratio (n_i/n), and then combining and sorting all realizations in the six groups based on their yellow times, and finally adding the weights up to 1. Applying the procedure to the data, the number of observations and percentage of drivers in each gender/age group and the overall distribution of yellow time and its corresponding statistics are shown in Figure 41.

	Female Drivers							Male Drivers						
Younger Drivers	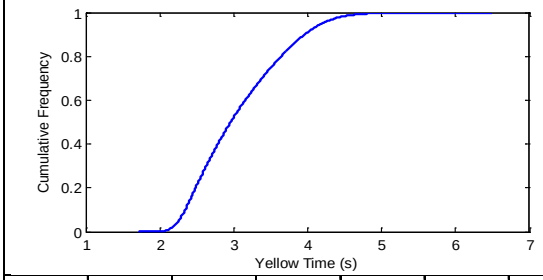							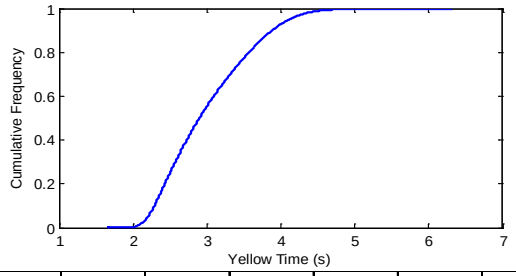						
	Min	**Max**	**Mean**	**50%**	**85%**	96.4%	**StD**	**Min**	**Max**	**Mean**	**50%**	**85%**	97.5%	**StD**
	1.7185	6.4972	3.0686	2.9580	**3.7973**	**4.3-s**	0.6234	1.6695	6.3251	3.0049	2.8977	**3.7225**	**4.3-s**	0.6130
Mid-age Drivers	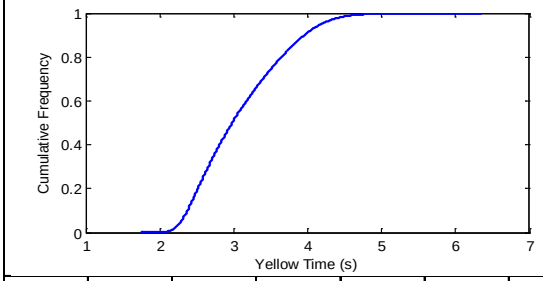							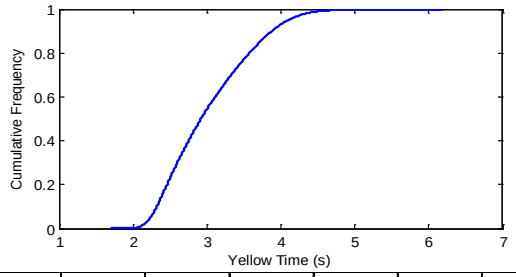						
	Min	**Max**	**Mean**	**50%**	**85%**	96.6%	**StD**	**Min**	**Max**	**Mean**	**50%**	**85%**	97.6%	**StD**
	1.7567	6.3545	3.0850	2.9792	**3.7973**	**4.3-s**	0.6081	1.7078	6.1904	3.0220	2.9192	**3.7232**	**4.3-s**	0.5982
Older Drivers	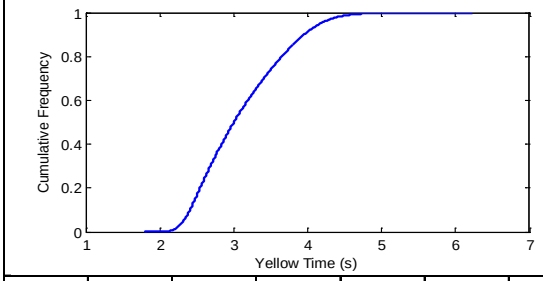							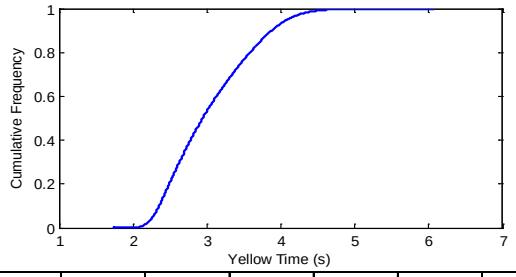						
	Min	**Max**	**Mean**	**50%**	**85%**	96.9%	**StD**	**Min**	**Max**	**Mean**	**50%**	**85%**	97.8%	**StD**
	1.7950	6.2235	3.1024	3.0012	**3.7979**	**4.3-s**	0.5935	1.7463	6.0667	3.0400	2.9414	**3.7250**	**4.3-s**	0.5840

Figure 40: Yellow Time Distributions for Different Gender and Age Groups

		Gender		
		Female	**Male**	**All**
Age	**Young (< 40)**	330 (16.4%)	298 (14.8%)	**628 (31.2%)**
	Mid-age (40 – 60)	337 (16.7%)	374 (18.6%)	**711 (35.3%)**
	Old (≥ 60)	284 (14.1%)	393 (19.5%)	**677 (33.6%)**
	All	**951 (47.2%)**	**1065 (52.8%)**	**2016 (100%)**

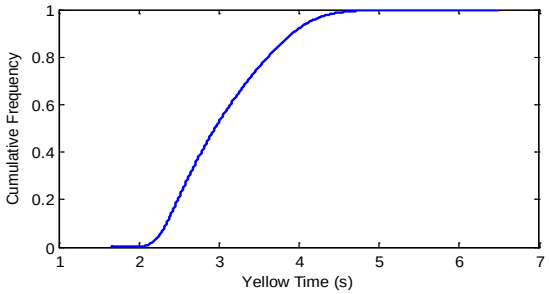

Min	**Max**	**Mean**	**50%**	**85%**	97.2%	**StD**
1.6695	6.4972	3.0538	2.9499	**3.7598**	**4.3-s**	0.6045

Figure 41: Overall Yellow Time Distribution for Weighted Gender and Age Groups

It can be seen from Figure 41 that in order to ensure that at least 85 percent of all the drivers in the data set do not encounter a dilemma zone, the yellow time should be approximately 3.76 s. Nevertheless, applying the recommended 4.3-second yellow time would decrease the percentage of drivers trapped in a dilemma zone to 3.8 percent. The proposed procedure is very useful and not only can be applied to different intersections with different driver population breakdowns, but also can be applied to different posted speed limits. Furthermore, the lookup table (Table 11) could be extended to cover effects of gender and age on the yellow time, and a set of six lookup tables for each age and gender group is developed and can be found in Appendix A. If the available information permits, the required yellow time for each age and gender group can be looked up from these tables and then the overall yellow time can be calculated as the weighted average across the various groups. Moreover, the concept of having the required yellow time as a function of the underlying variables can serve perfectly within the IntelliDrive^{SM} initiative, where each individual driver can receive advice on the specific time he/she needs in order to react before the signal turns to red. This novel advance not only provides each driver with his/her exact yellow-time duration, but also assists in reduction of the transition yellow time, given that each driver is informed of the change from green to red prior to the change occurring via an in-vehicle display.

7.6 SUMMARY AND CONCLUSIONS

The chapter developed a novel stochastic approach for estimating the yellow interval duration. The approach explicitly accounts for design reliability using a Monte Carlo simulation approach that accounts for the stochastic nature of driver PRT and deceleration behavior. Using

the proposed stochastic approach for estimating yellow clearance times, a lookup table was developed to assist practitioners in the design of yellow timings, that reflects the stochastic nature of driver PRT and deceleration levels. It was concluded that the proposed lookup table could yield average safety benefits between 5,450 and 54,500 potential savings in signalized intersection crashes, as well as average efficiency benefits between 0.2 and 0.8 seconds savings in the yellow time durations. Lookup tables could also be developed for different gender and age groups. Yellow timings can then be computed as a volume-weighted average yellow time considering the breakdown of drivers within the various gender and age categories.

Furthermore, the proposed lookup tables can be used in order to account for the design reliability in determining the clearance time duration. In addition, information about drivers' population attributes, whenever available, should be included in determining yellow times. It is worth mentioning here that the lookup tables proposed in this chapter are valid only for light duty vehicles on dry roadway surface and clear weather conditions. Finally, it is possible to develop driver-specific clearance warnings to drivers through some form of communication between the vehicle and the traffic signal controller. Consequently, the proposed approach can be integrated within the IntelliDrive^{SM} initiative, which can gather information on the driver, the subject vehicle, and surrounding traffic conditions to execute safe and customizable clearance timings.

CHAPTER 8 AGENT-BASED STOCHASTIC MODELING OF DRIVER DECISION AT THE ONSET OF YELLOW INDICATION

8.1 INTRODUCTION

In this chapter, a Bayesian statistical approach is used in order to develop an agent-based statistical model for the driver stop-run decision at the onset of yellow at signalized intersections to capture the stochastic nature of the driver stop-run decision. The Bayesian model parameters are calibrated using the Markov Chain Monte Carlo (MCMC) slice procedure implemented within the MATLAB® software using the stop-run records from dataset I. The classical frequentist statistical model calibrated earlier in Chapter 5 serves as the initial solution for the Bayesian model, and the variables included in the model are driver gender, age, TTI, yellow time, approaching speed and speed limit. In addition, two procedures for the agent-based Bayesian model application are proposed; namely Cascaded regression and Cholesky decomposition, in order to capture the Bayesian model parameter correlations without the need to store the set of parameters realizations. Furthermore, the Bayesian model is validated by replicating dataset I and is also tested for transferability using dataset II. The proposed Bayesian approach is ideal for modeling multi-agent systems in which each agent has its own unique set of parameters. It is worth mentioning here that the analysis in this chapter is published in [75].

8.2 MODELING DRIVER DECISION USING BAYESIAN STATISTICS

In order to explain the difference between the different statistics inferences, it can be said, simply, that the classical frequentist statistics disregards any prior knowledge about the process being measured, whereas the Bayesian statistics uses both the prior information available about the process and the information about the process contained in the present data using Bayes' theorem [76], which uses the conditional probability formula in Equation (20).

$$P(\theta \mid \text{Data}) = \frac{P(\text{Data} \mid \theta)\, P(\theta)}{P(\text{Data})} \tag{20}$$

where θ is the unknown parameter,
$P(\theta \mid \text{Data})$ is the posterior distribution,
$P(\text{Data} \mid \theta)$ is the sampling density of the data (likelihood),
$P(\theta)$ is the prior distribution,
$P(\text{Data})$ is the distribution of the present data (normalizing constant).

The Bayes' theorem is also often presented in its proportional form as in Equation (21).

$$posterior \propto prior \times likelihood \tag{21}$$

Furthermore, classical frequentist inferences are usually based on maximum likelihood estimation (MLE). MLE selects the parameters that maximize some likelihood function. In MLE, parameters are assumed to be unknown and fixed. On the other hand, in Bayesian statistics, the uncertainty about the unknown parameters is quantified so that the unknown parameters are regarded as random variables.

Accordingly, the Bayesian statistics approach can be used to calibrate the coefficients of the classical frequentist model calibrated earlier in Chapter 5, and given again (for convenience) in Equation (22), in order to generate stochastic estimates of those coefficients.

$$\ln\left(\frac{P_s}{P_r}\right) = \ln\left(\frac{P_s}{1-P_s}\right) = \text{logit}\left(P_s\right) = \beta_0 + \beta_1 r + \beta_2 A + \beta_3 \frac{TTI}{y} + \beta_4 \frac{v}{v_f} \tag{22}$$

where P_s is the probability of stopping,
P_r is the probability of running,
β_i's are model constants,
r is the gender (0 = female, 1 = male),
A *is* the age (years),
TTI is the time-to-intersection (s),
y is the yellow time (s),
v and v_f are the approaching speed and the speed limit (m/s).

Bayesian estimates of the model parameters, along with their posterior distributions, can be estimated using the Markov Chain Monte Carlo (MCMC) slice algorithm implemented within the MATLAB® software. Monte Carlo methods are often used in Bayesian data analysis to generate the posterior distributions when these distributions cannot be generated analytically. The approach generates random samples from these distributions to estimate the posterior distribution or derived statistics (e.g. mean, median, and standard deviation). The slice sampling algorithm that is implemented within MATLAB® is an algorithm designed to sample from a distribution with an arbitrary density function, known only up to a constant of proportionality – what is needed for sampling from a complicated posterior distribution whose normalization constant is unknown. The algorithm does not generate independent samples, but rather a Markovian sequence whose stationary distribution is the target distribution. This algorithm differs from other well-known MCMC algorithms because only the scaled posterior need to be

specified – no proposal or marginal distributions are needed. Still, the MCMC slice algorithm requires an initial solution for the model parameters, the prior distribution, the number of samples to be generated, a burn-in rate, and a thinning ratio. The initial solution was assumed to be the solution generated using the GLM logistic model, shown in Table 6. The prior distributions for the model parameters were assumed to be "non-informative" normal distributions with means equal to 0 and variances equal to 10^4. Different combinations were tested for the other parameters to set the number of samples at 500, the burn-in rate at 20 and the thinning ratio at 600. These parameters translate into a total sample size of 312,000 simulations, including a burn-in sample size of 12,000 observations. Of the remaining 300,000 sample simulations 500 are selected using a thinning rate of 600 (i.e. selecting 1 in every 600 simulations). Table 12 summarizes the different statistics for the 500 realizations for all the five model parameters. It can be seen that the mean value of all the model parameters are close to the parameter estimates from the classical frequentist GLM model in Table 6 in Chapter 5.

Table 12: Summary Statistics of the Different Model Parameters

Parameter	Mean (μ)	Quantiles		St. Dev. (σ)	Skewness (γ_3)	Kurtosis (γ_4)
		$Q_{0.025}$	$Q_{0.975}$			
β_0	- 6.3519	- 9.4564	- 3.2974	1.5966	- 0.0642	2.9560
β_1	0.5811	0.4031	0.7787	0.0957	0.1392	2.8463
β_2	0.0184	0.0131	0.0244	0.0029	0.0931	2.7080
β_3	12.5508	11.7688	13.4635	0.4445	0.2165	3.0193
β_4	- 4.1263	- 7.0724	- 1.1920	1.5367	0.0621	2.9789

In order to illustrate the results of the Bayesian model estimates in Table 12, the logit model is applied 500 times with the 500 realizations of the model parameters, and the resulting 500 stopping probability curves are plotted on the same chart, as shown in Figure 42. It can be seen from the figure that the agent-based Bayesian model yields a spectrum of 500 different stopping probability distributions for the various agents, in contrast to a single stopping probability curve from the classical Frequentist model. In other words, the Bayesian model captures the inter- and intra-agent variability while facing the same exact situation as opposed to the current approach of considering a single deterministic probability of stopping.

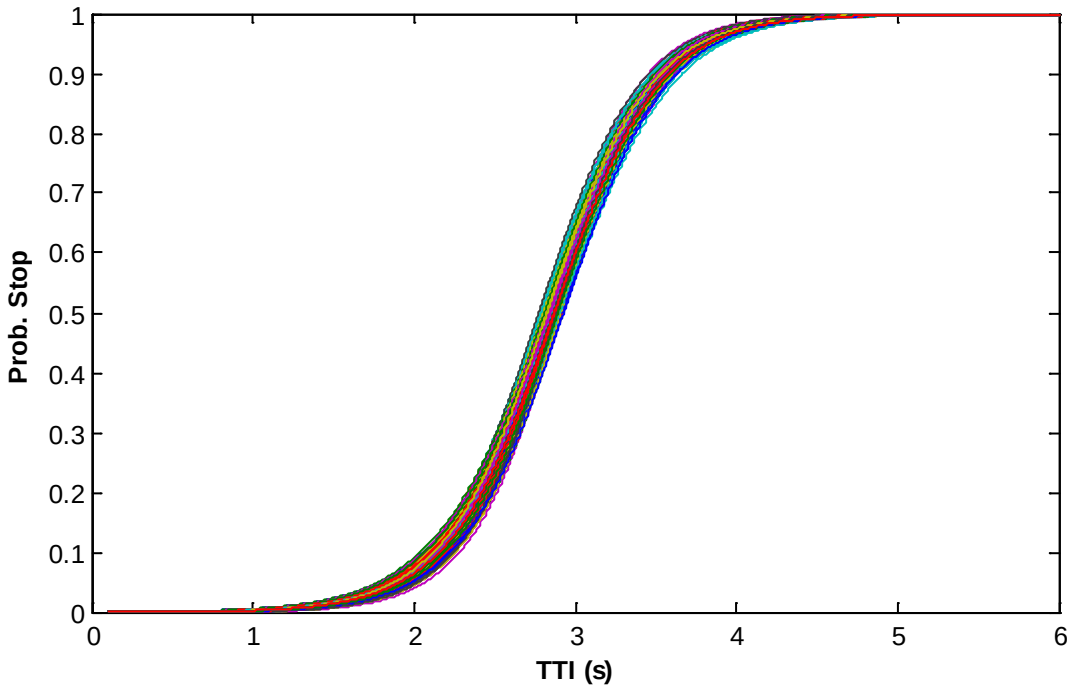

Figure 42: Probability of Stopping based on the Bayesian Model Parameters

Furthermore, inspection of the autocorrelation functions for each of the five coefficients demonstrates that the sample size is sufficient for convergence, as illustrated in Figure 43. The solid horizontal lines represent the 95% confidence limits while the stem lines represent the autocorrelation function. As would be expected an autocorrelation of 1.0 is observed for a lag of 0 while the values are within the confidence limits for larger lag times. In addition, a Kolmogorov-Smirnov goodness of fit test (K-S test) was run on the model parameter distributions and concluded that there was insufficient evidence to reject the null hypothesis that the model parameter distributions were different from the normal distribution at a level of significance of 0.05, as illustrated in Figure 44. It can be demonstrated from the figure that although all parameter distributions are not different from the normal distribution, the distribution of the gender and *TTI*/*y* parameters, β_1 and β_3, respectively are slightly right skewed. The normality of the parameter distributions are also verified by the skewness and Kurtosis values in Table 12, keeping in mind that a standard normal distribution has skewness (γ_3) value of zero and Kurtosis (γ_4) value of three [77]. Moreover, the model parameters are found consistently positive in the case of the β_1 (gender), β_2 (age), and β_3 (*TTI*/*y*) parameters, whereas they are consistently negative in the case of the β_0 and β_4 (v/v_f) parameters. Consequently, the parameter distributions are logical in terms of their signs. Noteworthy here is the fact that in

some rare instances the speed ratio coefficient (β_4) was more than zero, indicating that for these realizations the model stopping probability increases as the driver approaching speed increases.

Another important illustration of the model result is presented in Figure 45, which shows the different interactions between the five model parameters (β_0, β_1, β_2, β_3, and β_4), where in each subplot the relationship between each two parameters is established based on the parameter distributions. When comparing β_0 to the other parameters, it is clear that a linear relationship between β_4 and β_0 can be deduced. There also appears to be some evidence for a linear relationship between β_3 and β_0. However, there does not appear to be a relationship between β_1 and β_0, nor between β_2 and β_0. It is worth mentioning here that the level of noise generated in the different subplots of Figure 45 is limited to some extent due to the fact that the Bayesian approach used a thinning process that ensured that there was no autocorrelation between model parameters as shown in Figure 43.

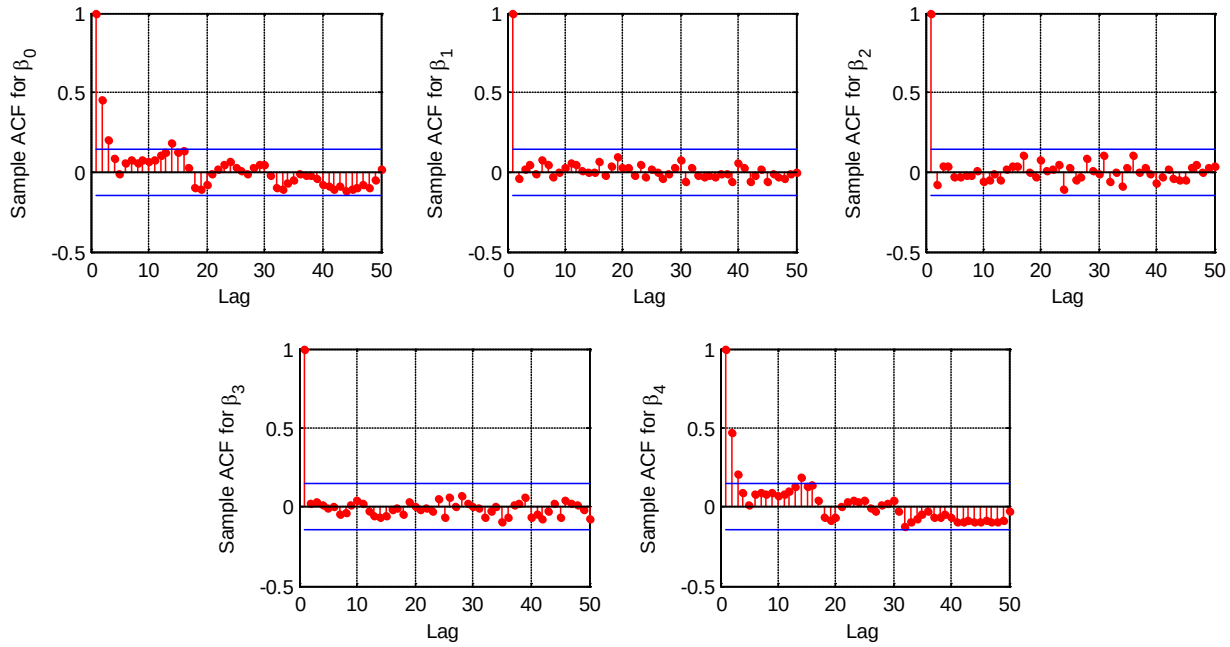

Figure 43: Variations in the Autocorrelation Function of the Model Parameters

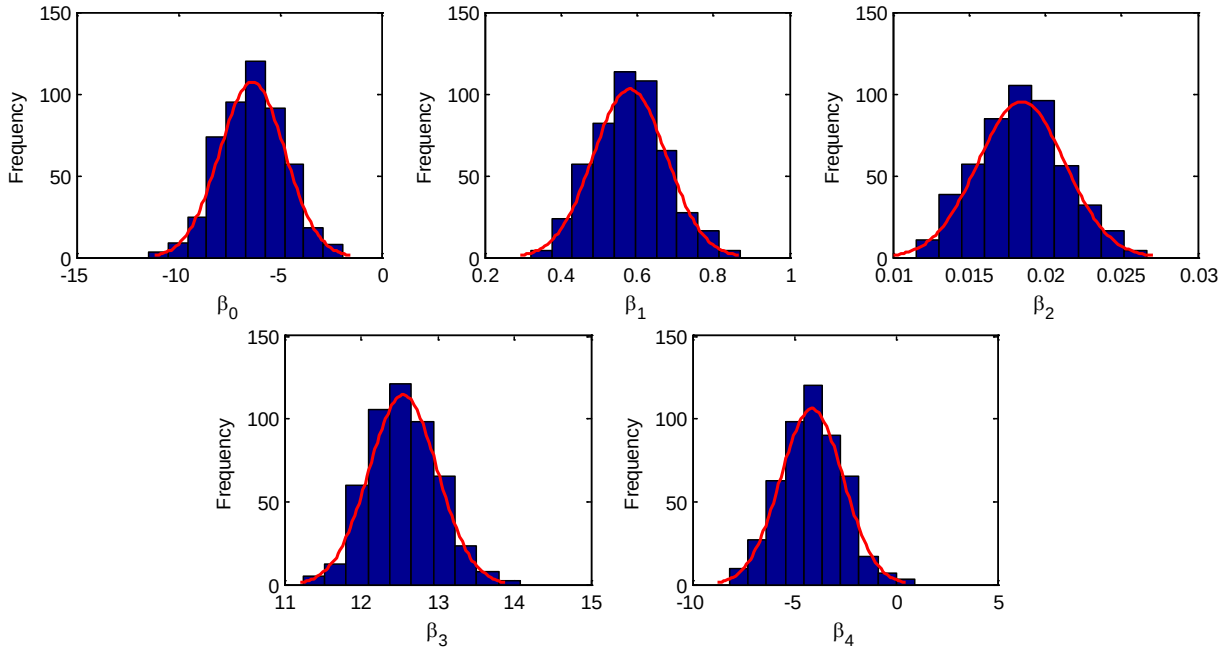

Figure 44: Histograms of the Model Parameter Distributions

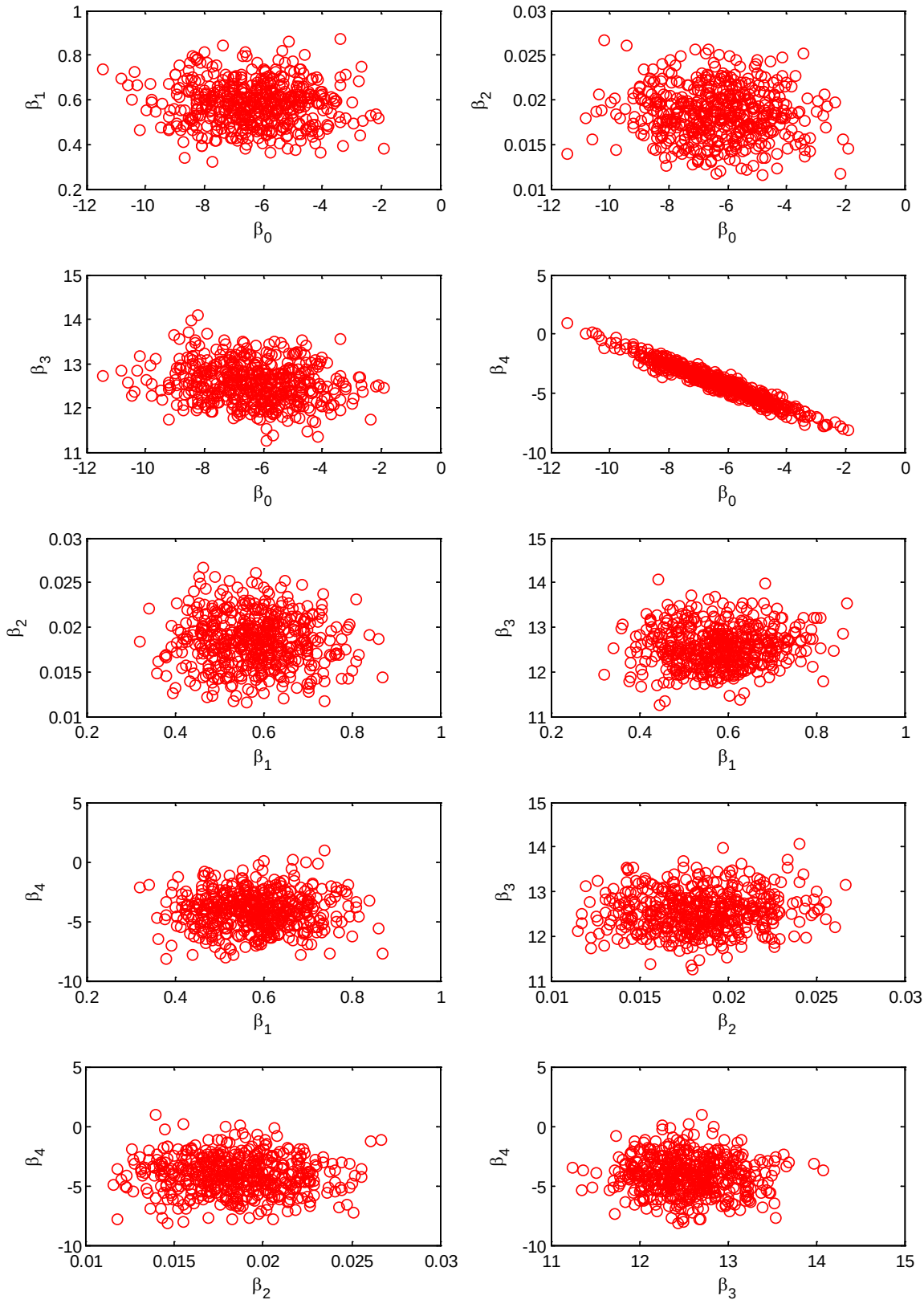

Figure 45: Inter-dependence of the Bayesian Model Parameters

8.3 APPLICATION OF THE BAYESIAN DRIVER DECISION MODEL

Modeling of the driver decision using the presented Bayesian approach entails that the realizations of the different model parameters (β_i) not be generated independently. Instead, the correlations between these parameters must be taken into consideration. As mentioned earlier, based on Figure 45, there is a strong linear relationship between β_4 and β_0 and there is a potential relationship between β_3 and β_0 as well. In general, the interactions between the different model parameters can be captured in several ways. One way is to store the parameter realizations from the Bayesian model; however, this would require extensive computation capabilities. Another technique is to use joint probability functions to capture the interaction, and that also is typically difficult to implement, where considering the five model parameters would yield a six-dimensional function. Alternatively, two suitable approaches are adopted and proposed in this analysis in order to simplify the application of the Bayesian model to account for the stochastic nature of the driver decision, without the need for extensive storage capabilities. The two approaches, namely Cascaded regression and Cholesky decomposition, are presented and compared hereinafter.

8.3.1 Model Application Using Cascaded Regression

In this approach the regression analysis is used to cascade the model parameters on each other, in order to account for the correlations between the parameters. Accordingly, the first parameter (β_0) is generated independently from a random normal distribution as in Equation (23).

$$\beta_0 \sim N\left(\mu_{\beta_0}, \sigma_{\beta_0}\right) \tag{23}$$

Subsequently, regression model is calibrated between the next parameter (β_1) and β_0, with a normally distributed error term (ε_{β_1}) as in Equation (24).

$$\beta_1 = a_{\beta_1} + b_{\beta_1}\beta_0 + \varepsilon_{\beta_1} \qquad \text{where} \quad \varepsilon_{\beta_1} \sim N\left(0, \sigma_{\varepsilon_{\beta_1}}\right) \tag{24}$$

The regression of the next parameter (β_2) on β_0 and β_1 is fit by another regression model, with a normally distributed error term (ε_{β_2}) as in Equation (25).

$$\beta_2 = a_{\beta_2} + b_{\beta_2}\beta_0 + c_{\beta_2}\beta_1 + \varepsilon_{\beta_2} \qquad \text{where } \varepsilon_{\beta_2} \sim N\left(0, \sigma_{\varepsilon_{\beta_2}}\right) \tag{25}$$

Based on the relation between β_1 and β_0 from Equation (24), this relation can be reduced to a relation between β_2 and β_0, with a new error term (ε'_{β_2}) that is also normally distributed because it is the summation of two normally distributed errors, as in Equation (26).

$$\beta_2 = \left(a_{\beta_2} + a_{\beta_1}c_{\beta_2}\right) + \left(b_{\beta_2} + b_{\beta_1}c_{\beta_2}\right)\beta_0 + \left(\varepsilon_{\beta_2} + \varepsilon_{\beta_1}c_{\beta_2}\right) = a'_{\beta_2} + b'_{\beta_2}\beta_0 + \varepsilon'_{\beta_2} \tag{26}$$

where $\varepsilon'_{\beta_2} \sim N\left(0, \sigma_{\varepsilon'_{\beta_2}}\right)$

The same exact procedure can be applied to the last two variables (β_3 and β_4) and their regression can be reduced to depend only on β_0, as in Equations (27) and (28).

$$\beta_3 = a_{\beta_3} + b_{\beta_3}\beta_0 + c_{\beta_3}\beta_1 + d_{\beta_3}\beta_2 + \varepsilon_{\beta_3} = a'_{\beta_3} + b'_{\beta_3}\beta_0 + \varepsilon'_{\beta_3} \tag{27}$$

where $\varepsilon'_{\beta_3} \sim N\left(0, \sigma_{\varepsilon'_{\beta_3}}\right)$

$$\beta_4 = a_{\beta_4} + b_{\beta_4}\beta_0 + c_{\beta_4}\beta_1 + d_{\beta_4}\beta_2 + e_{\beta_4}\beta_3 + \varepsilon_{\beta_4} = a'_{\beta_4} + b'_{\beta_4}\beta_0 + \varepsilon'_{\beta_4} \tag{28}$$

where $\varepsilon'_{\beta_4} \sim N\left(0, \sigma_{\varepsilon'_{\beta_4}}\right)$

As concluded from the analysis of Figure 45, applying this approach to the Bayesian model parameters yielded no linear relationship between β_0 and β_1 nor β_2. This means that β_1 and β_2 can be generated independently from β_0 based on Equation (29), whereas β_3 and β_4 can be generated using their regression equations based on the calibrated constants (a'_{β_i} and b'_{β_i}), as in Table 13.

$$\beta_1 \sim N\left(\mu_{\beta_1}, \sigma_{\beta_1}\right) \qquad \text{and} \qquad \beta_2 \sim N\left(\mu_{\beta_2}, \sigma_{\beta_2}\right) \tag{29}$$

Table 13: Cascaded Regression Model Coefficients

i	a'_{β_i}	b'_{β_i}	$\mu_{e'_{\beta_i}}/\mu_{\beta_i}$	$\sigma_{e'_{\beta_i}}/\sigma_{\beta_i}$
β_0	--	--	- 6.3519	1.5982
β_1	--	--	0.5811	0.0958
β_2	--	--	0.0184	0.0029
β_3	12.2523	- 0.0470	0	0.4390
β_4	- 10.0506	- 0.9327	0	0.3802

Accordingly, using the proposed Cascaded regression approach requires calibrating and storing 14 parameters (two of which are zeros) without the need to store complete sets of the parameters realizations. The generated normal distributions for the first three parameters (β_0, β_1, and β_2) and the error terms for the last two parameters (ε'_{β_3} and ε'_{β_4}) are presented in Figure 46.

In order to validate this approach, Table 14 summarizes the different statistics for 500 replications generated using the Cascaded regression for all five model parameters. Comparing these statistics to those of the Bayesian model in Table 12, it can be seen that although the proposed approach is simple to estimate and stores only 14 parameters, it is still valid and can be used for the model application. In addition, the inter-dependence of the generated 500 replications was plotted over those of the Bayesian model as in Figure 47, and both show similar behavior.

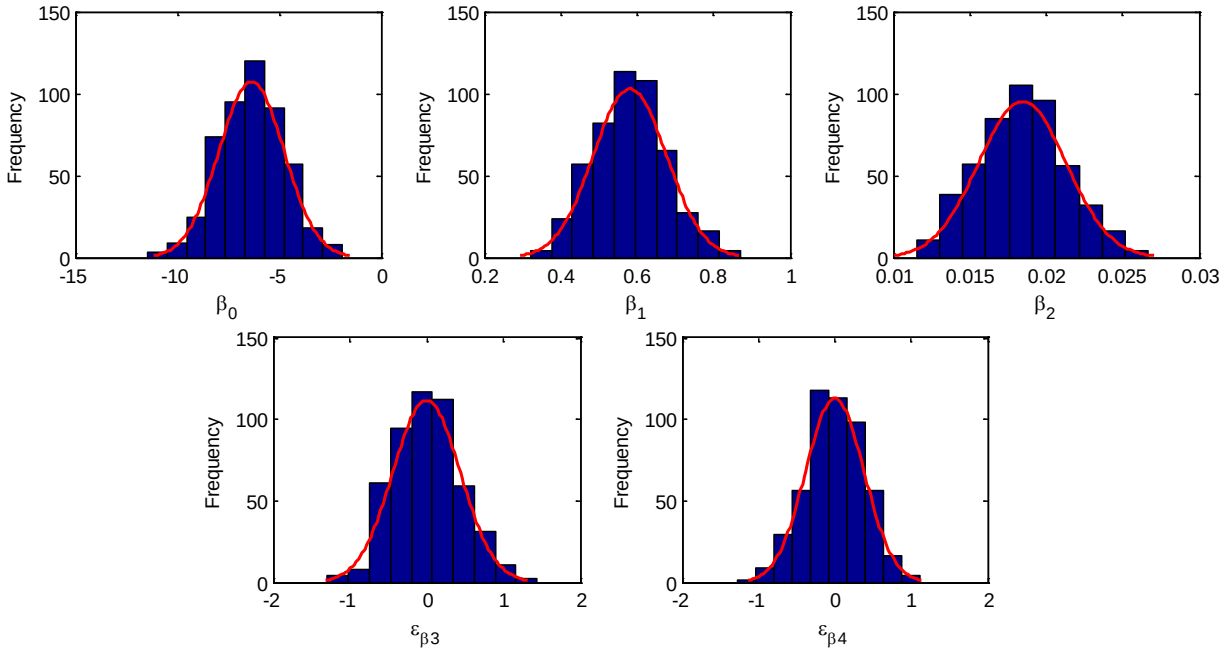

Figure 46: Histograms of the Cascaded Regression Generated Parameters

Table 14: Summary Statistics of the Cascaded Regression Model Parameters

Parameter	Mean (μ)	Quantiles		St. Dev. (σ)	Skewness (γ_3)	Kurtosis (γ_4)
		$Q_{0.025}$	$Q_{0.975}$			
β_0	- 6.2750	- 9.5477	- 2.8959	1.6599	0.0611	3.2105
β_1	0.5860	0.3938	0.7563	0.0929	0.0170	3.0261
β_2	0.0185	0.0125	0.0240	0.0029	- 0.0595	2.6446
β_3	12.5558	11.7087	13.4802	0.4389	0.0878	3.0718
β_4	- 4.1823	- 7.4036	- 1.3296	1.5455	- 0.0826	3.2280

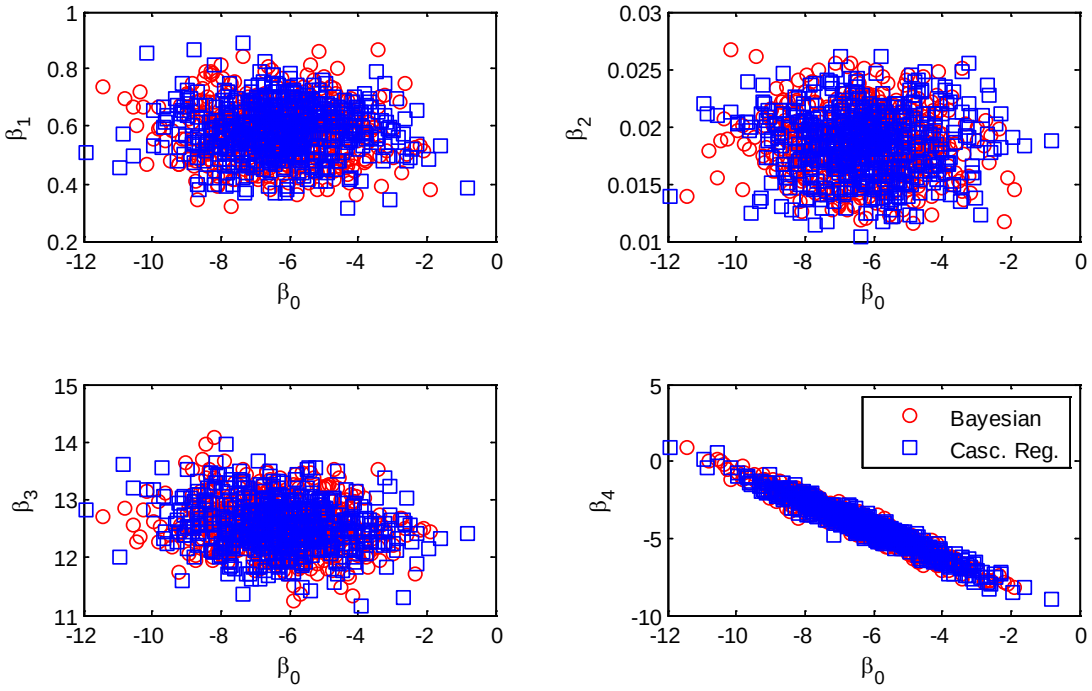

Figure 47: Inter-dependence of the Cascaded Regression Model Parameters

8.3.2 Model Application Using Cholesky Decomposition

In general, Cholesky decomposition [78] is a matrix calculus tool that can be used to break a symmetric positive-definite matrix into the product of a lower triangular matrix and its conjugate transpose. In order to apply the Bayesian driver decision model, this approach can be used to generate the desired parameter replications, given the correlations among the different parameters, as in Equation (30).

$$\left.\begin{array}{l}\beta_0 \sim N\left(\mu_{\beta_0}, \sigma_{\beta_0}\right) \\ \quad\vdots \\ \beta_4 \sim N\left(\mu_{\beta_4}, \sigma_{\beta_4}\right)\end{array}\right| \qquad \rho_{ij} = \operatorname{corr}\left(\beta_i, \beta_j\right) \qquad \forall i \neq j \tag{30}$$

Supposing that $Z_0,\ldots,Z_4$ are i.i.d. standard normal vectors (i.e. $Z_i \sim N(0,1)$), the problem can be formulated as in Equation (31).

$$\begin{array}{ll}\mu_{\beta_0} + c_{00}Z_0 & = \beta_0 \\ \mu_{\beta_1} + c_{10}Z_0 + c_{11}Z_1 & = \beta_1 \\ \quad\vdots & \quad\vdots \\ \mu_{\beta_4} + c_{40}Z_0 + c_{41}Z_1 + \cdots + c_{44}Z_4 & = \beta_4\end{array} \Longrightarrow \underset{\mu}{\begin{pmatrix}\mu_{\beta_0} \\ \mu_{\beta_1} \\ \vdots \\ \mu_{\beta_4}\end{pmatrix}} + \underset{C}{\begin{pmatrix}c_{00} & 0 & 0 & 0 \\ c_{10} & c_{11} & 0 & 0 \\ \vdots & & \ddots & 0 \\ c_{40} & c_{41} & \cdots & c_{44}\end{pmatrix}} \underset{Z}{\begin{pmatrix}Z_0 \\ Z_1 \\ \vdots \\ Z_4\end{pmatrix}} = \underset{\beta}{\begin{pmatrix}\beta_0 \\ \beta_1 \\ \vdots \\ \beta_4\end{pmatrix}} \tag{31}$$

where C is a lower triangle matrix that represents the coefficients that need to be determined by solving this formulation.

By taking the variance for both sides in Equation (31), and given that μ is constant and Z is standard normal, hence

$$\operatorname{Var}(\mu) = 0,\ \operatorname{Var}(C\,Z) = C\,\operatorname{Var}(Z)C^T,\ \operatorname{Var}(Z) = I \ \Rightarrow\ \operatorname{Var}(\mu + C\,Z) = C\,C^T \tag{32}$$

$$\operatorname{Var}(\beta) = \sum = \begin{pmatrix}\sigma^2_{\beta_0} & & \rho_{ij}\sqrt{\sigma^2_{\beta_i}\sigma^2_{\beta_j}} \\ & \ddots & \\ \rho_{ij}\sqrt{\sigma^2_{\beta_i}\sigma^2_{\beta_j}} & & \sigma^2_{\beta_4}\end{pmatrix} \Rightarrow \sum = C\,C^T \tag{33}$$

Matrix Σ can be calculated easily given the correlations between the parameters and their standard deviations. Thus, the Cholesky decomposition can be applied to Equation (33), to break Σ into C and C^T. Once C is obtained, it can be substituted in Equation (31) to generate the required parameter replications.

Similar to the validation of the cascaded regression approach, Table 15 summarizes the different statistics for 500 replications generated using the Cholesky decomposition for all the five model parameters. Comparing these statistics to those of the Bayesian model in Table 12, it can be seen that the Cholesky approach is valid and can be used for the model application. Again, the inter-dependence of the generated 500 replications was plotted over those of the Bayesian model as in Figure 48, and they both show similar fashion.

Table 15: Summary Statistics of the Cholesky Decomposition Model Parameters

Parameter	Mean (μ)	Quantiles		St. Dev. (σ)	Skewness (γ_3)	Kurtosis (γ_4)
		$Q_{0.025}$	$Q_{0.975}$			
β_0	- 5.8944	- 8.7273	- 2.8463	1.4577	0.1136	3.1350
β_1	0.5701	0.3841	0.7460	0.0933	0.0215	2.8945
β_2	0.0182	0.0123	0.0237	0.0029	- 0.0904	2.7460
β_3	12.4689	11.6832	13.2446	0.4119	0.0583	2.9967
β_4	- 4.4911	- 7.1837	- 1.6984	1.4103	- 0.0663	3.0973

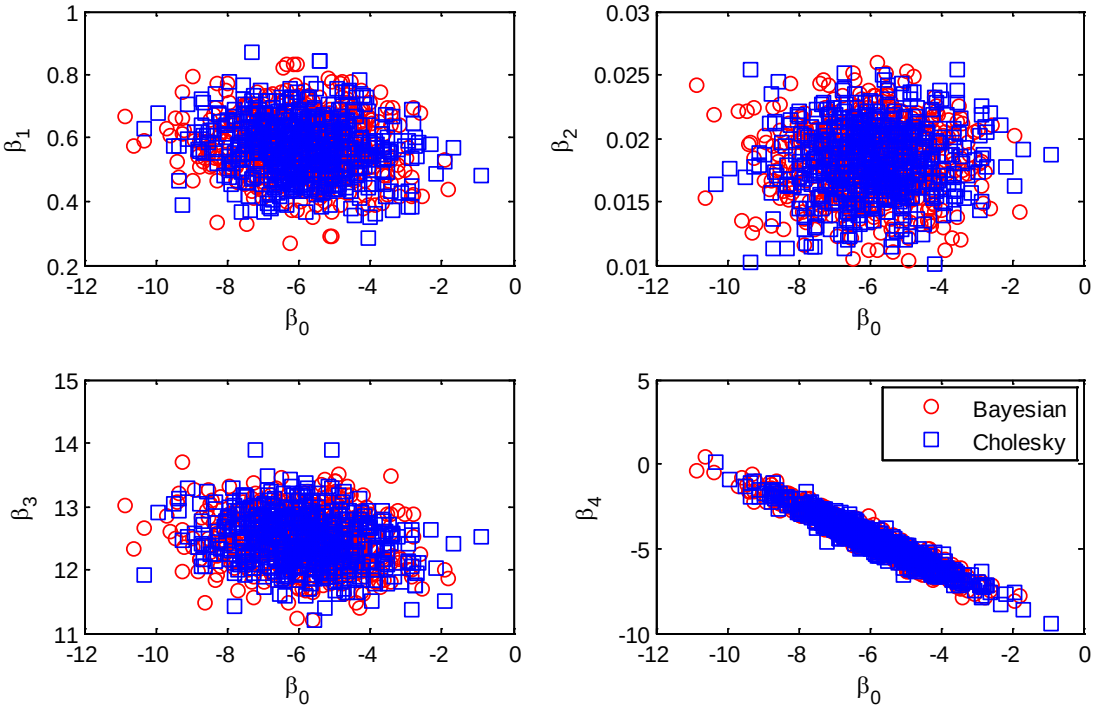

Figure 48: Inter-dependence of the Cholesky Decomposition Model Parameters

8.4 VALIDATION OF THE BAYESIAN DRIVER DECISION MODEL

In this section, the Bayesian driver decision model is applied using the Cascaded regression approach to validate the model success rate. The model is applied twice on the two available datasets I and II. The model first is applied to dataset I which is the original data used in the model calibration, in order to test the model ability to replicate the original data. Then, it is applied to dataset II, in order to test the model transferability. For each dataset, Monte Carlo simulation is used to replicate a sample of 1000 realizations and each time the model success rate is obtained. The summary statistics of the success rates of the 1000 realizations for both datasets

are presented in Table 16 and the histograms of success rates distributions are shown in Figure 49.

Table 16: Summary Statistics of the Bayesian Model Success Rate

Dataset	Min	Max	Mean	15%	50%	85%	St. Dev.
(I)	0.6905	0.8269	0.8114	0.8014	0.8149	0.8212	0.0134
(II)	0.6959	0.8719	0.8066	0.7633	0.8079	0.8509	0.0372

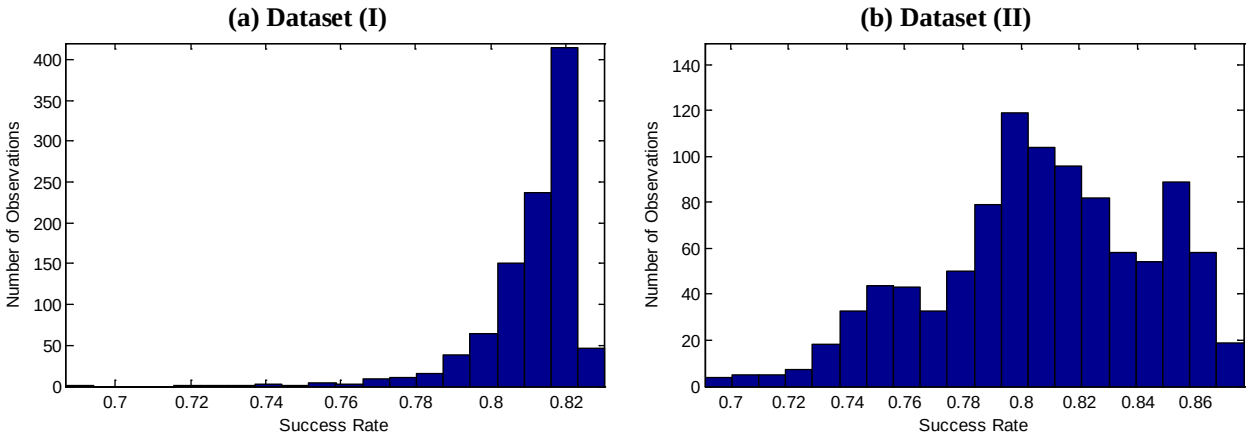

Figure 49: Histograms of the Bayesian Model Success Rate

It can be seen that the Bayesian model is capable replicating dataset I to a satisfactory level, compared to the GLM model. However, the Bayesian model is more advantageous than the GLM, as it is capable of generating a probabilistic distribution for the success rate rather than a deterministic single value as with the classical frequentist GLM model. Furthermore, the model is also transferable to other datasets, as it can replicate dataset II with acceptable success rates with small variance.

8.5 SUMMARY AND CONCLUSIONS

This chapter characterized the driver stop-run decision at the onset of a yellow indication by developing an agent-based Bayesian logistic model using dataset I. The Markov Chain Monte Carlo (MCMC) slice algorithm built in the MATLAB® software was used to calibrate the Bayesian model realizations. The variables that were considered in the model include driver gender, age, TTI, yellow time, approaching speed and speed limit. The Bayesian approach was found to be consistent with the classical frequentist model, with the advantage of being able to capture the stochastic nature of the driver decision. Nevertheless, the application of the Bayesian

model requires significant computational capabilities in order to store the model parameters realizations. Therefore, two approaches were adopted in order to simplify the application of the Bayesian model. The two approaches are the Cascaded regression and the Cholesky decomposition approaches, which capture the parameters correlations without the need to store the parameters realizations. Both approaches were found to be consistent and able to generate parameters replications comparable to the Bayesian model. In addition, the Bayesian model was validated and found to be transferable and able to replicate the driver decision in both datasets I and II.

Furthermore, the proposed agent-based Bayesian modeling framework can be easily implemented within traffic simulation software using any of the proposed application procedures (Cascaded regression or Cholesky decomposition). The agent-based modeling framework only requires the calibration of 14 parameters (Table 13) without the need to store complete sets of parameter realizations. The proposed agent-based Bayesian modeling approach can also be applied using a Monte Carlo simulation to derive stochastic dilemma zone boundaries for different driver gender and age groups. In other words, probabilistic distributions for the dilemma zone boundaries (the 10/90 percentages TTIs) can be developed using a multi-agent based modeling framework. Furthermore, the Bayesian model capability of generating a probabilistic distribution for each parameter can be utilized in order to conduct stochastic sensitivity analysis of different variables that affect the driver stop-run decisions, such as driver gender and age, yellow duration, approaching speed, etc. Instead of having single deterministic values for the change in stop/run probability corresponding to changing the explanatory variable, this stochastic sensitivity analysis provides a more realistic probabilistic distribution for the change in stop/run probability. Thus, practitioners as well as researchers can statistically test for significant differences in stop/run probability distributions corresponding to two different values of the explanatory variable. Such hypothesis testing provides more realistic sensitivity as opposed to comparing two single deterministic numbers.

CHAPTER 9 BEHAVIORAL MODELING FRAMEWORK OF DRIVER BEHAVIOR AT THE ONSET OF YELLOW INDICATION

9.1 INTRODUCTION

This chapter introduces a state-of-the-art behavioral model (BM) framework that can be used as a tool to simulate driver behavior after the onset of a yellow indication until he/she reaches the intersection stop line. First, the proposed general framework of the BM and its components are presented. Subsequently, the behavioral model ability to track Dilemma Zone (DZ) drivers and update the information available to them every time step until they reach a final decision, is discussed. The BM framework is ideal for testing dilemma zone mitigation strategies before actual implementation. The BM framework can be easily implemented in any traffic simulation software. The analysis in this chapter also characterizes the components involved in the BM framework using dataset I and the model is validated using Monte Carlo (MC) simulations. It is worth mentioning here that the analysis in this chapter is published in [70].

9.2 BEHAVIORAL MODELING FRAMEWORK OF DRIVER BEHAVIOR

Modeling the behavior of a driver at the onset of a yellow indication while approaching a signalized intersection; is key for evaluating dilemma zone mitigation strategies. All existing efforts made toward this objective are statistical approaches and ignore the behavioral aspects of the driver. This dissertation attempts to introduce a unique tool that can be used not only to predict the driver stop-run decision, but also to simulate the complete behavior of the driver during his/her journey from the onset of yellow to the instant the driver reaches the intersection stop line. The general structure of the proposed behavioral model (BM) is summarized in Figure 50 showing the different steps of the decision making process.

After the onset of the yellow indication, the decision making process is delayed by the time needed by the driver to recognize the change in the signal head indication and react to it, known as the PRT. Consequently, after the onset of yellow, the driver continues to travel at the approaching speed (u) for the duration of the PRT (t). Once the driver recognizes the yellow indication, he/she attempts to estimate his/her approaching speed (u), remaining yellow time (RYT), and DTI. Although the driver does not know precisely how long the remaining yellow time is, he/she makes an estimate based on the posted speed limit and being familiar with the

traffic signal he/she is approaching. Having the speed displayed on the vehicle speedometer almost eliminates any error in estimating the vehicle speed, whereas the error in estimating the DTI is unconstrained and still needs to be characterized in order to accurately simulate the behavior. At this point, the driver is capable of estimating the required acceleration rate (a_{req}) to be able to run through the intersection safely before the signal turns red, based on the perceived RYT, DTI, and speed. In addition, the driver is able to estimate the required deceleration rate (d_{req}) to stop before the stop line, based on the perceived DTI and speed. It is assumed that the driver makes his/her stop-run decision based on comparing the required acceleration/deceleration rates (a_{req} & d_{req}) with the maximum accepted acceleration/deceleration rates (a_{max} & d_{max}), respectively. These maximum accepted acceleration (a_{max}) and deceleration (d_{max}) rates vary between different drivers. The former, however, is constrained by the posted speed limit as well as the vehicle characteristics; whereas the latter varies widely and needs to be related to other parameters. Accordingly, the driver has four outcome decisions based on this logic; (1) to run through the intersection if $a_{req}<a_{max}$ and $d_{req}>d_{max}$, (2) to stop at the stop line if $a_{req}>a_{max}$ and $d_{req}<d_{max}$, (3) either to stop or to run if $a_{req}<a_{max}$ and $d_{req}<d_{max}$, and finally (4) neither to stop nor to run if $a_{req}>a_{max}$ and $d_{req}>d_{max}$.

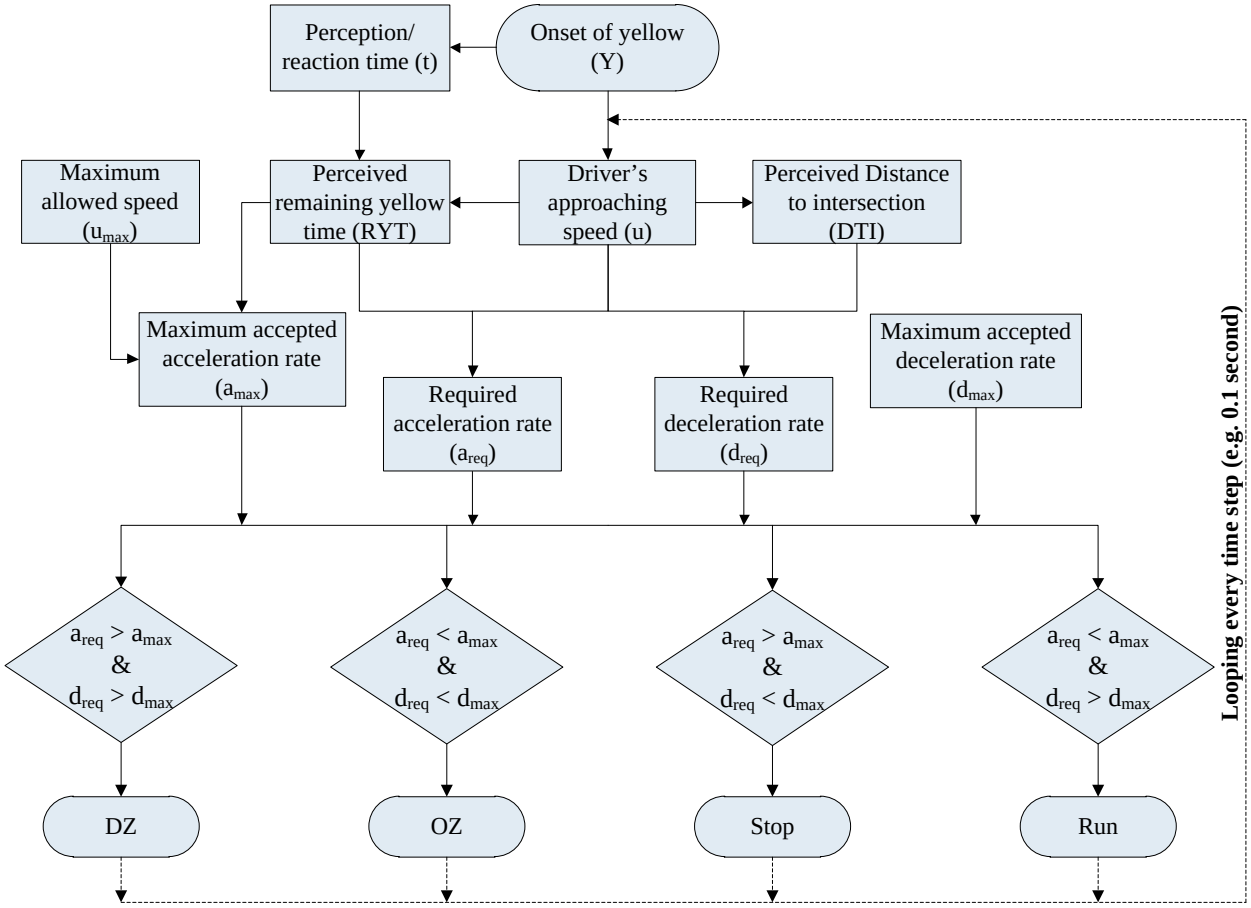

Figure 50: General Framework of the Behavioral Model

The third and fourth outcomes are commonly known as Option Zone (OZ) and Dilemma Zone (DZ), respectively. In the OZ, the driver has the choice either to stop or to run as he/she is capable of performing either action safely. However, logically the driver is more willing to minimize his/her travel time and thus would be more inclined to run rather than stop. Still, a binary logit model can be calibrated to determine the driver's choice. On the other hand, a driver in the DZ is not capable of either running or stopping safely and thus can be assumed to have a 50/50 stop-run probability. Theoretically, a well-timed traffic signal should have no DZ if the design assumptions are valid. Nevertheless, variations in driver/vehicle parameters (t, DTI, u, d_{max}…etc) may result in drivers being caught in the DZ. The exclusive feature of this proposed behavioral model (BM) is its capability of continuing the decision making process every desired simulation time step (e.g. every deci-second) until the vehicle reaches the stop line. Unlike statistical modeling of the stop-run decision, the BM simulates the complete driver behavior and tracks the vehicle motion through the intersection approach. This behavior includes, beside the

stop-run decision, information on the adopted acceleration or deceleration level, the new instantaneous speed, distance traveled during the time step and the corresponding travel time; which is available every time step. This exclusive feature of the BM allows the simulated driver to update the adopted stop-run decision every time step based on the new ambient situation. Accordingly, at the onset of yellow, a driver inevitably trapped in a DZ will randomly choose his/her stop-run decision and every time step he/she will continue to make decisions until he/she reaches a point where he/she converges to a final decision; either to run or to stop.

In order to be able to run the behavioral model accurately, the different components and steps in the framework must be characterized and fine-tuned to give an accurate input for the decision making process. In other words, the more well-defined the components of the BM framework are, the more accurate the simulated driver behavior will be. In the next section, the components of the BM framework are characterized and the BM is validated based on dataset I.

9.3 CHARACTERIZING BEHAVIORAL MODEL PARAMETERS

As described earlier, the available dataset I includes complete tracking data every deci-second of the subject vehicle within approximately 150 m (500 ft) before and after the intersection. The dataset includes 3328 stop-run records (1312 running records and 2016 stopping records).

In order to characterize the different parameters used in the BM framework, it was decided to characterize the constrained variables (a_{max} and u_{max}) based on their statistical means, whereas the unconstrained variables (t, d_{max}, and DTI error) were characterized based on their statistical correlations with possible predictors. Those predictors include age, gender, platoon, grade, actual DTI, TTI, yellow time, approaching speed, and speed limit.

9.3.1 Characterizing a_{max}, u_{max}, t, and d_{max}

Table 17 summarizes the descriptive statistical measures of the two constrained variables, namely a_{max} and u_{max}, which are characterized based on their statistical means. In addition, Table 17 summarizes the descriptive statistical measures of the unconstrained variables d_{max} and t. It is useful here to utilize the statistical models calibrated earlier in Chapter 6, in order to represent the characterization of t and d_{max}. The two statistical models are repeated here in Equations (34) and (35), for the reader's convenience.

Table 17: Descriptive Statistical Measures of the BM Parameters

Variable		Min	Max	Mean	15%	50%	85%	St. Dev.
a_{max}	m/s^2	0.0012	0.6959	0.1553	0.0300	0.1065	0.3030	0.1433
u_{max}	km/h	69.11	100.60	83.21	74.46	80.95	92.34	8.10
t	sec	0.1800	1.5300	0.7371	0.5700	0.7200	0.9200	0.1775
d_{max}	m/s^2	7.3068	2.3075	3.8084	4.5392	3.6840	3.1200	0.7344

$$t = 0.7775 - 0.0415\, r + 0.0025\, A + 1.1966\, G + 0.3980\, \frac{TTI}{y} - 0.4897\, \frac{v}{v_f} + e_t \quad (34)$$

$$d_{max} = 6.1048 + 0.0977\, r - 0.0008\, A - 2.8531\, G - 6.0033\, \frac{TTI}{y} + 1.9372\, \frac{v}{v_f} + 1.4575\, t + e_{d_{max}} \quad (35)$$

where t is the perception-reaction time (s),
d_{max} is the maximum accepted deceleration rate (m/s^2),
r is the gender (0 female and 1 male),
A is the age (years),
G is the roadway grade (percent/100),
TTI is the time-to-intersection (s),
y is the yellow time (s), and
v and v_f are the approaching speed and the speed limit (m/s).

9.3.2 Characterizing DTI error

In order to obtain the DTI error, the BM was run on the data using the actual values for all other parameters in order to optimize the estimated DTI that reproduce the actual decision and the DTI error is calculated as the difference between the actual DTI and the estimated DTI. If the driver stopped while he/she should have run, then he/she overestimated the DTI producing a positive DTI error, and if he/she ran while he/she should have stopped, then he/she underestimated the DTI producing a negative DTI error. Figure 51 shows the histograms of the DTI error for all trials, as well as its split between stopping and running trials. In addition, Table 18 summarizes the descriptive statistics of the three DTI error distributions.

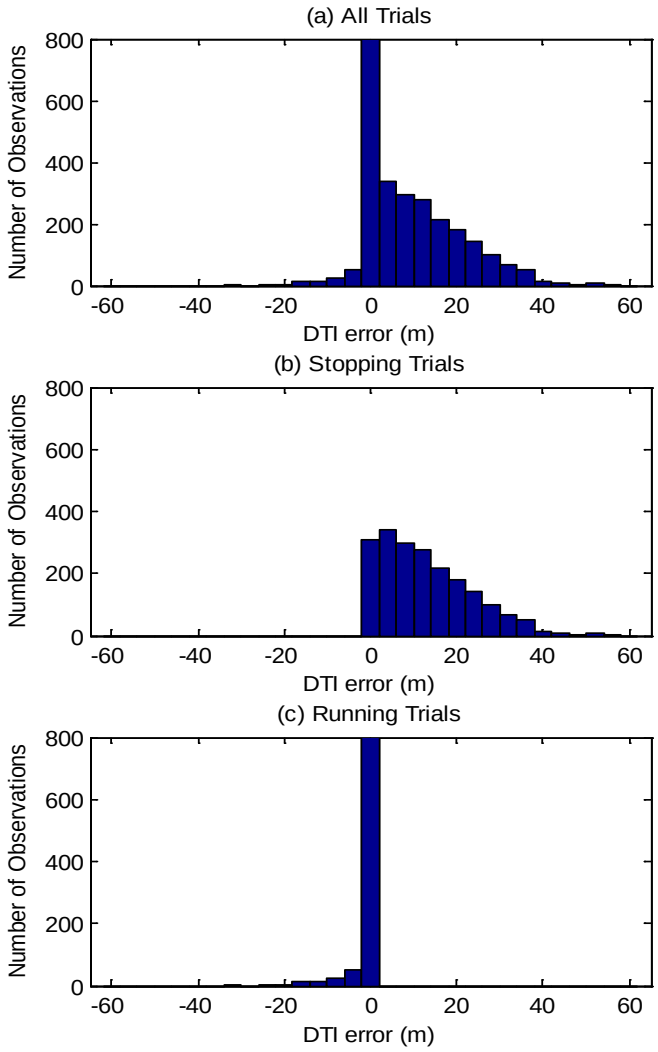

Figure 51: Histograms of DTI Error for All, Stopping, and Running Trials

Table 18: Descriptive Statistical Measures of the DTI Error

Trials	Min	Max	Mean	15%	50%	85%	St. Dev.
All	-32.00	58.00	7.78	0	3.00	20.00	10.82
Stopping	0	58.00	13.28	2.00	11.00	25.00	10.56
Running	-32.00	0	-0.66	0	0	0	2.79

It can be demonstrated from the distributions of the DTI error that many stopping drivers overestimated their DTI, while most of the running drivers estimated their DTI correctly. This appears to indicate that the drivers were not able to estimate their DTI accurately when they were stopping. Thus, the DTI error was based on the stopping trials only.

In order to characterize the DTI error, a stepwise linear regression model was fit to the data from stopping trials. After investigating different model forms, including absolute and normalized variables, the selected form is shown in Equation (36).

$$\text{DTI error} = \beta_0 + \beta_1 TTI + \beta_2 y + e_{\text{DTI error}} \quad (36)$$

where DTI error is the error in driver's perceived DTI (m),
β_i's are model constants,
TTI is the time-to-intersection (s), and
y is the yellow time (s).

The selected model form is then calibrated twice. First, the model is calibrated at the "system" level, by obtaining an aggregate set of parameters (β_i's) for all the drivers "agents". Then, the model is calibrated independently for each of the 24 drivers "agents" involved in the experiment. Unlike the system-based model, the agent-based model produced a set of model parameters (β_i's) for each driver "agent".

The model calibrated coefficients for the system-based model and their corresponding P-values are summarized in Table 17, showing a good statistical fit with adjusted-R^2 of 90.5 percent. With respect to the agent-based model, the calibrated parameters also showed good statistical fits with zero-P-values and adjusted-R^2 values ranging between 42.6% and 98.6% (mean adjusted-R^2 of 83%).

Table 19: System-Based DTI error Model Calibration Results

Coefficients	Coefficient Values	P-value
β_0	-27.3854	
β_1	-19.6098	0.0000
β_2	27.0055	0.0000

9.4 VALIDATION OF THE BEHAVIORAL MODEL

Having characterized the critical parameters included in the behavioral model, the next step is to validate the model and its success in reproducing the correct stop-run decisions. In order to do this, a Monte Carlo (MC) simulation is carried out to replicate the original dataset for 1000 times. Each time the residual errors associated with t, d_{max}, and DTI error are assigned randomly. Then, after each simulation, the success rate of the BM is calculated as in Equation (37).

$$\text{Success Rate} = \frac{\text{No. of successfully predicted decisions}}{\text{Total no. of simulated decisions}} \quad (37)$$

Nevertheless, before validating the behavioral model success rate, it would be interesting to see how the model will behave based on assuming the current state-of the-practice values of the t (1-s) and d_{max} (3 m/s^2), while neglecting the driver's error in estimating the DTI (DTI error = 0). Accordingly, the current state-of-the-practice values are input to the model to yield a very low success rate of 45.52%, as shown in Figure 52a. Moreover, the performance of the model is evaluated based on using the actual values for all the model variables, and as expected it returns a perfect success rate of 100%, as shown in Figure 52b.

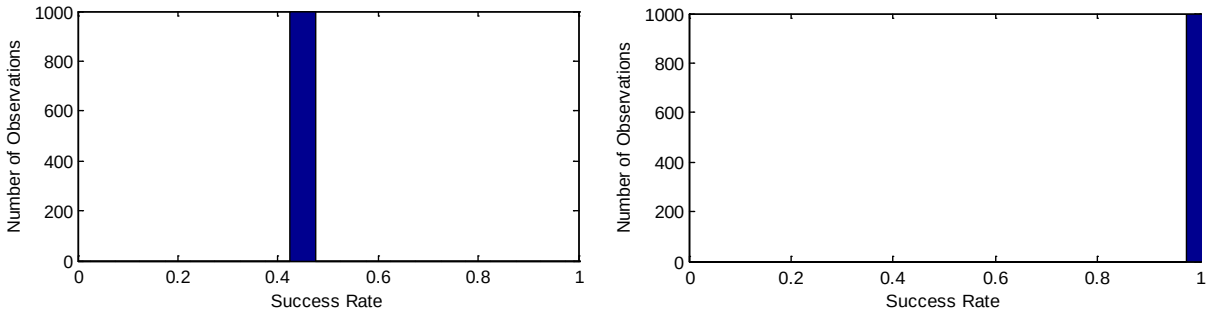

(a) State-of-the-Practice Values **(b) Actual Values**

Figure 52: Success Rate of the Behavioral Model Based on State-of-the-Practice Values and Actual Values

After exploring the model performance on the basic values of the model variables, Monte Carlo (MC) simulations are carried out using the variables (a_{max}, u_{max}, t, d_{max}, DTI error) characterization from the previous section in order to validate the success of the behavioral model in replicating the stop-run decisions from the original dataset. In addition, the MC simulations are made twice: one time with the system-based DTI error model, and another time with the agent-based DTI error model. Figure 53 a and b summarize the histograms and the descriptive statistical measures of the success rates for the behavioral model MC simulations using the system-based and the agent-based models of the DTI error.

As demonstrated from the results of the two figures, the success rate of the behavioral model using the system-based model range from 40% to 100% with mean value of 72.8%, whereas using the agent-based model, the success rate ranges from 70% to 100% with a mean success rate of 87.2%. Although, the BM success rate using the system-based model is not as high as that of the statistical model calibrated earlier in Chapter 5 (82%), the BM success rate is

considerably improved after adopting the agent-based model. In addition to the higher success rate of the behavioral model compared to the statistical model, the results demonstrate that a well-characterized behavioral model yields a promising tool for testing different signal timing and dilemma zone and red-light running mitigation policies before introducing them into the field. This tool can also be used for implementation in the traffic simulation software to better simulate the driver behavior after the onset of the yellow indication.

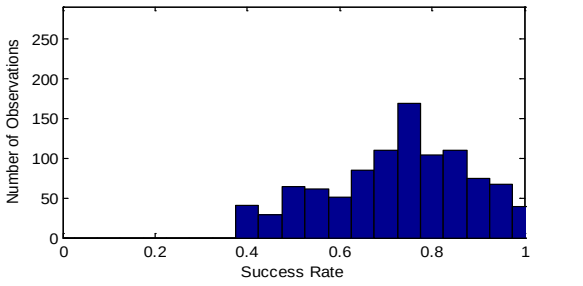

Min	Max	Mean	15%	50%	85%	StD
0.3954	1.0000	**0.7282**	0.5355	0.7449	0.8917	0.1535

(a) System-Based Model

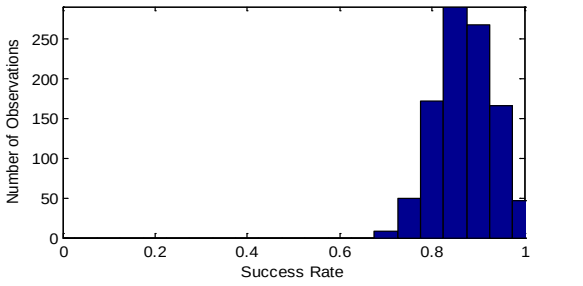

Min	Max	Mean	15%	50%	85%	StD
0.6980	1.0000	**0.8716**	0.8029	0.8730	0.9408	0.0618

(b) Agent-Based Model

Figure 53: Success Rates of the Behavioral Model Using System-Based and Agent-Based DTI error Models

9.5 SUMMARY AND CONCLUSIONS

In this chapter a state-of-the-art behavioral model (BM) was proposed to simulate driver behavior after the onset of a yellow indication until the driver reaches the intersection stop line. The approach tracks the driver behavior continuously at each time step (e.g. every deci-second). This feature allows for the modeling of changes in driver behavior as they travel towards the intersection. The chapter presented the general framework of the proposed BM and its different components and demonstrated the ability of the model to track the driver decision evolution. The BM is capable of updating the information available for drivers in the DZ every time step until they reach a final decision. However, for the BM to be able to simulate driver behavior accurately, information on a number of variables is required. This makes it a unique tool for testing new DZ mitigation strategies before their actual implementation. In addition, the BM can be implemented in a microscopic traffic simulation environment, where all the information is available. The analysis then characterized the components involved in the BM framework using the dataset I. These components include the maximum accepted acceleration, maximum accepted speed, PRT, maximum accepted deceleration rate, and the error in estimating the DTI. The first

two variables are constrained variables and were characterized based on their mean values. On the other hand, the other three variables are unconstrained variables and were characterized by statistical models. For the DTI error, two models were calibrated; a system-based model and an agent-based model. Both models were adopted to validate the behavioral model success rate, based on Monte Carlo (MC) simulations. The mean BM success rates using the system-based model and agent-based model are 72.8% and 87.2%, respectively. The behavioral model using the agent-based model performs better than the statistical model calibrated in Chapter 5 (success rate of 82%).

CHAPTER 10 CONCLUSIONS AND RECOMMENDATIONS

10.1 DISSERTATION CONCLUSIONS

The research presented in this dissertation characterizes the driver behavior when approaching high-speed signalized intersection approaches at the onset of the yellow indication. The conclusions of this dissertation can be summarized in four major categories; characterization of driver behavior attributes, stochastic procedure for yellow interval design, agent-based stochastic modeling of the driver decision, and a behavioral modeling framework of the driver behavior.

10.1.1 Characterization of Driver Behavior Attributes

The characterization of the driver behavior at the onset of yellow included characterizing four major attributes. The following contributions can be drawn regarding each attribute.

10.1.1.1 Yellow/red light running behavior

- Drivers are more likely to run at the onset of the yellow indication at shorter distances from the intersection.
- Approaching speed at the onset of yellow can be reasonably considered representative for the driver's speed at the intersection entry instant.
- Number of running drivers is inversely proportional with the intersection entry times after the onset of yellow indication.
- There is a potential risk that the legal yellow-light runners would not be able to completely clear the intersection at the instant the side-street traffic gains the right-of-way, if the adopted all-red interval is not well-timed.
- Finally, younger and female drivers are more willing to run than older and male drivers at the same TTI.

10.1.1.2 Driver stop-run decision

- Dataset II statistical model showed that TTI is the most significant explanatory variable, whereas dataset I model showed that TTI, gender, age, yellow time, and ratio of approaching speed to speed limit are significant variables.
- A data transformation technique can be applied to the statistical model to adjust for higher propensity for vehicle stopping in the controlled field test versus uncontrolled field test.

- Sensitivity analysis based on the statistical model showed that male drivers are more likely to stop than female drivers, and also older drivers are more likely to stop than younger drivers for both speed limits.

10.1.1.3 Driver perception-reaction time

- TTI, driver gender and age, and roadway grade did not show significant impact on the perception time component, whereas the reaction time was found to increase when TTI increases, and when going uphill than going downhill.
- Overall PRT from dataset II was not dependent on driver age and gender, whereas PRT from dataset I is higher for female and older drivers compared to male and younger drivers.
- PRT is also higher for vehicles traveling uphill and also when the TTI increases.
- Typically, PRT is higher if they are following a vehicle that runs a yellow light, whereas PRT decreases when they are followed by another vehicle.
- PRT values are found consistent with earlier studies, which demonstrates that the
- Driver behavior observed in the controlled field experiment appears to be consistent with naturalistic and non-obtrusive field-observed driver behavior, where PRT values are found consistent with earlier studies.
- Statistical model of PRT showed that gender, age, grade, TTI, yellow time, and ratio of approaching speed to speed limit; are significant explanatory variables.

10.1.1.4 Driver deceleration level

- Driver deceleration levels are significantly higher than the 3 m/s^2 deceleration level used in the state-of-the-practice traffic signal design guidelines.
- Deceleration levels are higher at shorter TTI at the onset of yellow.
- Younger (less than 40 years old) and older (60+ years old) drivers employ greater deceleration levels compared to middle-aged drivers (40 to 59 years old).
- Drivers following another vehicle that proceeds legally through the intersection without stopping exerts higher deceleration levels compared to drivers driving alone or leading another vehicle.
- Drivers leading a platoon of vehicles are not affected by the vehicles behind them with regards to their deceleration behavior.

- Deceleration behavior can be effectively modeled using a distribution of parameters rather than applying an average deceleration rate for the design of yellow times, given the extensive variations in the observed deceleration rates.
- Statistical modeling deceleration showed that gender, age, grade, TTI, yellow time, ratio of approaching speed to speed limit, and PRT; are significant explanatory variables.

10.1.2 Stochastic Procedure for Yellow Interval Design

A stochastic approach for estimating the yellow interval duration was proposed that accounts for design reliability using a Monte Carlo simulation approach that accounts for the stochastic nature of driver PRT and deceleration behavior. Further conclusions are listed hereinafter.

- Lookup tables are developed to assist practitioners in the design of yellow timings, that reflects the stochastic nature of driver PRT and deceleration levels.
- The proposed procedure could yield savings in signalized intersection between 1% and 10% and/or savings in the yellow time between 0.2 and 0.8 seconds.
- Lookup tables are also developed for different gender and age groups. Yellow timings can then be computed as a volume-weighted average yellow time considering the breakdown of drivers within the various gender and age categories.
- The lookup tables proposed in this dissertation are valid only for light duty vehicles on dry roadway surface and clear weather conditions.
- It is possible to develop driver-specific clearance timings by informing drivers of the possible changes in the signal indication through some form of communication between the vehicle and the traffic signal controller, which makes the proposed approach capable of integration within the IntelliDrive^{SM} initiative.

10.1.3 Agent-Based Stochastic Modeling of Driver Decision

An agent-based Bayesian logistic model for driver stop-run decision at the onset of a yellow indication that captures the stochastic nature of the driver decision was developed. The variables that were considered in the model include driver gender, age, TTI, yellow time, approaching speed and speed limit. The model development demonstrated the following.

- Application of the Bayesian model requires significant computational capabilities in order to store the model parameters realizations. Two approaches were adopted in order

to simplify the application of the Bayesian model, namely Cascaded regression and Cholesky decomposition, which capture the parameters correlations in only 14 parameters without the need to store the parameters realizations. Both approaches were found to be consistent and able to generate parameters replications comparable to the Bayesian model.

- The Bayesian model is validated and found to be transferable and able to replicate the driver decision in the different datasets.
- The proposed agent-based Bayesian modeling framework can be easily implemented within traffic simulation software using any of the proposed application procedures (Cascaded regression or Cholesky decomposition). In addition, the proposed approach can also be applied using a Monte Carlo simulation to derive stochastic dilemma zone boundaries for different driver gender and age groups.
- The Bayesian model can be able to conduct stochastic sensitivity analysis of different variables that affect the driver stop-run decisions, such as driver gender and age, yellow duration, approaching speed, etc. Thus, practitioners as well as researchers can statistically test for significant differences in stop/run probability distributions corresponding to two different values of the explanatory variable.

10.1.4 Behavioral Modeling Framework of Driver Behavior

The dissertation outlined the general framework for a state-of-the-art behavioral model (BM) that is capable of simulating the complete driver behavior while approaching an intersection approach from the instant of the onset of yellow to the instant the driver reaches the intersection stop line. The following conclusions are drawn.

- The behavioral framework can track the dilemma zone drivers and update the information available to them every time step until they reach a final decision.
- The BM simulates driver behavior every time step (e.g. every deci-second), which enables updating all the surrounding parameters that affect the driver stop-run decision. This makes it a unique tool for testing new signal timings and dilemma zone mitigation strategies before actual implementation. The BM could be implemented in any traffic simulation software, where all the information is available.

- The characterization of the BM components involves the maximum accepted acceleration, maximum accepted speed, PRT, maximum accepted deceleration rate, and the error in estimating the DTI.
- Drivers are overestimating their DTI when they decided to stop, whereas they accurately estimated their DTI when they decided to run.
- The agent-based modeling of DTI error demonstrates a considerably high success rate of the BM that is better than the stop-run decision statistical model, and better than using a system-based DTI error model.

10.2 RECOMMENDATIONS FOR FURTHER WORK

The following areas of research should be pursued in order to expand the research work introduced in this dissertation on the driver behavior modeling.

- Generalizing the calibration and the application of the models and the procedures presented in this dissertation with different datasets that cover different conditions other than those presented in the used datasets (e.g. inclement weather conditions and presence of heavy vehicles).
- Conducting further data collection in order to develop lookup table for the stochastic yellow timing procedure that extends to include heavy duty trucks, wet roadway conditions, and/or inclement weather conditions.
- Investigation of extending the stochastic yellow time procedure to develop customized clearance intervals for individual drivers in order to test its ability to be integrated within the IntelliDrive^{SM} initiative.
- Implementation of the proposed agent-based Bayesian driver decision model within simulation software in order to compare its performance to the existing traditional models.
- Investigating the implementation of the behavioral modeling framework within simulation software in order to test its ability of simulating the dilemma zone drivers.

REFERENCES

1. Federal Highway Administration (FHWA), *Manual on Uniform Traffic Control Devices (MUTCD)*. 2003, Washington, DC.
2. Lee, S. E., R. R. Knipling, M. C. DeHart, M. A. Perez, G. T. Holbrook, S. B. Brown, S. R. Stone, and R. L. Olson, *Vehicle-Based Countermeasures for Signal and Stop Sign Violation*. 2004, DOT HS 809 716, Virginia Tech Transportation Institute.
3. Zegeer, C. V., *Effectiveness of Green-Extension Systems at High-Speed Intersections*. 1977, Research Report 472, Kentucky Bureau of Highways, Lexington, KY.
4. Huang, H., H. C. Chin, and A. H. H. Heng, *Effect of Red Light Cameras on Accident Risk at Intersections.* Transportation Research Record: Journal of the Transportation Research Board, 2006. Vol. 1969 p. 18-26.
5. Federal Highway Administration (FHWA), *Traffic Signal Timing Manual*. 2008, United States. 274p.
6. Institute of Transportation Engineers (ITE), *Traffic Engineering Handbook*, ed. J.L. Pline. 1999, [Washington, D.C.]: Institute of Transportation Engineers.
7. Institute of Transportation Engineers (ITE), *Traffic Control Devices Handbook*, ed. J.L. Pline. 2001, Washington, DC: Institute of Transportation Engineers.
8. Pant, P. D. and Y. Cheng, *Dilemma zone protection and signal coordination at closely-spaced high-speed intersections: Final Report*. 2001, Federal Highway Administration (U.S. Department of Transportation).
9. Zegeer, C. and R. Deen, *Green-Extension Systems at High-Speed Intersections.* ITE Journal-Institute of Transportation Engineers, 1978. Vol. 48(11) p. 19-24.
10. Bonneson, J., D. Middleton, K. Zimmerman, H. Charara, and M. Abbas, *Development and Evaluation of a Detection-Control System for Rural Intersections*. 2001, 0-4022-1, Texas Transportation Institute, The Texas A&M University System, College Station, TX.
11. Bonneson, J., D. Middleton, K. Zimmerman, H. Charara, and M. Abbas, *Intelligent Detection-Control System for Rural Signalized Intersections*. 2002, 0-4022-2, Texas Transportation Institute, The Texas A&M University System, College Station, TX.
12. Zimmerman, K. and J. Bonneson, *In-Service Evaluation of a Detection-Control System for High-Speed Signalized Intersections*. 2005, 5-4022-01-1, Texas Transportation Institute, The Texas A&M University System, College Station, TX.
13. Kronborg, P., *MOVA and LHOVRA: traffic signal control for isolated intersections.* Traffic Engineering and Control, 1993. Vol. 34(4) p. 195-200.
14. Kronborg, P., F. Davidsson, and J. Edholm, *SOS-self optimising signal control: development and field trials of the SOS algorithm for self-optimising signal control at isolated intersections*. 1997, Report 1997:2E, Transport Research Institute, Stockholm, Sweden.
15. Peterson, A., T. Bergh, and K. Steen., *LHOVRA: a new traffic signal control strategy for isolated junctions.* Traffic Engineering and Control, 1986. Vol. 27(7/8) p. 388-389.
16. *ITS Strategic Research Plan, 2010-2014 - Executive Summary*. 2010.

17. Dimitropoulos, I. and G. Kanellaidis. *Highway Geometric Design: The Issue of Driving Behavior Variability*. in *International Symposium on Highway Geometric Design Practices*. 1998. Boston, MA: Transportation Research Board.

18. Thompson, B. A. and ITE Technical Council Task Force 4TF-1, *An informational report: Determining vehicle signal change and clearance intervals.* ITE Journal-Institute of Transportation Engineers, 1994. Vol. 64(8) p. 16.

19. Milazzo, J., J. Hummer, N. Rouphail, L. Prothe, and J. McCurry. *The Effect of Dilemma Zones on Red Light Running Enforcement Tolerances*, in *Transportation Research Board 81st Annual Meeting*, Washington D.C., 2002. 02-00346.

20. Taoka, G. T., *Brake reaction times of unalerted drivers.* ITE Journal-Institute of Transportation Engineers, 1989. Vol. 59(3) p. 19-21.

21. Gazis, D., R. Herman, and A. Maradudin, *The Problem of the Amber Signal Light in Traffic Flow.* Operations Research, 1960. Vol. 8(1) p. 112-132.

22. Green, M., *"How Long Does It Take to Stop?" Methodological Analysis of Driver Perception-Brake Times.* Transportation Human Factors, 2000. Vol. 2(3) p. 195 - 216.

23. Bates, J. T., *Perception-reaction time.* ITE Journal-Institute of Transportation Engineers, 1995. Vol. 65(2) p. 35-36.

24. Kai, G. P. and W. Y. Diew, *Driver Perception Response Time During the Signal Change Interval.* Applied Health Economics and Health Policy, 2004. Vol. 3(1) p. 9-15.

25. Summala, H., *Brake Reaction Times and Driver Behavior Analysis.* Transportation Human Factors, 2000. Vol. 2(3) p. 217 - 226.

26. Diew, W. Y. and G. P. Kai, *Perception-Braking Response Time of Unalerted Drivers at Signalized Intersections.* ITE Journal-Institute of Transportation Engineers, 2001. Vol. 71(6) p. 73-76.

27. Chang, M., C. J. Messer, and A. Santiago, *Timing Traffic Signal Change Intervals Based on Driver Behavior*. Transportation Research Record: Journal of the Transportation Research Board, 1985. Vol. 1027 p. 20-23.

28. Gates, T., D. Noyce, L. Laracuente, and E. Nordheim, *Analysis of Driver Behavior in Dilemma Zones at Signalized Intersections.* Transportation Research Record: Journal of the Transportation Research Board, 2007. Vol. 2030 p. 29-39.

29. Doerzaph, Z. R., *Intersection Stopping Behavior as Influenced by Driver State: Implications for Intersection Decision Support Systems*, in *Industrial and Systems Engineering*. 2004, Unpublished Thesis, Virginia Polytechnic Institute and State University: Blacksburg, VA.

30. Wortman, R. H. and J. S. Matthias, *Evaluation of Driver Behavior at Signalized Intersections.* Transportation Research Record: Journal of the Transportation Research Board, 1983. Vol. 904 p. 10-20

31. Van der Horst, R. and A. Wilmink, *Drivers' Decision-Making at Signalised Intersections: An Optimisation of the Yellow Timing.* Traffic Engineering & Control, 1986. Vol. 27(12) p. 615-617.

32. Williams, W. L., *Driver Behavior during the Yellow Interval (Abridgment).* Transportation Research Record: Journal of the Transportation Research Board, 1977. Vol. 644 p. p. 75-78.

33. Caird, J. K., S. L. Chisholm, C. J. Edwards, and J. I. Creaser, *The effect of yellow light onset time on older and younger drivers' perception response time (PRT) and intersection behavior.* Transportation Research Part F: Traffic Psychology and Behaviour, 2007. Vol. 10(5) p. 383-396.

34. Parsonson, P. S. and A. Santiago. *Design Standards for Timing the Traffic Signal Clearance Period Must be Improved to Avoid Liability*. in *ITE Compendium of Technical Papers*. 1980. Washington, DC: Institute of Transportation Engineers.

35. Wortman, R. H., J. M. Witkowski, and T. C. Fox, *Traffic Characteristics During Signal Change Intervals.* Transportation Research Record: Journal of the Transportation Research Board, 1985. Vol. 1027 p. p. 4-6.

36. Bennett, C. R. and R. C. M. Dunn, *Driver deceleration behavior on a freeway in New Zealand.* Transportation Research Record: Journal of the Transportation Research Board, 1995. Vol. 1510 p. 70-75.

37. Haas, R., V. Inman, A. Dixson, and D. Warren, *Use of Intelligent Transportation System Data to Determine Driver Deceleration and Acceleration Behavior.* Transportation Research Record: Journal of the Transportation Research Board, 2004. Vol. 1899 p. 3-10.

38. Wang, J., K. Dixon, H. Li, and J. Ogle, *Normal Deceleration Behavior of Passenger Vehicles at Stop Sign-Controlled Intersections Evaluated with In-Vehicle Global Positioning System Data.* Transportation Research Record: Journal of the Transportation Research Board, 2005. Vol. 1937 p. 120-127.

39. Hicks, T., R. Tao, and E. Tabacek. *Observations of Driver Behavior in Response to Yellow at Nine Intersections in Maryland*, in *Transportation Research Board 84th Annual Meeting*, Washington D.C., 2005.

40. El-Shawarby, I., H. Rakha, V. Inman, and G. Davis, *Evaluation of Driver Deceleration Behavior at Signalized Intersections.* Transportation Research Record: Journal of the Transportation Research Board, 2007. Vol. 2018 p. 29-35.

41. Sheffi, Y. and H. Mahmassani, *A model of driver behavior at high speed signalized intersections.* Transportation Science, 1981. Vol. 15(1) p. 50-61.

42. Senders, J. W., *Analysis of an Intersection.* Ergonomics in Design, 1998. Vol. 6(2) p. 4-6.

43. Parsonson, P. S., *Signal Timing Improvement Practices*. National Cooperative Highway Research Program Synthesis of Highway Practice No. 172. 1992, Washington, D.C.: Transportation Research Board.

44. El-Shawarby, I., H. A. Rakha, V. W. Inman, and G. W. Davis. *Age and Gender Impact on Driver Behavior at the Onset of a Yellow Phase on High-Speed Signalized Intersection Approaches*, in *Transportation Research Board 86th Annual Meeting*, 2007. Compendium of Papers CD-ROM (#07-0208).

45. Tarnoff, P. J., *Traffic Signal Clearance Intervals.* ITE Journal-Institute of Transportation Engineers, 2004. Vol. 74(4) p. 20-24.

46. Virginia Department of Transportation (VDOT), *Memo TE-306: Calculation of Clearance Intervals*. 2001.

47. Lum, K. M. and Y. D. Wong, *Impacts of Red Light Camera on Violation Characteristics.* Journal of Transportation Engineering, 2003. Vol. 129(6) p. 648-656.

48. Li, P., *Stochastic Methods for Dilemma Zone Protection at Signalized Intersections*, in *Civil Engineering*. 2009, Unpublished Dissertation, Virginia Polytechnic Institute and State University: Blacksburg, VA.

49. Vincent, R. A. and J. R. Peirce, *MOVA: Traffic responsive, self-optimising signal control for isolated intersections.* 1988, Crowthorne, Berkshire: Transport and Road Research Laboratory (TRRL).

50. Zimmerman, K., *Additional Dilemma Zone Protection for Trucks at High-Speed Signalized Intersections.* Transportation Research Record: Journal of the Transportation Research Board, 2007. Vol. 2009 p. 82-88.

51. McCoy, P. and G. Pesti, *Improving Dilemma-Zone Protection of Advance Detection with Advance-Warning Flashers.* Transportation Research Record: Journal of the Transportation Research Board, 2003. Vol. 1844 p. 11-17.

52. Messer, C. J., S. R. Sunkari, H. A. Charara, and R. T. Parker, *Development of Advance Warning Systems for End-of-Green Phase at High Speed Traffic Signals*. 2003, 0-4260-4, Texas Transportation Institute, The Texas A&M University System, College Station, TX.

53. Sunkari, S., C. Messer, and H. Charara, *Performance of Advance Warning for End of Green System for High-Speed Signalized Intersections.* Transportation Research Record: Journal of the Transportation Research Board, 2005. Vol. 1925 p. 176-184.

54. Chaudhary, N., M. Abbas, and H. Charara, *Development and Field Testing of Platoon Identification and Accommodation System.* Transportation Research Record: Journal of the Transportation Research Board, 2006. Vol. 1978 p. 141-148.

55. Li, P. and M. Abbas, *Stochastic Dilemma Hazard Model at High-Speed Signalized Intersections.* Journal of Transportation Engineering, 2010. Vol. 136(5) p. 448-456.

56. Jones, S. L., Jr and V. P. Sisiopiku, *Safety Treatments at Isolated High-Speed Signalized Intersections: Synthesis.* Journal of Transportation Engineering, 2007. Vol. 133(9) p. 523-528.

57. Shinar, D. and R. Compton, *Aggressive driving: an observational study of driver, vehicle, and situational variables.* Accident Analysis & Prevention, 2004. Vol. 36(3) p. 429-437.

58. Yager, R. R., *Measuring Tranquillity and Anxiety in Decision Making: An Application of Fuzzy Sets.* International Journal of General Systems, 1982. Vol. 8(3) p. 139 - 146.

59. Kikuchi, S., V. Perincherry, P. Chakroborty, and H. Takahashi, *Modeling of Driver Anxiety during Signal Change Intervals.* Transportation Research Record: Journal of the Transportation Research Board, 1993. Vol. 1399 p. 27-35.

60. Yager, R. R. and S. Kikuchi, *On the Role of Anxiety in Decisions under Possibilistic Uncertainty.* Systems, Man, and Cybernetics, Part B: Cybernetics, IEEE Transactions on, 2004. Vol. 34(2) p. 1224-1234.

61. Retting, R. A., S. A. Ferguson, and C. M. Farmer, *Reducing Red Light Running Through Longer Yellow Signal Timing and Red Light Camera Enforcement: Results of a Field Investigation.* Accident Analysis & Prevention, 2008. Vol. 40(1) p. 327-333.

62. Retting, R. A., A. F. Williams, C. M. Farmer, and A. F. Feldman, *Evaluation of Red Light Camera Enforcement in Oxnard, California.* Accident Analysis & Prevention, 1999. Vol. 31(3) p. 169-174.

63. Retting, R. A., R. G. Ulmer, and A. F. Williams, *Prevalence and Characteristics of Red Light Running Crashes in the United States.* Accident Analysis & Prevention, 1999. Vol. 31(6) p. 687-694.

64. Porter, B. E. and K. J. England, *Predicting Red-Light Running Behavior: A Traffic Safety Study in Three Urban Settings.* Journal of Safety Research, 2000. Vol. 31(1) p. 1-8.

65. Bonneson, J. and H. Son, *Prediction of Expected Red-Light-Running Frequency at Urban Intersections.* Transportation Research Record: Journal of the Transportation Research Board, 2003. Vol. 1830 p. 38-47.

66. Yang, C. Y. D. and W. G. Najm, *Examining Driver Behavior Using Data Gathered from Red Light Photo Enforcement Cameras.* Journal of Safety Research, 2007. Vol. 38(3) p. 311-321.

67. Rakha, H., I. El-Shawarby, and A. Amer, *Development of a Framework for Evaluating Yellow Timing at Signalized Intersections (In Press).* 2010, 87584, Virginia Transportation Research Council (VTRC), Virginia Department of Transportation (VDOT), Charlottesville, VA.

68. Rakha, H., I. Lucic, S. H. Demarchi, J. R. Setti, and M. Van Aerde, *Vehicle dynamics model for predicting maximum truck acceleration levels.* Journal of Transportation Engineering, 2001. Vol. 127(5) p. 418-425.

69. Rakha, H., A. Amer, and I. El-Shawarby, *Modeling Driver Behavior Within a Signalized Intersection Approach Decision-Dilemma Zone.* Transportation Research Record: Journal of the Transportation Research Board, 2008. Vol. 2069 p. 16-25.

70. Amer, A., H. Rakha, and I. El-Shawarby. *A Behavioral Modeling Framework of Driver Behavior at Onset of Yellow Indication at Signalized Intersections,* in *Transportation Research Board 89th Annual Meeting* Washington, DC, 2010. Compendium of Papers DVD (#10-0520).

71. El-Shawarby, I., A. Amer, A.-S. Abdel-Salam, and H. Rakha. *Empirical Study of Yellow/Red Light Running Behavior on High-Speed Signalized Intersection Approaches (In Press),* in *Transportation Research Board 90th Annual Meeting*, Washington, DC, 2011. Compendium of Papers DVD (#11-2204).

72. El-Shawarby, I., A. Amer, and H. Rakha, *Driver Stopping Behavior on High-Speed Signalized Intersection Approaches.* Transportation Research Record: Journal of the Transportation Research Board, 2008. Vol. 2056 p. 60-69.

73. El-Shawarby, I., H. Rakha, A. Amer, and C. McGhee. *Characterization of Driver Perception-Reaction Time at Onset of Yellow Indication,* in *Transportation Research Board 89th Annual Meeting* Washington, DC, 2010. Compendium of Papers DVD (#10-0520).

74. El-Shawarby, I., H. Rakha, A. Amer, and C. McGhee. *Driver and Surrounding Traffic Impact on Vehicle Deceleration Behavior at the Onset of a Yellow Indication (In Press)*, in *Transportation Research Board 90th Annual Meeting*, Washington, DC, 2011. Compendium of Papers DVD (#11-1512).

75. Amer, A., H. Rakha, and I. El-Shawarby. *Stochastic Modeling of Driver Decision at the Onset of a Yellow Indication at Signalized Intersections (In Press)*, in *Transportation Research Board 90th Annual Meeting*, Washington, DC, 2011.

76. Bolstad, W. M., *Introduction to Bayesian statistics*. 2nd ed. 2007, Hoboken, N.J.: John Wiley.

77. *Measures of Skewness and Kurtosis (Section 1.3.5.11)*, in *Engineering Statistics Handbook*. 2010, National Institute of Standards and Technology.

78. Jin, W. and L. Chunlei. *Generating Multivariate Mixture of Normal Distributions using a Modified Cholesky Decomposition*. in *Simulation Conference, 2006. WSC 06. Proceedings of the Winter*. 2006.

APPENDIX A

YELLOW TIME LOOKUP TABLES FOR SPECIFIC AGE AND GENDER GROUPS

Table A-1 Yellow Clearance Interval Lookup Table for Young Female Drivers

G	-4%			-3%			-2%			*G*
v_f *(mi/h)*	**35**	**45**	**55**	**35**	**45**	**55**	**35**	**45**	**55**	v_f *(mi/h)*
50%	2.6	3.1	3.6	2.6	3.1	3.6	2.5	3.0	3.5	**50%**
60%	2.8	3.3	3.9	2.8	3.3	3.8	2.7	3.2	3.7	**60%**
70%	3.1	3.6	4.1	3.0	3.5	4.0	3.0	3.5	4.0	**70%**
80%	3.4	3.9	4.4	3.4	3.8	4.3	3.3	3.8	4.3	**80%**
85%	3.6	4.1	4.6	3.5	4.0	4.5	3.5	3.9	4.4	**85%**
90%	3.9	4.3	4.8	3.8	4.2	4.7	3.7	4.1	4.6	**90%**
95%	4.2	4.6	5.1	4.1	4.5	5.0	4.0	4.4	4.9	**95%**
96%	4.3	4.7	5.2	4.2	4.6	5.1	4.0	4.5	4.9	**96%**
97%	4.4	4.8	5.3	4.3	4.7	5.2	4.2	4.6	5.0	**97%**
98%	4.6	5.0	5.5	4.4	4.8	5.3	4.3	4.7	5.2	**98%**
99%	4.8	5.2	5.7	4.7	5.1	5.5	4.5	4.9	5.4	**99%**
99.9%	5.8	6.1	6.6	5.5	5.8	6.3	5.2	5.6	6.0	**99.9%**

Reliability Factor (left) / **Reliability Factor** (right)

G	-1%			0%			1%			*G*
v_f *(mi/h)*	**35**	**45**	**55**	**35**	**45**	**55**	**35**	**45**	**55**	v_f *(mi/h)*
50%	2.5	3.0	3.5	2.5	3.0	3.4	2.5	2.9	3.4	**50%**
60%	2.7	3.2	3.7	2.7	3.2	3.6	2.6	3.1	3.6	**60%**
70%	2.9	3.4	3.9	2.9	3.4	3.9	2.9	3.3	3.8	**70%**
80%	3.2	3.7	4.2	3.2	3.6	4.1	3.1	3.6	4.1	**80%**
85%	3.4	3.9	4.3	3.3	3.8	4.3	3.3	3.7	4.2	**85%**
90%	3.6	4.1	4.5	3.5	4.0	4.4	3.5	3.9	4.4	**90%**
95%	3.9	4.3	4.8	3.8	4.2	4.7	3.7	4.1	4.6	**95%**
96%	3.9	4.4	4.8	3.9	4.3	4.7	3.8	4.2	4.6	**96%**
97%	4.0	4.5	4.9	3.9	4.4	4.8	3.8	4.3	4.7	**97%**
98%	4.2	4.6	5.0	4.0	4.5	4.9	3.9	4.4	4.8	**98%**
99%	4.4	4.8	5.2	4.2	4.7	5.1	4.1	4.5	5.0	**99%**
99.9%	5.0	5.4	5.9	4.9	5.3	5.8	4.7	5.1	5.5	**99.9%**

Reliability Factor (left) / **Reliability Factor** (right)

G	2%			3%			4%			*G*
v_f *(mi/h)*	**35**	**45**	**55**	**35**	**45**	**55**	**35**	**45**	**55**	v_f *(mi/h)*
50%	2.4	2.9	3.4	2.4	2.9	3.3	2.4	2.8	3.3	**50%**
60%	2.6	3.1	3.5	2.6	3.0	3.5	2.6	3.0	3.5	**60%**
70%	2.8	3.3	3.8	2.8	3.2	3.7	2.8	3.2	3.7	**70%**
80%	3.1	3.5	4.0	3.0	3.5	3.9	3.0	3.4	3.9	**80%**
85%	3.2	3.7	4.1	3.2	3.6	4.1	3.1	3.6	4.0	**85%**
90%	3.4	3.8	4.3	3.3	3.8	4.2	3.3	3.7	4.1	**90%**
95%	3.6	4.0	4.5	3.5	4.0	4.4	3.5	3.9	4.3	**95%**
96%	3.7	4.1	4.5	3.6	4.0	4.5	3.5	3.9	4.4	**96%**
97%	3.8	4.2	4.6	3.7	4.1	4.5	3.6	4.0	4.4	**97%**
98%	3.9	4.3	4.7	3.8	4.2	4.6	3.7	4.1	4.5	**98%**
99%	4.0	4.4	4.9	3.9	4.3	4.8	3.8	4.2	4.7	**99%**
99.9%	4.5	5.0	5.4	4.4	4.8	5.3	4.3	4.7	5.1	**99.9%**

Reliability Factor (left) / **Reliability Factor** (right)

Table A-2 Yellow Clearance Interval Lookup Table for Young Male Drivers

G	-4%			-3%			-2%			*G*
v_f *(mi/h)*	35	45	55	35	45	55	35	45	55	v_f *(mi/h)*
50%	2.5	3.0	3.6	2.5	3.0	3.5	2.5	3.0	3.5	50%
60%	2.7	3.3	3.8	2.7	3.2	3.7	2.7	3.2	3.7	60%
70%	3.0	3.5	4.0	3.0	3.5	4.0	2.9	3.4	3.9	70%
80%	3.3	3.8	4.3	3.3	3.8	4.3	3.2	3.7	4.2	80%
85%	3.5	4.0	4.5	3.5	3.9	4.4	3.4	3.9	4.3	85%
90%	3.8	4.2	4.7	3.7	4.1	4.6	3.6	4.0	4.5	90%
95%	4.1	4.5	5.0	4.0	4.4	4.9	3.9	4.3	4.8	95%
96%	4.2	4.6	5.1	4.1	4.5	5.0	4.0	4.4	4.9	96%
97%	4.3	4.7	5.2	4.2	4.6	5.1	4.1	4.5	5.0	97%
98%	4.4	4.9	5.4	4.3	4.7	5.2	4.2	4.6	5.1	98%
99%	4.7	5.1	5.6	4.6	5.0	5.4	4.4	4.8	5.3	99%
99.9%	5.7	5.9	6.3	5.4	5.8	6.2	5.2	5.5	5.9	99.9%

Reliability Factor

G	-1%			0%			1%			*G*
v_f *(mi/h)*	35	45	55	35	45	55	35	45	55	v_f *(mi/h)*
50%	2.4	2.9	3.4	2.4	2.9	3.4	2.4	2.9	3.3	50%
60%	2.6	3.1	3.6	2.6	3.1	3.6	2.6	3.1	3.5	60%
70%	2.9	3.4	3.8	2.8	3.3	3.8	2.8	3.3	3.7	70%
80%	3.2	3.6	4.1	3.1	3.6	4.0	3.1	3.5	4.0	80%
85%	3.3	3.8	4.3	3.3	3.7	4.2	3.2	3.7	4.1	85%
90%	3.5	4.0	4.4	3.5	3.9	4.3	3.4	3.8	4.3	90%
95%	3.8	4.2	4.7	3.7	4.1	4.6	3.6	4.0	4.5	95%
96%	3.9	4.3	4.7	3.8	4.2	4.6	3.7	4.1	4.6	96%
97%	3.9	4.4	4.8	3.8	4.3	4.7	3.8	4.2	4.6	97%
98%	4.1	4.5	4.9	4.0	4.4	4.8	3.9	4.3	4.7	98%
99%	4.3	4.7	5.1	4.1	4.6	5.0	4.0	4.4	4.9	99%
99.9%	4.9	5.3	5.7	4.7	5.2	5.6	4.6	4.9	5.4	99.9%

Reliability Factor

G	2%			3%			4%			*G*
v_f *(mi/h)*	35	45	55	35	45	55	35	45	55	v_f *(mi/h)*
50%	2.4	2.8	3.3	2.4	2.8	3.3	2.3	2.8	3.2	50%
60%	2.6	3.0	3.5	2.5	3.0	3.4	2.5	3.0	3.4	60%
70%	2.8	3.2	3.7	2.7	3.2	3.6	2.7	3.1	3.6	70%
80%	3.0	3.5	3.9	3.0	3.4	3.9	2.9	3.4	3.8	80%
85%	3.2	3.6	4.0	3.1	3.5	4.0	3.1	3.5	3.9	85%
90%	3.3	3.7	4.2	3.3	3.7	4.1	3.2	3.6	4.1	90%
95%	3.5	4.0	4.4	3.5	3.9	4.3	3.4	3.8	4.2	95%
96%	3.6	4.0	4.5	3.5	3.9	4.4	3.4	3.9	4.3	96%
97%	3.7	4.1	4.5	3.6	4.0	4.4	3.5	3.9	4.4	97%
98%	3.8	4.2	4.6	3.7	4.1	4.5	3.6	4.0	4.4	98%
99%	3.9	4.3	4.8	3.8	4.2	4.7	3.7	4.1	4.6	99%
99.9%	4.4	4.9	5.3	4.3	4.7	5.1	4.2	4.6	5.0	99.9%

Reliability Factor

Table A-3 Yellow Clearance Interval Lookup Table for Mid-Age Female Drivers

G	-4%			-3%			-2%			*G*
v_f *(mi/h)*	35	45	55	35	45	55	35	45	55	v_f *(mi/h)*
50%	2.6	3.1	3.6	2.6	3.1	3.6	2.6	3.1	3.5	50%
60%	2.8	3.3	3.9	2.8	3.3	3.8	2.8	3.3	3.7	60%
70%	3.1	3.6	4.1	3.0	3.5	4.1	3.0	3.5	4.0	70%
80%	3.4	3.9	4.4	3.3	3.8	4.3	3.3	3.8	4.3	80%
85%	3.6	4.1	4.6	3.5	4.0	4.5	3.5	3.9	4.4	85%
90%	3.8	4.3	4.8	3.8	4.2	4.7	3.7	4.1	4.6	90%
95%	4.2	4.6	5.1	4.0	4.5	5.0	3.9	4.4	4.8	95%
96%	4.2	4.7	5.2	4.1	4.6	5.0	4.0	4.5	4.9	96%
97%	4.4	4.8	5.3	4.2	4.7	5.1	4.1	4.5	5.0	97%
98%	4.5	4.9	5.4	4.4	4.8	5.3	4.3	4.7	5.1	98%
99%	4.8	5.1	5.6	4.6	5.0	5.5	4.5	4.9	5.3	99%
99.9%	5.6	6.0	6.4	5.4	5.8	6.2	5.2	5.6	6.1	99.9%

Reliability Factor

G	-1%			0%			1%			*G*
v_f *(mi/h)*	35	45	55	35	45	55	35	45	55	v_f *(mi/h)*
50%	2.5	3.0	3.5	2.5	3.0	3.5	2.5	2.9	3.4	50%
60%	2.7	3.2	3.7	2.7	3.2	3.7	2.7	3.1	3.6	60%
70%	3.0	3.4	3.9	2.9	3.4	3.9	2.9	3.3	3.8	70%
80%	3.2	3.7	4.2	3.2	3.6	4.1	3.1	3.6	4.1	80%
85%	3.4	3.9	4.3	3.3	3.8	4.3	3.3	3.7	4.2	85%
90%	3.6	4.0	4.5	3.5	4.0	4.4	3.5	3.9	4.3	90%
95%	3.8	4.3	4.7	3.8	4.2	4.7	3.7	4.1	4.6	95%
96%	3.9	4.4	4.8	3.8	4.3	4.7	3.7	4.2	4.6	96%
97%	4.0	4.4	4.9	3.9	4.3	4.8	3.8	4.2	4.7	97%
98%	4.1	4.6	5.0	4.0	4.4	4.9	3.9	4.3	4.8	98%
99%	4.3	4.7	5.2	4.2	4.6	5.1	4.1	4.5	5.0	99%
99.9%	5.0	5.4	5.8	4.8	5.2	5.7	4.7	5.0	5.5	99.9%

Reliability Factor

G	2%			3%			4%			*G*
v_f *(mi/h)*	35	45	55	35	45	55	35	45	55	v_f *(mi/h)*
50%	2.5	2.9	3.4	2.4	2.9	3.3	2.4	2.9	3.3	50%
60%	2.6	3.1	3.6	2.6	3.1	3.5	2.6	3.0	3.5	60%
70%	2.8	3.3	3.8	2.8	3.3	3.7	2.8	3.2	3.7	70%
80%	3.1	3.5	4.0	3.1	3.5	3.9	3.0	3.4	3.9	80%
85%	3.2	3.7	4.1	3.2	3.6	4.1	3.1	3.6	4.0	85%
90%	3.4	3.8	4.3	3.3	3.8	4.2	3.3	3.7	4.1	90%
95%	3.6	4.0	4.5	3.5	4.0	4.4	3.5	3.9	4.3	95%
96%	3.7	4.1	4.5	3.6	4.0	4.5	3.5	3.9	4.4	96%
97%	3.7	4.2	4.6	3.7	4.1	4.5	3.6	4.0	4.4	97%
98%	3.8	4.3	4.7	3.8	4.2	4.6	3.7	4.1	4.5	98%
99%	4.0	4.4	4.8	3.9	4.3	4.7	3.8	4.2	4.7	99%
99.9%	4.5	4.9	5.3	4.4	4.7	5.2	4.2	4.7	5.1	99.9%

Reliability Factor

Table A-4 Yellow Clearance Interval Lookup Table for Mid-Age Male Drivers

Reliability Factor	G	-4%			-3%			-2%			G	Reliability Factor
	v_f (mi/h)	35	45	55	35	45	55	35	45	55	v_f (mi/h)	
	50%	2.5	3.1	3.6	2.5	3.0	3.5	2.5	3.0	3.5	50%	
	60%	2.8	3.3	3.8	2.7	3.2	3.7	2.7	3.2	3.7	60%	
	70%	3.0	3.5	4.0	3.0	3.5	4.0	2.9	3.4	3.9	70%	
	80%	3.3	3.8	4.3	3.3	3.8	4.3	3.2	3.7	4.2	80%	
	85%	3.5	4.0	4.5	3.5	3.9	4.4	3.4	3.9	4.3	85%	
	90%	3.8	4.2	4.7	3.7	4.1	4.6	3.6	4.0	4.5	90%	
	95%	4.1	4.5	5.0	4.0	4.4	4.9	3.9	4.3	4.8	95%	
	96%	4.2	4.6	5.1	4.0	4.5	4.9	3.9	4.4	4.8	96%	
	97%	4.3	4.7	5.2	4.1	4.6	5.0	4.0	4.5	4.9	97%	
	98%	4.4	4.8	5.3	4.3	4.7	5.2	4.2	4.6	5.0	98%	
	99%	4.7	5.0	5.5	4.5	4.9	5.4	4.3	4.8	5.2	99%	
	99.9%	5.5	5.8	6.3	5.3	5.6	6.1	5.0	5.4	6.0	99.9%	

Reliability Factor	G	-1%			0%			1%			G	Reliability Factor
	v_f (mi/h)	35	45	55	35	45	55	35	45	55	v_f (mi/h)	
	50%	2.5	2.9	3.4	2.4	2.9	3.4	2.4	2.9	3.3	50%	
	60%	2.7	3.1	3.6	2.6	3.1	3.6	2.6	3.1	3.5	60%	
	70%	2.9	3.4	3.8	2.9	3.3	3.8	2.8	3.3	3.7	70%	
	80%	3.2	3.6	4.1	3.1	3.6	4.0	3.1	3.5	4.0	80%	
	85%	3.3	3.8	4.2	3.3	3.7	4.2	3.2	3.7	4.1	85%	
	90%	3.5	4.0	4.4	3.4	3.9	4.3	3.4	3.8	4.3	90%	
	95%	3.8	4.2	4.7	3.7	4.1	4.6	3.6	4.0	4.5	95%	
	96%	3.8	4.3	4.7	3.8	4.2	4.6	3.7	4.1	4.5	96%	
	97%	3.9	4.4	4.8	3.8	4.3	4.7	3.7	4.2	4.6	97%	
	98%	4.0	4.5	4.9	3.9	4.4	4.8	3.8	4.3	4.7	98%	
	99%	4.2	4.6	5.1	4.1	4.5	5.0	4.0	4.4	4.9	99%	
	99.9%	4.9	5.3	5.7	4.7	5.1	5.5	4.5	4.9	5.4	99.9%	

Reliability Factor	G	2%			3%			4%			G	Reliability Factor
	v_f (mi/h)	35	45	55	35	45	55	35	45	55	v_f (mi/h)	
	50%	2.4	2.9	3.3	2.4	2.8	3.3	2.4	2.8	3.3	50%	
	60%	2.6	3.0	3.5	2.6	3.0	3.5	2.5	3.0	3.4	60%	
	70%	2.8	3.2	3.7	2.8	3.2	3.6	2.7	3.2	3.6	70%	
	80%	3.0	3.5	3.9	3.0	3.4	3.9	3.0	3.4	3.8	80%	
	85%	3.2	3.6	4.0	3.1	3.6	4.0	3.1	3.5	3.9	85%	
	90%	3.3	3.8	4.2	3.3	3.7	4.1	3.2	3.6	4.1	90%	
	95%	3.5	4.0	4.4	3.5	3.9	4.3	3.4	3.8	4.2	95%	
	96%	3.6	4.0	4.5	3.5	3.9	4.4	3.5	3.9	4.3	96%	
	97%	3.7	4.1	4.5	3.6	4.0	4.4	3.5	3.9	4.4	97%	
	98%	3.8	4.2	4.6	3.7	4.1	4.5	3.6	4.0	4.4	98%	
	99%	3.9	4.3	4.8	3.8	4.2	4.7	3.7	4.1	4.6	99%	
	99.9%	4.4	4.8	5.2	4.3	4.7	5.1	4.1	4.6	5.0	99.9%	

Table A-5 Yellow Clearance Interval Lookup Table for Old Female Drivers

G	-4%			-3%			-2%			*G*
v_f *(mi/h)*	35	45	55	35	45	55	35	45	55	v_f *(mi/h)*
50%	2.6	3.1	3.6	2.6	3.1	3.6	2.6	3.1	3.6	50%
60%	2.8	3.4	3.9	2.8	3.3	3.8	2.8	3.3	3.8	60%
70%	3.1	3.6	4.1	3.1	3.6	4.1	3.0	3.5	4.0	70%
80%	3.4	3.9	4.4	3.4	3.8	4.3	3.3	3.8	4.3	80%
85%	3.6	4.1	4.6	3.5	4.0	4.5	3.5	3.9	4.4	85%
90%	3.8	4.3	4.8	3.7	4.2	4.7	3.7	4.1	4.6	90%
95%	4.1	4.6	5.0	4.0	4.5	4.9	3.9	4.4	4.8	95%
96%	4.2	4.6	5.1	4.1	4.5	5.0	4.0	4.4	4.9	96%
97%	4.3	4.7	5.2	4.2	4.6	5.1	4.1	4.5	5.0	97%
98%	4.4	4.9	5.4	4.3	4.8	5.2	4.2	4.6	5.1	98%
99%	4.7	5.1	5.6	4.5	5.0	5.4	4.4	4.8	5.3	99%
99.9%	5.5	5.8	6.2	5.2	5.6	6.1	5.1	5.5	5.9	99.9%

Reliability Factor

G	-1%			0%			1%			*G*
v_f *(mi/h)*	35	45	55	35	45	55	35	45	55	v_f *(mi/h)*
50%	2.6	3.0	3.5	2.5	3.0	3.5	2.5	3.0	3.4	50%
60%	2.7	3.2	3.7	2.7	3.2	3.7	2.7	3.1	3.6	60%
70%	3.0	3.5	3.9	2.9	3.4	3.9	2.9	3.4	3.8	70%
80%	3.2	3.7	4.2	3.2	3.7	4.1	3.2	3.6	4.1	80%
85%	3.4	3.9	4.3	3.3	3.8	4.3	3.3	3.7	4.2	85%
90%	3.6	4.0	4.5	3.5	4.0	4.4	3.5	3.9	4.3	90%
95%	3.9	4.3	4.7	3.7	4.2	4.6	3.7	4.1	4.5	95%
96%	3.9	4.3	4.8	3.8	4.3	4.7	3.7	4.2	4.6	96%
97%	4.0	4.4	4.9	3.9	4.3	4.8	3.8	4.2	4.7	97%
98%	4.1	4.5	5.0	4.0	4.4	4.9	3.9	4.3	4.8	98%
99%	4.3	4.7	5.2	4.2	4.6	5.0	4.1	4.5	4.9	99%
99.9%	4.9	5.3	5.8	4.7	5.2	5.6	4.6	4.9	5.4	99.9%

Reliability Factor

G	2%			3%			4%			*G*
v_f *(mi/h)*	35	45	55	35	45	55	35	45	55	v_f *(mi/h)*
50%	2.5	2.9	3.4	2.5	2.9	3.4	2.5	2.9	3.3	50%
60%	2.7	3.1	3.6	2.6	3.1	3.5	2.6	3.1	3.5	60%
70%	2.9	3.3	3.8	2.8	3.3	3.7	2.8	3.2	3.7	70%
80%	3.1	3.6	4.0	3.1	3.5	3.9	3.0	3.5	3.9	80%
85%	3.2	3.7	4.1	3.2	3.6	4.1	3.2	3.6	4.0	85%
90%	3.4	3.8	4.3	3.4	3.8	4.2	3.3	3.7	4.1	90%
95%	3.6	4.0	4.5	3.5	4.0	4.4	3.5	3.9	4.3	95%
96%	3.7	4.1	4.5	3.6	4.0	4.4	3.5	3.9	4.4	96%
97%	3.7	4.2	4.6	3.7	4.1	4.5	3.6	4.0	4.4	97%
98%	3.8	4.2	4.7	3.7	4.2	4.6	3.7	4.1	4.5	98%
99%	4.0	4.4	4.8	3.9	4.3	4.7	3.8	4.2	4.6	99%
99.9%	4.4	4.9	5.3	4.3	4.7	5.2	4.2	4.6	5.0	99.9%

Reliability Factor

Table A-6 Yellow Clearance Interval Lookup Table for Old Male Drivers

G	-4%			-3%			-2%			*G*
v_f *(mi/h)*	35	45	55	35	45	55	35	45	55	v_f *(mi/h)*
50%	2.6	3.1	3.6	2.5	3.0	3.5	2.5	3.0	3.5	50%
60%	2.8	3.3	3.8	2.7	3.2	3.7	2.7	3.2	3.7	60%
70%	3.0	3.5	4.0	3.0	3.5	4.0	3.0	3.4	3.9	70%
80%	3.3	3.8	4.3	3.3	3.8	4.2	3.2	3.7	4.2	80%
85%	3.5	4.0	4.5	3.5	3.9	4.4	3.4	3.9	4.3	85%
90%	3.7	4.2	4.7	3.7	4.1	4.6	3.6	4.0	4.5	90%
95%	4.0	4.5	5.0	3.9	4.4	4.8	3.8	4.3	4.7	95%
96%	4.1	4.6	5.0	4.0	4.5	4.9	3.9	4.3	4.8	96%
97%	4.2	4.6	5.1	4.1	4.5	5.0	4.0	4.4	4.9	97%
98%	4.4	4.8	5.3	4.2	4.7	5.1	4.1	4.5	5.0	98%
99%	4.6	5.0	5.5	4.4	4.9	5.3	4.3	4.7	5.2	99%
99.9%	5.4	5.8	6.2	5.2	5.5	6.0	5.0	5.4	5.8	99.9%

Reliability Factor

G	-1%			0%			1%			*G*
v_f *(mi/h)*	35	45	55	35	45	55	35	45	55	v_f *(mi/h)*
50%	2.5	3.0	3.4	2.5	2.9	3.4	2.5	2.9	3.4	50%
60%	2.7	3.2	3.6	2.7	3.1	3.6	2.6	3.1	3.6	60%
70%	2.9	3.4	3.9	2.9	3.3	3.8	2.8	3.3	3.8	70%
80%	3.2	3.6	4.1	3.1	3.6	4.0	3.1	3.5	4.0	80%
85%	3.3	3.8	4.2	3.3	3.7	4.2	3.2	3.7	4.1	85%
90%	3.5	4.0	4.4	3.5	3.9	4.3	3.4	3.8	4.3	90%
95%	3.8	4.2	4.6	3.7	4.1	4.5	3.6	4.0	4.5	95%
96%	3.8	4.3	4.7	3.7	4.2	4.6	3.7	4.1	4.5	96%
97%	3.9	4.3	4.8	3.8	4.2	4.7	3.7	4.1	4.6	97%
98%	4.0	4.4	4.9	3.9	4.3	4.8	3.8	4.2	4.7	98%
99%	4.2	4.6	5.1	4.1	4.5	4.9	4.0	4.4	4.9	99%
99.9%	4.8	5.1	5.7	4.7	5.0	5.5	4.5	4.9	5.3	99.9%

Reliability Factor

G	2%			3%			4%			*G*
v_f *(mi/h)*	35	45	55	35	45	55	35	45	55	v_f *(mi/h)*
50%	2.4	2.9	3.3	2.4	2.9	3.3	2.4	2.8	3.3	50%
60%	2.6	3.1	3.5	2.6	3.0	3.5	2.6	3.0	3.4	60%
70%	2.8	3.3	3.7	2.8	3.2	3.7	2.7	3.2	3.6	70%
80%	3.0	3.5	3.9	3.0	3.4	3.9	3.0	3.4	3.8	80%
85%	3.2	3.6	4.1	3.1	3.6	4.0	3.1	3.5	3.9	85%
90%	3.3	3.8	4.2	3.3	3.7	4.1	3.2	3.6	4.1	90%
95%	3.5	4.0	4.4	3.5	3.9	4.3	3.4	3.8	4.2	95%
96%	3.6	4.0	4.4	3.5	3.9	4.4	3.5	3.9	4.3	96%
97%	3.7	4.1	4.5	3.6	4.0	4.4	3.5	3.9	4.3	97%
98%	3.8	4.2	4.6	3.7	4.1	4.5	3.6	4.0	4.4	98%
99%	3.9	4.3	4.7	3.8	4.2	4.6	3.7	4.1	4.6	99%
99.9%	4.3	4.8	5.2	4.2	4.6	5.1	4.1	4.5	4.9	99.9%

Reliability Factor